SCIENTIFIC COUNCIL DSC.27.06.2017.FM/T.33.01 ON AWARD OF SCIENTIFIC DEGREES AT THE INSTITUTE OF NUCLEAR PHYSICS, ASTRONOMICAL INSTITUTE, NATIONAL UNIVERSITY OF UZBEKISTAN

INSTITUTE OF NUCLEAR PHYSICS

A manuscript
UDC: 539.173.4+7+8

TASHKHODJAEV RUSTAM BAKHODIRKHODJAEVICH

MECHANISMS OF COLLINEAR CLUSTER TRIPARTITION

01.04.08 – Physics of elementary particles and atomic nuclei, accelerator technique

DISSERTATION
written to get the Doctor of Philosophy degree of physical and mathematical sciences

Supervisor: Nasirov Avazbek Karimovich,
doctor of physical and mathematical sciences

Tashkent – 2017

CONTENTS

INTRODUCTION

Topicality and relevance of the theme of the dissertation. Today most experimental data have been collected on the physics of nuclear reactions in heavy ion collisions. These data require to be understood by suitable and non-contradictory models. The topicality of theoretical investigation of the spontaneous and induced fission of heavy nuclei is related to the absence of full understanding of fission processes. It requires new theoretical methods to analyze the known experimental data of fission products. Systematization of the obtained experimental results and establishment of analyses and regularities in them allow studying the realistic mechanisms of heavy nuclear fission. There are a lot of theoretical models created in various scientific centers, but no one of them can fully descript ternary fission with the yield of products with almost the same mass numbers.

During the years of independence of our country, the science has been developed by providing theoretical and experimental investigations on nuclei fission and events to solve fundamental problems in the world, and defined results have been reached. Increasing the efficiency of nuclear technology area through the application of innovative technologies of theoretical and applied investigations in the area of nuclear reactions with heavy nuclei and particular binary and ternary fission of nuclei has significant meaning in the Strategy of Actions on Further Development of Uzbekistan.

Now, in the world, there are different theoretical models created in various scientific centres, but no one model can explain ternary fission with almost the same fragments. The current dissertation work is the original investigation of the ternary and multicluster fission by the author. Of course, these processes constitute less than one percent out of all events of fission, but knowledge of their nature allows us to better understand the conventional nuclear fission process. Multicluster fission exists due to the shell structure of nuclear matter, so both theoretical and experimental

knowledge of the nature of multicluster fission in different nuclei contribute to build a full fission mechanism that increases practical application of its regularity.

This research corresponds to the tasks stipulated in governmental regulatory documents and Decree of the President of the Republic of Uzbekistan No.PD-4512 “On works of further development of alternative energy sources” of 1 March 2013, Resolution No.PR-2789 “On measures of further improvement of the activities of the Academy of Sciences, organization, management and financing of scientific research works” of 17 February 2017, and Decree No.PD-4947 “On the Strategy of Actions on Further Development of the Republic of Uzbekistan” of 7 February 2017 and others.

Relevance of the research to the priority areas of science and technology development of the Republic of Uzbekistan. The dissertation research was carried out in accordance with the priority areas of science and technology development of the Republic of Uzbekistan: II. “Power, energy and resource saving”.

Degree of study of the problem. Until today leading scientists of the world, for example, German scientists (A.R. Degheidy, J.A. Maruhn, H. Diehl, W. Greiner, F. Gonnenwein, W. von Oertzen, J.P. Theobald, P. Heeg and M. Mutterer), Russian scientists (Yu.V. Pyatkov, D.V. Kamanin, A.V. Karpov, V.A. Rubchenya and S.G. Yavshits), American scientists (M.L. Muga and C.R. Rice), Swedish scientists (P. Holmvall and U. Köster), Indian scientists (K. Manimaran, K.R. Vijayaraghavan and M. Balasubramaniam) and others have done a number of investigations to study the statistic and dynamic properties of fission of heavy nuclei experimentally and theoretically.

Properties of heavy ion (U, Cf, Th, Pu etc.) fission products, like yield, kinetic energy, and angular distribution have been studied by such Uzbek scientists as V.P. Pikul, Yu.N. Koblik, A.K. Nasirov and others. To describe nuclear reactions with heavy ions, the dinuclear system model has been created by the scientists of the Joint Institute of Nuclear Researches (Russia) and the Institute of Nuclear Physics (Uzbekistan).

Earlier the investigation of ternary fission included only a binary fission with accompanied light charged particles, i.e. He, Li, Be etc. In this mode of ternary fission, middle fragment (light nucleus) flies perpendicular to binary fission line and the heaviest emitted cluster is sulfur nucleus. But later the experimental group (FOBOS) from Russia started to study another type of ternary fission – collinear cluster tripartition (hereinafter CCT). These ternary fission products (clusters) fly almost in one line and their masses have around the same value, i.e. middle fragment can have larger mass numbers (<100).

After publication of the results of the FOBOS experiments, the number of the theoretical researches by Indian scientists has increased. Especially, charge and mass numbers of fragments were estimated by calculating the yield of products, and possible configuration by calculating the total potential energy in their theoretical papers. Main deficiency of this theory is that one barrier was used for two necks (or overlapping surfaces), which means that the fragments can be separated only simultaneously. This limitation was not taken into account by authors.

Taking into account the current status of the problem, we tried to investigate various mechanisms of ternary fission of heavy nuclei, especially uranium and californium nuclei.

Connection of the theme of dissertation with the scientific researches of the higher educational institution, where the dissertation was conducted. The dissertation was carried out within the framework of the scientific projects of the Institute of Nuclear Physics: FA-F2-F055 “A study of the reaction yield with heavy ions and nuclear fission” (2007-2011), FA-F2-F115 “Investigation of reaction mechanisms of multinucleon transmissions and fusion-fission of nuclei” (2012-2016).

The aim of the research is development of a theoretical formalism describing mechanisms of collinear cluster ternary fission of heavy nuclei and identification of conditions leading to collinearity of fission.

The tasks of the research:

calculating the total interaction potential of dinuclear system for describing the sequential collinear (prolate) ternary fission in the $^{235}U(n_{th},f)$ reaction;

finding the charge distribution (yield of products) of the sequential collinear (prolate) ternary fission in the $^{235}U(n_{th},f)$ reaction;

studying the dependence of the total interaction potential on the distance between the heaviest (^{132}Sn) and middle (^{50}Ca) clusters in collinear (prolate) configuration in spontaneous ternary fission of ^{252}Cf;

calculating the yield of products formed by the almost sequential mechanism collinear cluster tripartition of ^{252}Cf;

studying the role of the distance between edge fragments (^{70}Ni and ^{132}Sn) in shape of total interaction potential in non-collinear (oblate) configuration in the $^{252}Cf(sf)$ reaction;

getting the Lagrange equation of motion for the true ternary fission in the $^{252}Cf(sf)$ reaction;

solving the equation of motion with different initial conditions (Cauchy problem);

finding the initial conditions which lead to collinear ternary fission.

The objects of the research are heavy nuclei, products of ternary fission and clusters.

The subjects of the research are total interaction potential between two (and three) nuclei, yield of ternary fission products, initial states of the system which consist of three interacting nuclei.

The methods of research. On the theoretical level, the research methods are mathematical apparatus of phenomenological potential of strong interaction and macroscopic statistical mechanics, analytical and numerical methods for solving differential equations.

The scientific novelty of the research is as follows:

a new trinuclear system model to describe true ternary fission process was developed, and it was revealed that in some cases collinear ternary fission takes place in nature;

it was found that in sequential collinear ternary fission more possible channel is $^{82}Ge+^{72}Ni+^{82}Ge$ in the $^{235}U(n_{th},f)$ reaction;

it was shown that the location of ^{132}Sn close to the $^{72}Ni+^{50}Ca$ is important to be collinear ternary fission at the same time way;

it was also shown that fission the barrier between ^{72}Ni and ^{50}Ca is higher than that of ^{50}Ca and ^{132}Sn, i.e. separation of ^{132}Sn from the system $^{72}Ni+^{50}Ca$ is easier;

it was shown that the initial condition at pre-scission stage of trinuclear system is important for its decay which leads to a collinear fission.

Practical results of the research consist of the following:

more possible channel of sequential collinear cluster tripartition of the excited ^{236}U is $^{82}Ge+^{72}Ni+^{82}Ge$ in agreement with experimental data was obtained;

it was shown that at spontaneous fission of ^{252}Cf the probability of collinear ternary fission of the $^{70}Ni+^{50}Ca+^{132}Sn$ channel is more comparing with other channels, and rupture of neck between Ca and Sn nuclei occurs earlier than Ni and Ca. The difference of the rupture time should be too short;

at the spontaneous fission of ^{252}Cf the velocity of the middle fragment (^{50}Ca) is close to zero, and hence the possibility of the experimental observation of this fragment is rather small;

it was found that if the relative distance between Ni and Sn nuclei is less than 21 fm, then repulsive Coulomb force extrudes Ca nuclei from the collinear position, meanwhile the minimum position of Ca moves to collinear line with the increasing of the relative distance;

it was shown that from the dynamical calculation of true ternary fission of ^{252}Cf there is just one initial condition that leads to collinear fission: mass centres of three nuclei lie in one line and the perpendicular component of the middle fragment's

velocity to the collinear line is zero. All other initial conditions of the pre-scission state result in non-collinear ternary fission;

it was found that the breakup of ^{50}Ca from ^{70}Ni occurs around 1.35×10^{-21} seconds later than the separation of ^{132}Sn from ^{70}Ni+^{50}Ca system. This time is very small compared with the time of a usual binary fission (~10^{-19} s).

The reliability of the research results is substantiated by the use of modern methods of nuclear and theoretical physics and highly effective numerical methods and algorithms; careful check of a consistence of the received theoretical results with experimental data and results of other authors; consistency of conclusions with the main provisions of the nuclear reactions at low energy.

Scientific and practical significance of the research results. The scientific significance of the research results is determined by the ability of the developed formalism in the dissertation to analyze the properties of ternary fission fragments obtained by new experimental data and results of different theoretical models. For the first time, theoretical investigation of collinearity of products was carried out by the researcher, and this is important in understanding the nature of ternary fission of heavy nuclei.

The practical significance of the research results lies in the fact that they can be used to obtain more possible configurations of a ternary system and to define its fission channels. Created calculation method can be used to estimate different parameters of ternary fission products such as charge, mass, temperature, as well as the angular distribution that shows the type of ternary fission. The results can also be useful for the analysis of the nature and dynamics of nuclear reaction mechanisms, and in the development of observational experiments and criteria for the detection and identification of clusters.

Implementation of the research results. Great probability of collinear ternary fission of the ^{70}Ni+^{50}Ca+^{132}Sn channel at spontaneous fission of ^{252}Cf comparing with other channels was used by international journals (Journal of Physics G, 2017;

Physical Review C, 2016; Physical Review, 2017) to define a channel of collinear cluster tripartition. The use of the scientific research result has given chance to define collinear ternary fission of heavy nuclei.

Possibility of non collinear ternary decay at more than 24 fm of the distance between Ni and Sn at ternary fission of ^{252}Cf was used used by international journals (International Journal of Physics E, 2016; European Physical Journal A, 2017; Physical Review C, 2017) to define collinearity or non collinearity of fission. The use of the scientific research result has given chance to define cases of non collinear fission.

Testing of the research results. The research results were reported and tested at 7 international and local scientific conferences.

Publication of the research results. On the theme of the dissertation 17 scientific works were published, including 8 scientific papers in international scientific journals recommended by the Supreme Attestation Commission of the Republic of Uzbekistan for publishing basic scientific results of PhD dissertations.

Structure and volume of the dissertation.

The dissertation is presented on 103 pages consisting of an introduction, four chapters, a conclusion, an appendix and a bibliography.

CHAPTER I. COLLINEAR CLUSTER TRIPARTITION AS SEQUENTIAL BINARY FISSION IN THE $^{235}U(n_{th},f)$ REACTION

1.1. Introduction

The problem of ternary fission of heavy ions at low energy is one of oldest problem in the physics of atomic nuclei area. The interest to ternary fission process was appeared after discovery of binary fission of nuclei. As reported by Farwell [1], for the first time experimentally obtained evidence for light nuclei (especially helium nucleus) accompanied by a binary fission is referred to as a ternary fission by L. W. Alvarez in 1947. Later various experimental works which were dedicated to this type of ternary fission (i.e. binary fission with emission of light nuclei) were provided by different authors [2-4]. In 1958 ternary fission process was discussed theoretically using the liquid drop model by Swiatecki [5]. Starting from 1960 the interest to this area of nuclear physics was increased rapidly, and a lot of different experimental and theoretical papers were appeared (see, for example [6-11]).

In the work [6] the long-range alpha particles associated with the spontaneous-fission decay of californium-252 have been studied by means of nuclear-emulsion techniques. It was shown that alpha emission occurs at the time of scission of two massive nuclei and also the direction of alpha particle is determined by the extent of electrostatic repulsion by the fragments. Authors of the work [8] Diehl and Greiner tried to explain fission of compound nucleus into three equal fragments within the framework of the liquid drop model. Two different parameterizations for the prolate and oblate direct fission modes are calculated, and it is concluded that the prolate ternary fission turned out to be energetically much more favored than the oblate fission. Theobald et. al. (see Ref. [11]) investigated the α-particle accompanied ternary fission. It has been shown that there are manifold correlations between the

measured kinematic observables which can be interpreted in terms of the initial parameters of the ternary system.

This chapter of the dissertation is devoted to study true ternary fission in cascade mechanism: firstly, a compound nucleus decays into heavy and light fragments, and then heavy fragment breaks-up into two fragments. Finally we get three fission products with comparable masses. The chapter is based on our published paper [12].

The observation of three and more nuclear fission products in the fission of ^{235}U with thermal neutrons and in the spontaneous fission of ^{252}Cf has opened a new area of study in the nuclear reactions. This phenomenon relates to the appearance of cluster states in nuclear reactions and it is the manifestation of the shell structure which is responsible for the production of isotopes with magic numbers of neutrons and protons. When a massive nucleus loses its stability, and goes to fission, first of all clusters are formed as future fragments having the neutron or/and proton number nearby the magic numbers 28, 50, 82 and 126. In the case of ternary fission one observes fragments with the charge number 28.

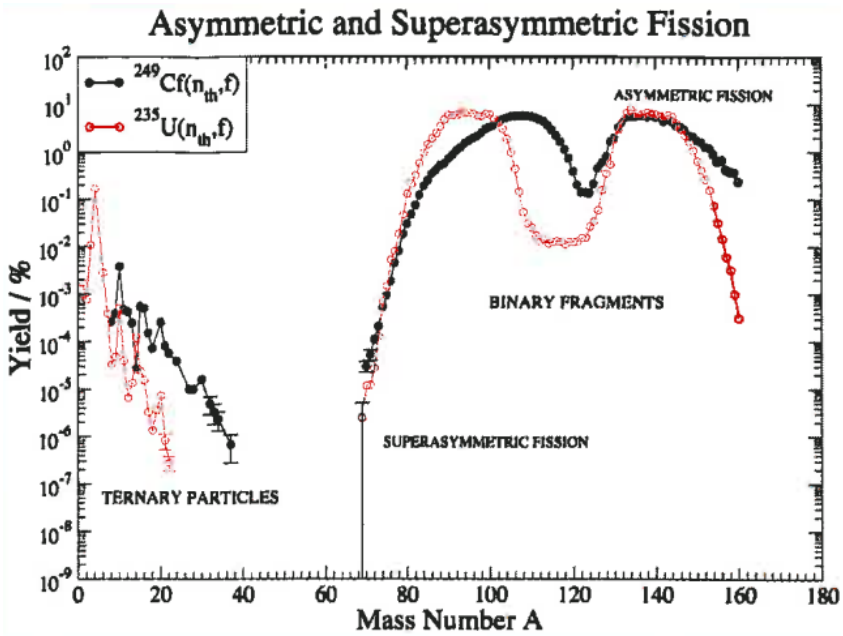

Fig.1.1. Experimental yields of the conventional ternary (left part) and binary (right part) fission products reproduced from Ref. [13].

An interesting example is illustrated in the Fig. 1.1 where the experimental [13] yields of the conventional ternary (left part) and binary (right part) fission products are presented. As it is shown there is a gap between product masses of two types of fission. Light mass area (until ~ 40) was called as “ternary particles”, heavier mass (~90÷160) areas were called as “binary fragments” and “asymmetric fission”. In our point of view the “superasymmetric fission” region around the mass 70 corresponds to the yield of Ni nucleus in the collinear cluster tripartition. The mass distribution of the new type of fission – the collinear cluster tripartition fills this gap in the known experimental data.

This chapter is devoted to the study of and induced fission of heavy nuclei. There is no full understanding of the fission process and the dependence of the probability of formation of reaction products on the fission stages. Though one event of the collinear cluster tripartition (hereinafter CCT) process occurs against 1000 events of binary fission, the knowledge of its mechanism gives us a better understanding of the process of spontaneous and induced fission. A theoretical and experimental knowledge of the nature of multicluster fission of various nuclei will promote the construction of a full picture of fission.

The role of the nuclear shell structure in the formation of fission products appears in the observed asymmetric mass distributions depending on the full number of neutrons and the excitation energy of the system undergoing to fission. The other manifestation of the nuclear shell structure occurs at collinear cluster tripartition which was investigated by the FOBOS collaboration [14-21]. In this chapter, the author explains reasons for the yield of the observed fragments in the collinear cluster tripartition in the $^{235}U(n_{th},f)$ reaction. The cross sections of multicluster fission of the U, Pu and Cf isotopes are less than one percent of the corresponding cross sections of binary fission. So the cross section of CCT is comparable with one of the well-known ternary fission with the emission of an alpha particle. Therefore, a theoretical interpretation of these processes is required for a full understanding of the

mechanism. The ternary fission fragmentation of ^{252}Cf for all possible third fragments using the recently proposed three-cluster model [22] was studied in Refs. [23,24]. The authors concluded that the theoretical relative yields imply that the emission of ^{14}C, ^{34,36,38}Si, ^{46,48}Ar, and ^{48,50}Ca as the most probably third particle in the spontaneous ternary fission of ^{252}Cf. The defect of the three-cluster model is related with the simplification of the decay process by the use of one barrier for the decay of the ternary fission. Therefore, this method does not give a physically relevant explanation of the decay of the ternary system in present. This problem is solved by this dissertation.

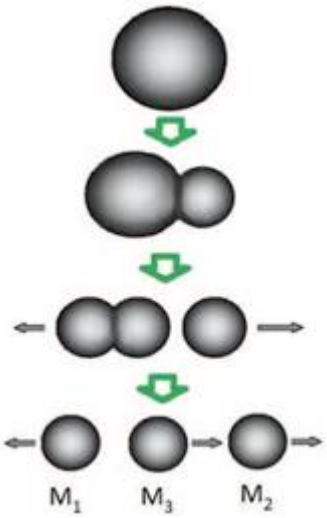

Fig. 1.2. The illustration of the sequential collinear cluster tripartition of a heavy nucleus

1.2. Theoretical model.

For the description of the mass and charge distributions of fission products of heavy nuclei the concept of the dinuclear system (DNS) [25–28] has been applied. The formation of the DNS is an inevitable stage in fission as in fusion. Indeed, at the descent from the saddle point to the scission point, the fissile nucleus looks like a dumbbell and changes its shape and mass (charge) asymmetry by nucleon exchange. The initial stage of fission when the shape of the fissionable nucleus transforms from

the compact form into the double nuclear system is not considered here. The charge distribution of the fragments is calculated after the crossing of the saddle point and the formation of DNS. In the case of the DNS with a large-neck parameter the DNS model is not acceptable because the DNS concept proposes the smallness of the neck connecting the two interacting nuclei relatively to their whole volume.

A similar conception was used in Ref. [29] to estimate the yield of the ^{4}He, ^{8}Be, and ^{10}Be in the ternary fission of ^{252}Cf and ^{56}Ni. The authors of Ref. [29] assumed the ternary fission as a two-step process: the binary system is firstly formed and then the ternary system is formed from it by extracting the light charged particle (^{4}He or ^{8,10}Be) into the region between the two heavy fragments. Then this ternary system decays. According to their concept, the ternary system exists as a whole for a short time then it decays into three parts, while in this chapter the heavy products undergo fission after scission from the light fragment of the previous binary fission of the compound nucleus.

CCT can be assumed to be the two-stage fission of the sequential binary fissions. In Fig. 1.2, a sketch of the sequential mechanism is presented. It is obvious that such a way of division is possible when the initial nuclei decay through the asymmetric channel. It should be stressed that the tri-partition axes are collinear because the fission axes of both stages are in coincidence: the heavy fragment of the primary fission does not change the momentum direction at its fission into two fragments forming the second and third products of ternary fission. We do not exclude the fluctuation of the fission axis. But this physical quantity is not explored by us. Thus, in the consecutive ternary fission of the compound nucleus first two fragments with asymmetric masses and charges are formed. Then the heavy fragment decays again into two parts.

The mass and charge distributions of fission products of heavy nuclei can be calculated if the descent from the saddle point up to the scission points continues long enough. During the evolution of the DNS along the mass asymmetry it should not

decay into fragments. The DNS concept assumes an interaction between two nuclei by nucleon exchange between them and retaining their shell properties. The validity of the application of the DNS concept to describe deep inelastic transfer and quasifission reactions is evident: we have a DNS in the entrance channel. But its application to explain the yield of products in the fusion-fission, fast-fission and spontaneous fission processes requires more thoughts on why it is reasonable. With the DNS concept a number of features of deep inelastic transfer reactions, fusion of nucleus, fission, quasifission, fusion-fission and fast fission [28,30,31] can be well explained. In calculation of the DNS total energy the charge Z and mass A asymmetries of the system and the relative distance R between the DNS fragments centers (see Fig. 1.3a) are the main degrees of freedom. The change of the DNS total energy is the sum of the changes of the energy reaction balance (Q_{gg}-value) and nucleus-nucleus interaction potential $V(Z,A,R)$ between its constituents:

$$V(Z,A,R) = V_{int}(Z,A,R) + Q_{gg}(Z,A). \tag{1.1}$$

The Q_{gg}-value represents the change of the internal energy of the system during the reaction: $Q_{gg} = B_1(Z,A) + B_2(Z_{\mathrm{CN}} - Z, A_{\mathrm{CN}} - A) - B_{\mathrm{CN}}(Z_{\mathrm{CN}}, A_{\mathrm{CN}})$, where $Z_{\mathrm{CN}} = Z_1 + Z_2$; B_1 and B_2 (Z_1 and Z_2) are binding energies (charge numbers) of the DNS constituents. In Fig. 1.3(a) the potential energy surface $V(Z,R)$ is presented as a function of the relative distance between the fragments and the charge number Z of a fragment. The nucleus-nucleus potential $V_{int}(R)$ shown in Fig. 1.3(b) corresponds to the interaction between fragments ${}^{A_1}Z_1$ and ${}^{A_2}Z_2$. The mass numbers A_1 and A_2 corresponding to the charge numbers Z_1 and Z_2 provide minimal values of the potential-energy surface. The mass number A of a fragment was found from the minimization of the total potential energy of the fissioning system at the given charge number Z.

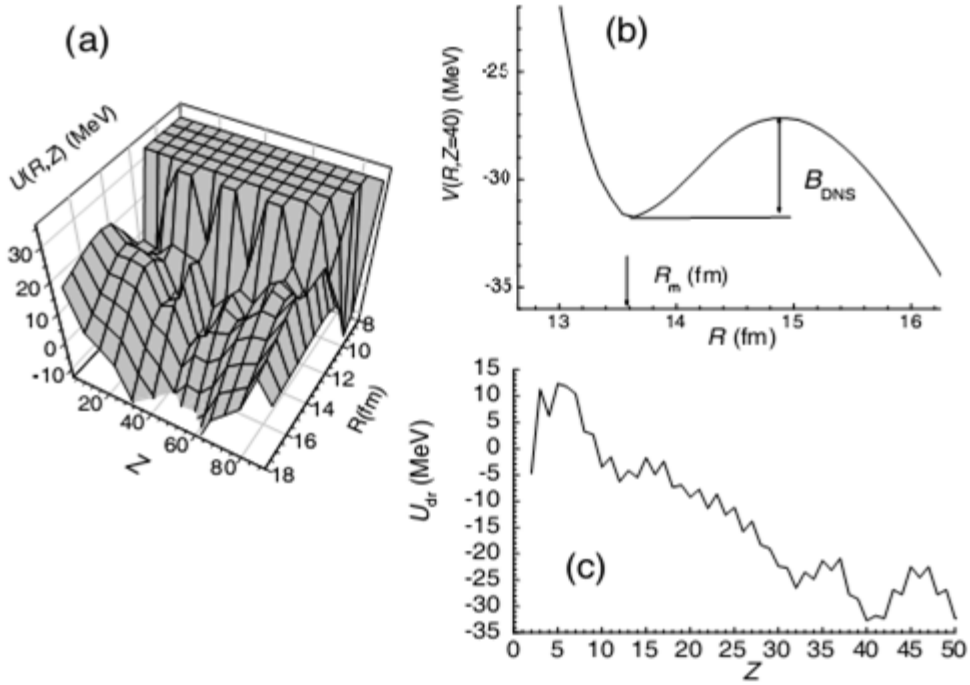

Fig. 1.3. Potential-energy surface for ^{236}U as a function of the relative distance *R* and a fragment's charge number *Z* (a); nucleus-nucleus potential *V(R)* corresponding to interaction of DNS ^{102}Zr+^{134}Te; the depth of the potential well is the barrier B_{DNS} against to decay of DNS (b); driving potential for ^{236}U (c).

The DNS model supposes the knowledge of the interaction potential between deformed nuclei with different orientation angles of their axial symmetry axes [28]. Details of the method of calculation of interaction potential $V_{int}(Z, A, R)$ are presented in the appendix. The advance of the use of the effective nucleon-nucleon potential by Migdal is its sensitivity to the nucleon density of the surrounded area. The behavior of the short range nuclear forces is very important in calculation of the formation and decay probability of DNS. The combination collective Coulomb and nuclear interaction potentials between two nuclei creates a well as a function of *R* (see Fig. 1.3(b)). The presence of the potential well allows DNS nuclei to be in interaction by multinucleon transfer before the decay into two fragments. The depth of this potential to decay of DNS is B_{DNS} (see Fig. 1.3(b)).

The driving potential has been found by connecting the minima of the potential well ($V_{int}(R_m)$) of the nucleus-nucleus interaction (see Fig. 1.3(b)) calculated for

each charge asymmetry of the DNS, i.e. it is the curve lying on the bottom of a valley of the potential-energy surface along the Z-axis $2<Z<90$. If we use $R_m(Z)$ to show the value of R corresponding to the bottom of the potential well for the DNS with the charge asymmetry Z, then the driving potential is defined by using (1.1) as

$$U_{dr}(Z,A) = V_{int}(Z,A,R_m(Z)) + Q_{gg}(Z,A). \tag{1.2}$$

The driving potential U_{dr} used to describe the charge distribution of the DNS fragments formed in the fission of ^{236}U is shown in Fig.1.3(c). The advantage of such method of calculation of the driving potential for the fissionable nuclear system is the possibility to use the experimental values of the binding energy of nuclei B_1 and B_2 [32] that allow us to take the shell effects into account. The shell effects play a crucial role in the formation of the fission products. The neutron and proton numbers corresponding to the maximum values of the shell correction are close to the magic numbers which are inherent to the clusters. In our calculations, for the values of binding energy of isotopes which have not been measured yet, we use those obtained from the well-known mass tables [33].

Theoretical calculation of the binding energies of the nucleus with the deformation parameter β_i providing the minimal energy for the given charge Z and mass A numbers is complicated task. The large set of mass numbers should be checked to find the value of A providing the minimum value of the total energy of the ternary system.

The peculiarities of the potential-energy surface for DNS allow us to find the basic directions of the evolution and main modes of the decay. The potential well of $V(R)$ corresponds to the scission point barrier which was discussed in Ref. [34]. This is one of the circumstance which is used to explain the fission process. The scission barrier can be considered as one of reasons calling the delay of the fission. So, the delay of scission is connected by the potential well with a definite depth (B_{DNS}, see Fig. 1.3 (b)).

The fact of the delay of the fission process results from the analysis of experimental data shows a competition between particle (neutrons, protons or alpha-particles) emission and fission of fusion-fission reactions. To explain this phenomenon large friction forces or viscosity of nuclear matter have been assumed [35]. It means that the descent from the saddle point up to the scission point occurs by nucleon exchange between already formed nuclei during a long time ($(35\pm15)\cdot10^{-21}$ s) in competition with the neutron emission. During the descent time, mass (charge) equilibrium in DNS can be reached [36] by nucleon exchange which is affected by the driving potential (see Fig. 1.3 (c)). The information which is used in our model about crossing of the saddle point is the excitation energy generated at the descent from there.

1.3. Application of the concept of the DNS for the explanation of binary fission.

The DNS evolution is determined by the potential-energy surface and especially by the driving potential. The driving potential determines the form and position of the maximum of the mass (charge) distribution, as well as the total kinetic energy of the products of the DNS decay. Therefore, the correct description of the experimental data or their interpretation depends on the accuracy of the calculation of the potential-energy surface of the DNS [37]. Large probabilities of the formation of fragments with magic numbers 20, 28, 40, 50, 82 and 126 of protons and neutrons (clusters) are obtained by including the quantum shell effects into the consideration. Formation and yields of the fission products with given mass and charge numbers are defined by the landscape of the potential-energy surface. The shell corrections to the binding energy of the DNS fragments are considered to explain features of the yields of products in asymmetric fission, which are observed in experiment. The simplest way to take into account shell effects is the use of binding energy values of atomic nuclei from the well-known tables [33].

The decay of the DNS may be analyzed as statistical process [29], i.e. statistical equilibrium in the charge (mass) distribution of the system can be established in dependence on the given excitation energy and height of the barrier hindering its decay into two fragments. In Ref. [29], the ternary system with a light nucleus between two heavy fragments is assumed to appear from the binary configuration near scission. The theoretical results of the authors for the charge distributions of the light charged particles which are emitted in spontaneous ternary fission of ^{252}Cf and in induced ternary fission of ^{56}Ni are in a good agreement with the available experimental data.

The charge (mass) distribution of the fission fragments yield $Y(Z)$ depends on the charge distribution of the DNS fragments $P(Z)$ and decay probability $W(Z)$ of the DNS from the given charge-asymmetry state Z:

$$Y(Z) = Y_0 P(Z) W(Z), \tag{1.3}$$

where Y_0 is a normalizing coefficient for the yield probabilities. The probability of formation of the DNS $P(Z)$ can be found from the condition of a statistical equilibrium as in Ref. [36]:

$$P(Z) = P_0 e^{-U_{dr}(Z)/T_{DNS}(Z)}, \tag{1.4}$$

where $T_{DNS}(Z) = \sqrt{\frac{E^*_{DNS}}{a}}$ is the effective temperature of the DNS with the charge asymmetry Z and $U_{dr}(Z)$ is determined by formula (1.2), $a = \frac{A_{CN}}{12\ \mathrm{MeV}}$ is level density parameter, and A_{CN} is the mass of a compound nucleus. $E^*_{DNS} = U_{dr}(Z_{BG}) - U_{dr}(Z)$ is excitation energy of DNS, to the maximum value of driving potential corresponds Z_{BG} which is called Businaro-Gallone point. The decay probability of the DNS $W(Z)$ can be found as in Ref. [29]:

$$W(Z) = W_0 e^{-B_{DNS}(Z)/T_B(Z)}, \tag{1.5}$$

where $T_B(Z) = \sqrt{\frac{B_{DNS}}{a}}$ is the effective temperature of the system on the barrier (or at the scission point), $B_{DNS}(Z)$ is the scission barrier for the decay of the DNS (see Fig.

2(b)). Its value is determined by the depth of the potential well of the nucleus-nucleus interaction; P_0 and W_0 are normalizing coefficients for the corresponding probability distributions.

From equations (1.3)–(1.5) we can see that the yield of the fragments at the decay of the DNS depends strongly on the driving potential $U_{dr}(Z)$. Equation (1.4) means that the position of the maxima of the mass distribution corresponds to the minima of driving potential, which is calculated for a given decaying nucleus. Therefore, we have to consider the minima of the driving potential. For the theoretical research of the yield of fission fragments, which are observed in experiment, the driving potential must be defined accurately. The knowledge about the driving potential U_{dr} of a fissionable system allows us to make predictions concerning the shape of the mass distribution of fission products. There is the possibility of the explanation of the ternary fission process with specialties of the driving potential which is calculated for the $^{235}U(n_{th},f)$ reaction.

1.4. Explanation of ternary fission as cascade fission in the $^{235}U(n_{th},f)$ reaction.

The authors of Ref. [17] used the “missing mass” method, when the setup consisting of two detectors placed opposite relative to the ^{235}U target, can register only two of the three fragments of the tripartition and the third fragment is missed. According to the sequential mechanism of CCT (see Fig. 1.1), when two reaction products are registered in coincidence by the two detectors then the first product of the primary fission is obligatorily registered while the other product is one of two secondary fission products. So, another product of the secondary fission is missed.

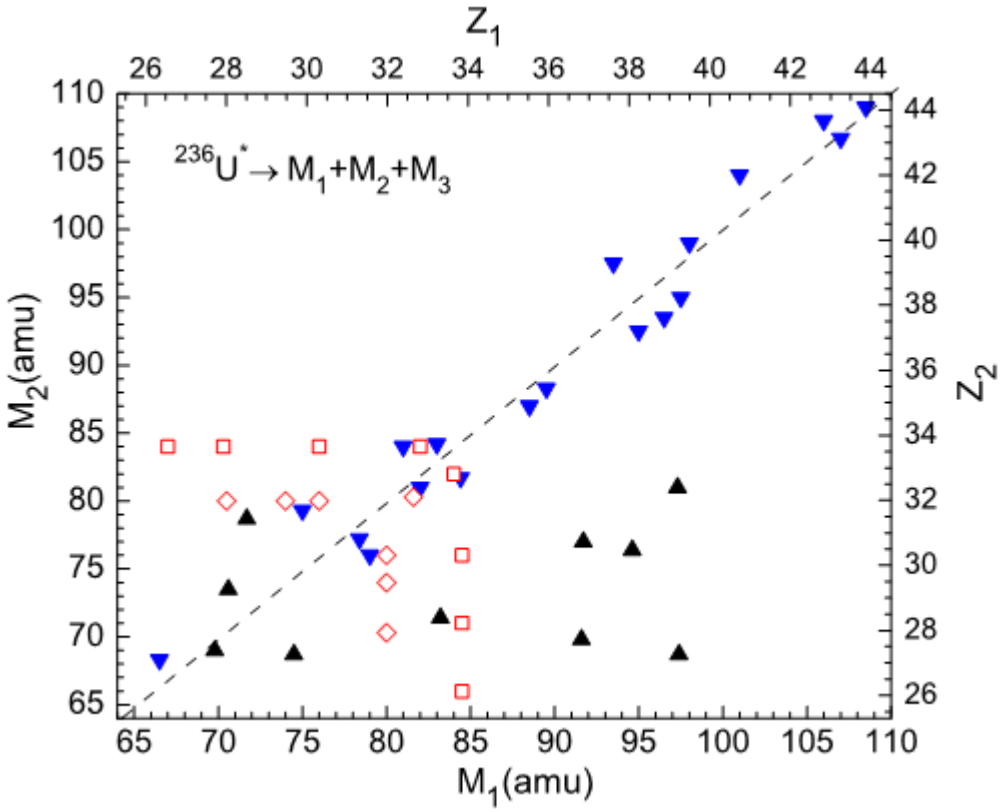

Fig. 1.4. Comparison of the maximum values of the calculated yield of the collinear cluster tripartition products by the sequential fission ^{82}Ge+(^{154}Nd→{^{72}Ni+^{82}Ge, ^{76}Zn+^{78}Zn}) (diamonds) and ^{86}Se+(^{150}Ce→{^{68}Fe+^{82}Ge,^{72}Ni+^{78}Zn}) (squares) mechanisms with the experimental data of the mass-mass distribution of the CCT products in the ^{235}U(n_{th},f) reaction registered in coincidence with approximately equal momenta (up triangles, the data were taken from Fig. 6b of Ref. [17]) and the CCT products with approximately equal masses with the momentum values up to 120 a.m.u. (cm ns)$^{-1}$ (down triangles, the data from Fig. 7d of Ref. [17]). The charge numbers corresponding to the presented mass numbers are shown on the top and right axes.

The experimental data (filled up and down triangles) presented in Fig. 1.4 are the mass-mass distribution of the ^{235}U(n_{th},f) fission fragments registered in coincidence by two detectors opposite relative to the ^{235}U target. Different filled symbols correspond to the CCT events which are selected from the whole data by different conditions: 1) the CCT products with approximately equal momenta,

velocities (filled up triangles, the results were taken from Fig. 6b of Ref. [17]) and 2) the CCT products with approximately equal masses with the momentum values up to 120 a.m.u. (cm ns)$^{-1}$. The maximum values of the calculated yield of the tripartition products in the analyzed fission channels (open squares and diamonds) are compared with experimental data in Fig. 1.4. Calculated fragment masses are not more than ~84 a.m.u. in the framework of the current cascade mechanism of collinear cluster tripartition.

The theoretical results of this work describing the yield of products with masses M_1 and M_2 in the ^{80}Ge+^{76}Zn+^{76}Zn+4n and ^{80}Ge+^{70}Ni+^{82}Ge+4n channels are shown by open diamonds while the ones corresponding to the yields of the CCT products in the ^{84}Se+^{66}Fe+^{82}Ge+4n and ^{84}Se+^{72}Ni+^{76}Zn+4n channels are shown by open squares. The charge numbers corresponding to the presented mass numbers are shown on the top and right axes in Fig. 1.4. Further we discuss the details of the calculation leading to our results presented in this figure.

According to the sequential mechanism, the first CCT product is formed in the asymmetric fission of an initial compound nucleus and the fission of the heaviest fragment in the first fission stage produces the second and third fragments. Firstly, we shall consider the first binary fission,

$$n_{th}+^{235}U\rightarrow^{236}U^{*}\rightarrow f_1+f_2,$$

by the thermal neutron with energy $E_{n_{th}} = 0.025$ eV. The excitation energy of the compound nucleus $^{236}U^{*}$ is 6.54 MeV. The potential-energy surface is calculated by formula (1.1) which includes the shell effects due to the use of realistic binding energies of the interacting nuclei. The energy balances for the different fission modes (f_1+f_2) are presented in table 1.1.

Table 1.1. Energy balance (Q_{gg}) and theoretical (*TKE*(theor)) and experimental (*TKE*(exp)) values [26] of the total kinetic energy (in MeV) of the fragments for the different fission modes of ^{236}U (the first stage). B_f^H is the fission barrier of the heavy fragment formed in the first stage of the sequential fission. $\beta_2^{(1)}$ and $\beta_2^{(2)}$ are the

quadrupole deformation parameters of the first and second fragments, respectively, which correspond to the 2^+ state and are taken from Ref. [38].

Fission modes	^{82}Ge+^{154}Nd	^{86}Se+^{150}Ce	^{92}Kr+^{144}Ba
Q_{gg} (MeV)	-173.75	-177.98	-193.91
TKE (theor)	159.83	168.46	190.69
TKE (exp)			170.0 [39]
B_f^H (MeV)	36.33	37.92	39.17
$\beta_2^{(1)}$ $\beta_2^{(2)}$	0.26 0.35	0.19 0.32	0.15 0.19

According to the energy conservation law the total kinetic energy should not be larger than the energy balance (Q_{gg}-value) of the corresponding channel. Therefore, in the calculation of the potential-energy for the $^{236}U^* \rightarrow f_1+f_2$ reaction the static deformation parameters of the constituents of DNS were used as free parameters to make the barrier of the nucleus-nucleus potential for the exit channel lower than the maximal value of *TKE*. The theoretical value of *TKE* included the energy carried away by 2 neutrons which are emitted. Therefore, there is a difference between theoretical and experimental values of *TKE* for the ^{92}Kr+^{144}Ba fission channel.

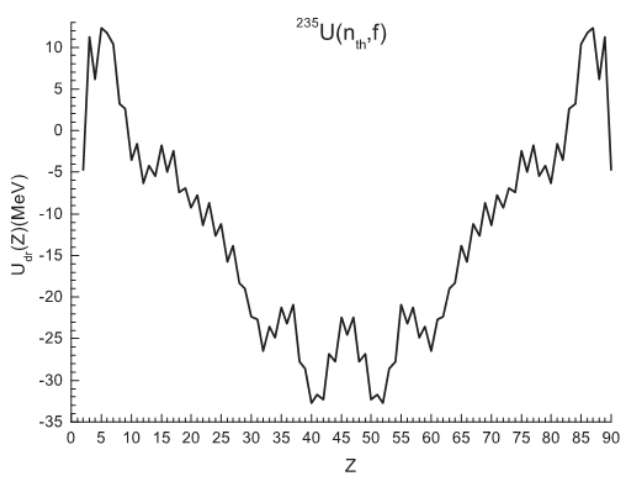

Fig. 1.5. Driving potential for the $^{235}U(n_{th},f)$ reaction calculated by the use of the binding energies with the shell effects.

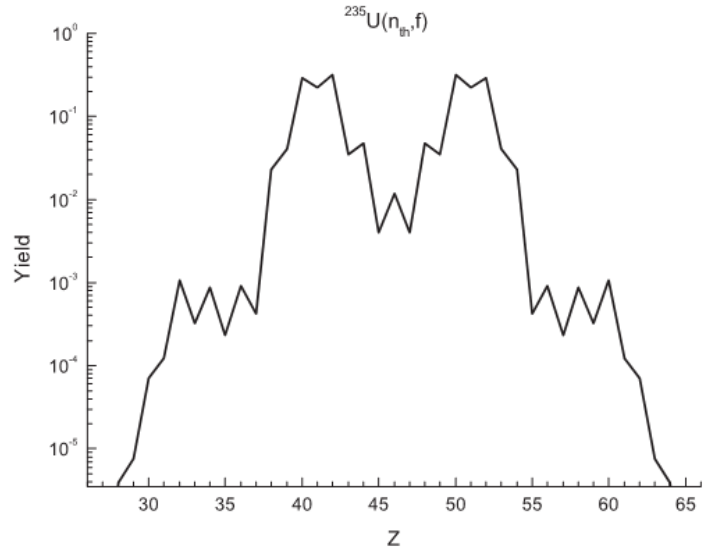

Fig. 1.6. Yields of the reaction products at fission of ^{236}U calculated with formula (1.3).

The driving potential calculated with the formula (1.2) is presented in Fig. 1.5. In Fig. 1.5 three minima of the driving potential located at Z = 56, 58, 60 are responsible for the corresponding maxima at these charge numbers in Fig. 1.6. As shown in Fig. 1.6, the yields of the products with the charge numbers Z = 30, 32, 34, 36, 40, 42, 50, 52, 54, 56, 58 and 60 are well pronounced. The light fragments with the most probable charge numbers Z_L = 40 and 42, which are products of the main fission channels, and the corresponding heavy fragments with Z_H = 52 and 54 are produced with larger fission barriers in comparison with the one of the heavier fragments Z = 58 and 60 (see table 1.1). The barrier values are obtained for the ground state of nuclei by the Sierk's model with the rotating liquid-drop model [40]. The shape of fission products is not expected to be in the ground state: as soon as they have prolated shape since the nucleus going to fission has the elongated shape. So, we shall consider the fragments Ba, Ce, Nd as fissionable nuclei in the second stage of the CCT:

$$\mathrm{n_{th}} + {}^{235}\mathrm{U} \rightarrow {}^{236}\mathrm{U}^{*} \rightarrow \begin{cases} {}^{92}\mathrm{Kr} + {}^{144}\mathrm{Ba} \\ {}^{86}\mathrm{Se} + {}^{150}\mathrm{Ce} \\ {}^{82}\mathrm{Ge} + {}^{154}\mathrm{Nd} \end{cases}$$

The results of the calculations for the yields of fragments in the fission of Ba, Ce and Nd are presented in Figures 1.7, 1.8 and 1.9, respectively.

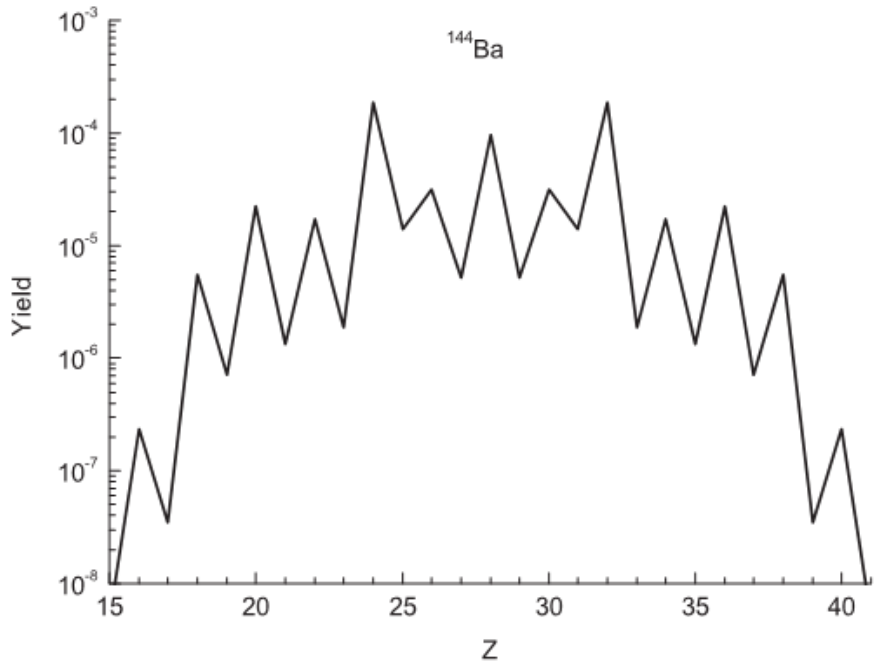

Fig. 1.7. Yields of the reaction fragments for fission of ^{144}Ba

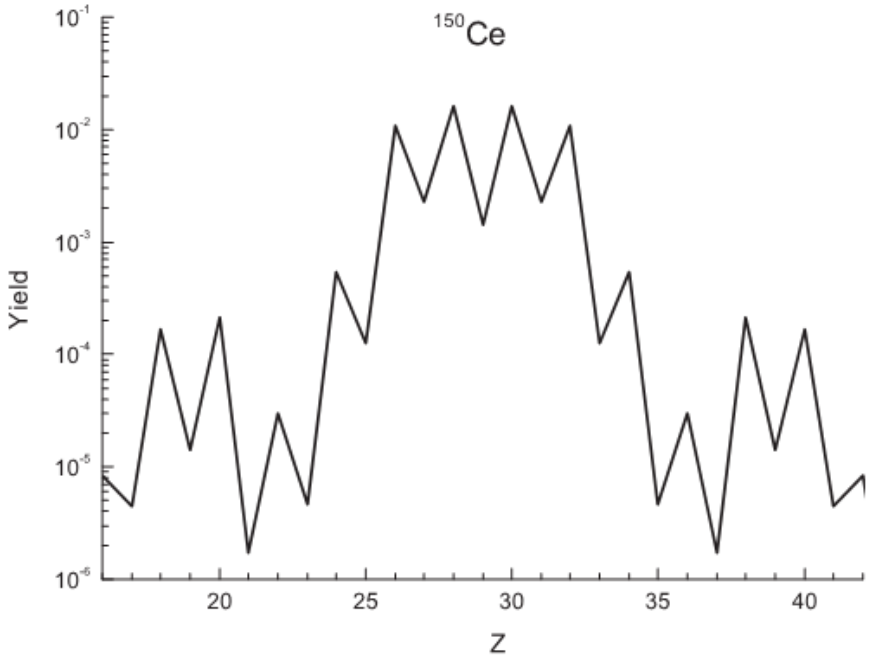

Fig. 1.8. Yields of the reaction fragments at fission for the ^{150}Ce

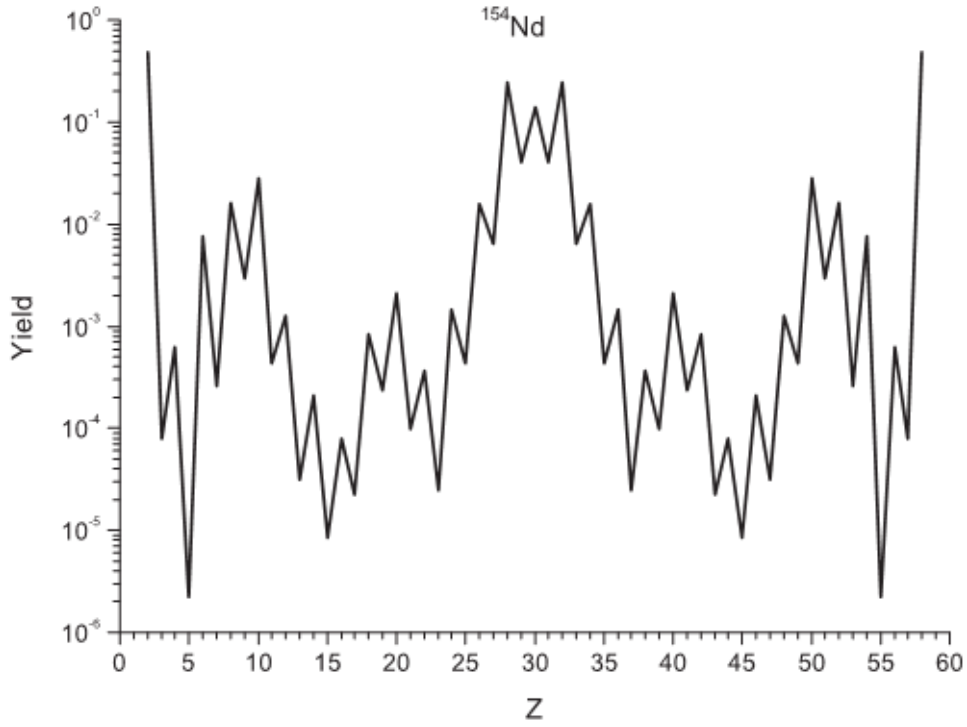

Fig. 1.9. Yields of the reaction fragments at fission for the ^{154}Nd.

In table 1.2 we presented the main CCT channels leading to formation and yield of the products with the relatively larger probabilities in the first- and sequential-fission processes of the excited compound nucleus $^{236}U^{*}$. As it can be seen from Fig. 1.6, the probabilities of the yield of Ba, Ce, Nd in the fission of $^{236}U^{*}$ are comparable. But the largest values of the formation and yield of the CCT products in the sequential fission of these heavy fragments are different: Y(^{144}Ba)=10^{-4}–10^{-3} in the fission of Ba, Y(^{150}Ce)=10^{-2}–10^{-1} in the fission of Ce and Y(^{154}Nd)=0.1–1 in the fission of Nd. It means that the formation of the intermediate nuclei Nd and Ce and the case of their sequential fission can be considered as more likely the second stage of the ternary sequential fission to interpret the observed yield of the Ni, Ge and Se isotopes (see Fig. 1.4).

Table 1.2. The calculated realization probabilities of the different sequential channels for the collinear cluster tripartition of $^{236}U^{*}$.

Fission channel $^{236}U^{*}\rightarrow f_1+f_2$	Fission channel of primary heavy fragment	Probability of CCT
$^{82}Ge+^{154}Nd^{*}$	$^{154}Nd^{*}\rightarrow^{72}Ni+^{82}Ge^{*}$ $^{154}Nd^{*}\rightarrow^{76}Zn^{*}+^{78}Zn^{*}$	$3\cdot10^{-4}$ $1.5\cdot10^{-4}$
$^{82}Se^{*}+^{154}Ce^{*}$	$^{154}Ce^{*}\rightarrow^{68}Fe^{*}+^{86}Ge^{*}$ $^{154}Ce^{*}\rightarrow^{72}Ni^{*}+^{82}Zn^{*}$	$1.0\cdot10^{-5}$ $1.4\cdot10^{-5}$

The number of emitted neutrons from the excited fission fragments was calculated as in Ref. [41]:

$$v_i = \frac{E_i^*}{B_i^{(n)} + 2T_i}, \tag{1.6}$$

where $B_i^{(n)}$ is the separation energy of the neutron from the fragment i and T_i is its temperature. In Figs. 1.9 and 1.10, the yields of reaction products for the fission of ^{154}Nd and the corresponding driving potential are presented, respectively. Assuming the distribution of the excitation energy between those fragments is proportional to their masses we calculate the number of the evaporated neutrons after decay of DNS by formula (1.6). The excitation energy of the nascent system consisting of the excited $^{82}Ge^{*}$ and $^{154}Nd^{*}$ fragments is 38.8 MeV (the origination of this energy we discuss in the next section 1.5). The neutron separation energy from ^{82}Ge and ^{81}Ge isotopes is equal to 7.39 and 4.93 MeV, respectively. The results of the calculations show that $^{82}Ge^{*}$ and $^{154}Nd^{*}$ can emit one or two neutrons each of them. After emission of two neutrons the isotope ^{80}Ge becomes the first product of CCT and it should be registered by one of detectors.

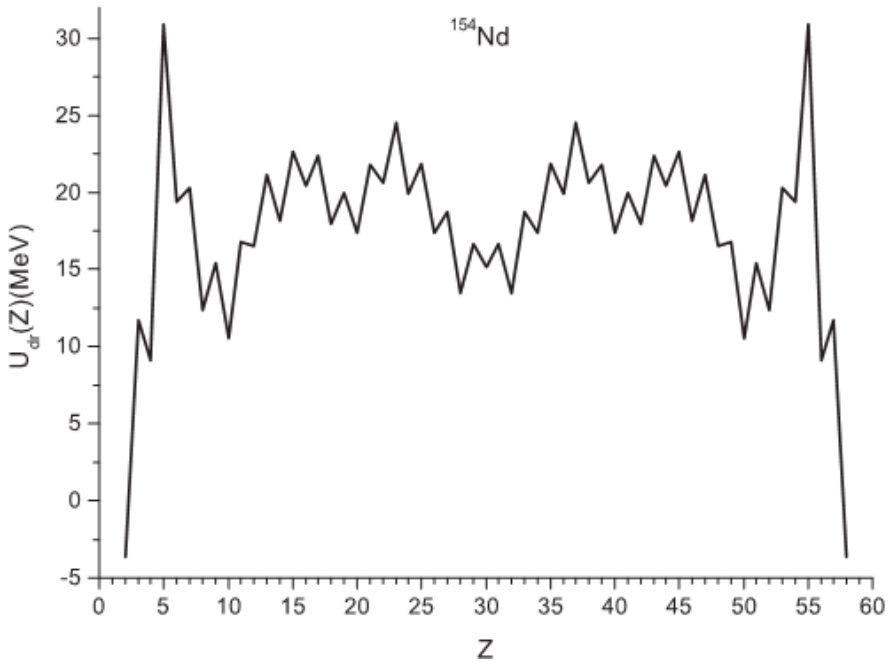

Fig. 1.10. Driving potential used to calculate the yields of the fission fragments of ^{154}Nd.

The fission of ^{154}Nd* competes with the emission of two neutrons. In the second stage of ternary fission, due to the excitation energy 25.3 MeV the nucleus ^{154}Nd* fissions into two fragments ^{72}Ni* and ^{82}Ge*. The maxima of the charge and mass distribution of the second-stage fission products lie at these reaction products. Two neutrons are emitted from the ^{72}Ni nucleus: the two neutrons separation energy is equal to 10.93 MeV. A similar energy for the two-neutron emission from the ^{82}Ge nucleus is larger, namely 12.25 MeV because ^{82}Ge is a double magic nucleus. The probability that the excited ^{72}Ni nucleus emits two neutrons is larger than the probability that one ^{82}Ge nucleus emits two neutrons. Therefore, we can state that the main channel of CCT of ^{236}U* is ^{80}Ge+^{70}Ni+^{82}Ge+4n. The events corresponding to the yield of ^{80}Ge and products formed in the fission of the primary product ^{154}Nd are shown by diamonds in Fig. 1.4: the first product ^{80}Ge (M_1=80) is registered in coincidence with ^{70}Ni (M_2=70) or ^{82}Ge (M_1=82).

The probability of the ternary fission into this channel having the strong possibility to be realized is $1.06\cdot10^{-3}\times2.46\cdot10^{-1}\approx 3\cdot10^{-4}$. The relative probability of

CCT to binary fission presented in Ref. [17] is approximately 10^{-3} that is in good agreement with our theoretical results. These results are comparable with the yields of the very asymmetric fission fragments with mass numbers A=70–75 which were observed in the ^{236}U(n,f) reaction (E_n=1 MeV) by Goverdovski et al. [42] but the authors of the mentioned paper did not consider the possibility of those fission fragments as CCT products.

The yields of the CCT product ^{80}Ge and the ^{76,78}Zn isotopes formed in the charge symmetric fragmentation ^{154}Nd→^{76}Zn*+^{78}Zn* channel are also shown in Fig. 1.4 by diamonds. The realization probability of this channel is smaller than the one of the ^{72}Ni*+^{82}Ge* channel as can be seen from the comparison of the yields in the fission of ^{154}Nd* presented in Fig. 1.9. The probability of the ternary fission of ^{236}U* by the ^{80}Ge+^{76}Zn +^{76}Zn+4n channel is $\approx 1.5\times 10^{-4}$. But the experimental data presented in Fig. 1.4 and in Ref. [17] show the yield of products formed in this CCT channel too.

The yield of the CCT products with masses *M*=84 a.m.u. is explained by the analysis of the asymmetric fission channel ^{236}U*→^{86}Se*+^{150}Ce*. It can be seen, from a comparison of Figs. 1.7 and 1.8, that the yield probabilities of the ^{68}Fe*+^{82}Ge* or ^{72}Ni*+^{78}Zn* products at decay of the excited primary product ^{150}Ce* are one order of magnitude less than the ones in the fission of the primary product ^{154}Nd*. The relative probabilities of CCT ^{84}Se+^{66}Fe+^{82}Ge+4n and ^{84}Se+^{72}Ni+^{76}Zn+4n channels to binary fission are equal to 10^{-5} and $1.4\cdot 10^{-5}$, respectively. We can conclude that the formation and yield of the ^{80}Ge and ^{70}Ni isotopes occur in both the considered CCT channels due to the magic neutron number *N*=50 (in ^{80}Ge) and proton number *Z*=28 (^{70}Ni).

It can be seen, from Fig. 1.4, that the theoretical results corresponding to yields of the ^{80}Ge and ^{84}Se isotopes as the first CCT products in the ^{82}Ge*+^{154}Nd* and ^{86}Se*+^{150}Ce* primary fission channels form two arms of the rectangles presented by diamonds and rectangles, respectively. The yield of ^{66}Fe, ^{70}Ni, ^{76}Zn and ^{82}Ge are accompanied by the first CCT products. Some events in the experimental data of the

mass distributions of the CCT products registered in coincidence and presented in Ref. [17] are close to the theoretical results in the mass region populated by products of the considered CCT channels in this work. We should note that the experimental data of the mass distribution of the two CCT products in Fig. 1.4 were selected by the authors of Ref. [17] with the definite conditions mentioned above in the beginning of this section.

The theoretical results obtained in this work for the CCT by the primary fission $^{72}Ni^{*}+^{164}Gd^{*}$ and $^{92}Kr^{*}+^{144}Ba^{*}$ channels have showed very small (10^{-7}) probabilities of the yield of the ^{70}Ni and ^{142}Ba isotopes in the sequential fission process. This situation induces us to conclude that ^{70}Ni and ^{142}Ba isotopes are mainly formed in the CCT mechanism with the simultaneous (not sequential) fission of $^{236}U^{*}$.

The agreement of our theoretical results of the yield of ^{80}Ge and ^{84}Se isotopes as the first CCT products and products ^{70}Ni, $^{74,76}Zn$ and ^{82}Ge of the sequential fission of the first heavy fragments with the corresponding experimental data of the mass distribution measured in coincidence by two collinear detectors allows us to conclude that these events can be associated with the sequential two-stage mechanism of CCT which is shown in Fig. 1.2.

1.5. Total kinetic energy of fission products.

Total kinetic energy of fission products is the sum of their energies related with acceleration of them by the Coulomb repulsive forces and gained at descent from the saddle point before scission point. The sources of these energies are the intrinsic binding energy of the fissioning nucleus and neutron energy E^{*}_{CN} brought at capture. During the whole process, the energy conservation rule must be fulfilled. The energy balance equation of the fission induced by the neutron capture can be written as follows

$$E^{*}_{\mathrm{CN}} + B_{\mathrm{CN}} = B_1 + B_2 + E^{*}_1 + E^{*}_2 + V_{int}(Z, A, R) + K_1 + K_2, \qquad (1.7)$$

where E_i^* and K_i (i = 1, 2) are the excitation energies and kinetic energies of the constituents of the DNS.

The total kinetic energy (*TKE*) and excitation energy of the dinuclear system are determined by the sum of the corresponding energies of the fragments $K_1 + K_2 = TKE$. The total kinetic energy of the fragments is restricted by the value which is found from the total-energy conservation law:

$$TKE(Z, A, R) = E_{\mathrm{CN}}^* - Q_{gg}(Z, A) - V_{int}(Z, A, R) - E_1^* - E_2^*, \tag{1.8}$$

at large values of R without interaction, i.e. $V_{int}(R \to \infty) \to 0$, we get

$$TKE(Z, A, R \to \infty) = E_{\mathrm{CN}}^* - Q_{gg}(Z, A) - E_1^*(Z, A) - E_2^*(Z, A). \tag{1.9}$$

E_{CN}^* is the excitation energy of the compound nucleus. The value of *TKE*, which includes kinetic energy of the relative motion and surface vibrational energies of the nuclei, depends on the value of $E_1^* + E_2^*$. One can say that the fixed intrinsic energy $E_{\mathrm{CN}}^* - Q_{gg}$ is distributed between *TKE* and $E_1^* + E_2^*$. The latter energy may be spent for emission of nucleons from the system and for its deformation.

For the initial stage, when ^{236}U is formed by the capture of a neutron by ^{235}U, the excitation energy of the compound nucleus is determined from the energy balance of the reaction:

$$E_{\mathrm{CN}}^*\left(^{236}\mathrm{U}\right) = E_{n_{th}} + Q_{gg} = E_{n_{th}} + B_1(n) + B_2\left(^{235}\mathrm{U}\right) - B_{\mathrm{CN}}\left(^{236}\mathrm{U}\right) = 6.5\ \mathrm{MeV}.$$

As we discussed above, in the first fission stage of ^{236}U*, two excited fragments are formed: ^{154}Nd* and ^{82}Ge*. The excitation energy of ^{154}Nd* is calculated from the assumption of a full thermodynamic equilibrium between the formed two fragments $E_{\mathrm{CN}}^*\left(^{154}\mathrm{Nd}\right) = \frac{A_{\mathrm{Nd}}}{A_{\mathrm{U}}}\left(U_{dr}(BG) - U_{dr}(Z = 60)\right) = 25.3$ MeV, where $U_{dr}(BG)$ is the driving potential at the Businaro-Gallone point of ^{236}U which is equal to 12.3 MeV; $U_{dr}(Z = 60) = -26.5$ MeV is the value of the driving potential for Z = 60 (see Fig. 1.4). We did not calculate the fission probability for ^{154}Nd* but its excitation energy is

enough for fission of $^{154}Nd^{*}$. The charge and mass distributions of its fission fragments are determined by the driving potential presented in Fig. 1.10.

As shown in Table 1.1, the total kinetic energy of the fragments at the first stage of CCT *TKE* (^{82}Ge + ^{154}Nd) is 159.83 MeV, so the total kinetic energy for the second stage *TKE* (^{72}Ni+^{82}Ge)=72.9 MeV can be found.

The driving potential of the $^{235}U(n_{th},f)$ reaction has minima corresponding to the magic numbers of the protons or neutrons equal to 2, 8, 20, 28, 50, 82, but the decay probability depends on the splitting barrier height $B_{DNS}(Z)$ as a function of the charge number. From this dependence it is clearly seen that the reaction products Ni, Sn and Ge are clusters.

1.6. Conclusion.

The sequential fission mechanism of the ternary fission of a heavy atomic nucleus has been considered within the framework of the DNS model. Herewith, first the mother nucleus decays into two non-alike fragments (asymmetrical fission mode). Then the heavy product decays into two fragments. The axes of both fission events are in coincidence according to the momentum-conservation rule if we assume that the averaged initial angular momentum of the compound nucleus $^{236}U^{*}$ generated by thermal neutrons is very small. The purposes of this chapter are an estimation of the values of charge and mass numbers of the ternary fission products, which are formed with large probabilities, and a comparison of the theoretical results of this work with the experimental data of the charge and mass distributions of the CCT products registered in coincidence by two detectors [17] placed on the opposite sides of the target. For the estimation of these values we calculated the driving potential and yields of fragments of fissionable nuclei. The total potential energy is introduced as the sum of the balance energy of the reaction (Q_{gg} value) and the nuclear interaction potential of the DNS constituents. The use of real binding energies of nuclei, taken

from Ref. [32] allows us directly to take into account the shell (quantum) effects in atomic nuclei. Due to the shell effects, there is the possibility of formation of clusters having charge or neutron numbers near the magic numbers 28, 50, 82 in the binary and ternary fission of nuclei. The DNS model allows taking into account the shell effects in the calculation of the potential energy surface of the fissioning system. The present method has been applied for the description of the yields of the products of the ternary fission of $^{236}U^*$ in reactions $^{235}U(n_{th},f)$. As the first primary channel of the sequential ternary fission we took the $^{82}Ge^*+^{154}Nd^*$ and $^{86}Se^*+^{150}Ce^*$ channels. After scission the excited nuclei $^{82}Ge^*$ and $^{86}Se^*$ can evaporate two neutrons and they can be registered as the first fission fragment of the former and latter channels, respectively. At the same time, there are two sequential fission channels for each of the heavy fragments $^{154}Nd^*$ and $^{150}Ce^*$ of the two primary fission channels of $^{236}U^*$ having the relatively large realization probabilities: $^{154}Nd^*\rightarrow^{72}Ni^*+^{82}Ge^*$ and $^{154}Nd^*\rightarrow^{76}Zn^*+^{78}Zn^*$; $^{150}Ce^*\rightarrow^{68}Fe^*+^{82}Ge^*$ and $^{150}Ce^*\rightarrow^{72}Ni^*+^{78}Zn^*$ channels. The neutrons emission from the primary fragments $^{72}Ni^*$, $^{76,78}Zn^*$, $^{82}Ge^*$ and $^{86}Se^*$ leads to the formation of the CCT products ^{70}Ni, $^{74,76}Zn$, ^{80}Ge and ^{84}Se which can be observed in coincidence with corresponding partner nucleus.

The yield probabilities of the $^{68}Fe^*+^{82}Ge^*$ or $^{72}Ni^*+^{78}Zn^*$ products in fission of the excited primary product $^{150}Ce^*$ are one order of magnitude less than the ones in the fission of the primary product $^{154}Nd^*$. The production of probability of ^{70}Ni in the CCT channel $^{72}Ni^*+^{82}Ge^*$ relative to the binary fission is large and it is equal to 3×10^{-4}, while this quantity is smaller for its formation in the $^{72}Ni^*+^{76}Zn^*$ channel, 1.4×10^{-5}. These results explain the observed yields of the ternary fission products Ni and Ge in coincidence with the Ge and Se isotopes in Ref. [17]. The relative probability of these events to binary fission is approximately 10^{-4} which is close to the results of the estimations presented in Ref. [17].

The agreement of our theoretical results of the yield of ^{80}Ge and ^{84}Se isotopes as the first CCT products and products ^{70}Ni, $^{74,76}Zn$ and ^{82}Ge of the sequential fission

of the first heavy fragments with some of the corresponding experimental data of the mass distribution measured in coincidence with two detectors allows us to conclude that these events can be associated with the sequential two stage mechanism of CCT.

The investigated mechanism of CCT – sequential binary fission gives products with masses not more than ~84 a.m.u. (or charge number ~34), but in experiment Sn-like masses ($A \approx 132$) were also detected (see Fig. 1.4). This reason motivates to consider the ternary fission in different ways. So, another mechanism of ternary fission will be discussed in the next chapter.

Sequential mechanism of the collinear cluster tripartition in the $^{235}U(n_{th},f)$ reaction partially has been studied in the frame of the program "Leonhard-Euler Program DAAD" (supported by the German Academic Exchange Service).

CHAPTER II. ALMOST SEQUENTIAL MECHANISM OF TRUE TERNARY FISSION

2.1. Introduction

Recently experimental group called FOBOS (in Flerov Laboratory of Nuclear Reactions of the Joint Institute for Nuclear Research, Dubna, Russia) has developed a new type ternary fission – collinear cluster tripartition [14-21]. The difference between this type of ternary fission and the conventional ternary one is that in collinear cluster tripartition (CCT) fission products (mainly clusters) fly almost in one line and their masses are nearly the same. Nowadays, the fission of a compound nucleus into three almost the same (in mass) fragments is called “true ternary fission”. The term “true” is used to distinguish this mechanism from the ternary fission with emission of light nuclei (mass number is around 34) in perpendicular direction to the fission axis. Authors of the experimental works [14-21] mainly used the missing-mass method. It means that they measure masses of two fragments in detectors (angle between detectors is around 180^0), while the mass of the third (middle) fragment can be estimated by conservation law of total mass during a reaction. This dissertation is dedicated to the theoretically investigation mechanisms of CCT.

Besides, there many various works in which the CCT mode of ternary fission is studied theoretically [22-24,43-46] in different aspects. For example, authors of the Ref. [22] developed the three-cluster model basing on preformed cluster model. Total interaction potential and yield of fission products were calculated as a sum of the interaction between 3 fragments, but separation (or relative) distances between the surfaces of three nuclei were reduced from two into one variable. As a result one fission barrier is used as a function of this variable for all three nuclei. In reality, three fission barriers should be used since there are three necks. Authors of Ref. [22] considered the mechanism of ternary fission when separation distance was changed

equivalently. But they did not notice about this physical phenomenon. Also it had not discussed that can be fragments separated such this way or not, and how does it explain experimental results. This kind of lack of the theory was repeated in later publications [23,24]. But in another paper [43], the authors considered ternary fission process as sequential mechanism, and mainly calculated kinetic energies of fragments. Also, in Refs. [44-46] collinear and triangular configurations of the pre-scission system (when three nuclei are connected) were compared by calculating the total interaction potential. The difference between such theoretical model and our one is that we try to distinguish mechanism of ternary fission, and to know reason which leads to collinearity of fission process.

In this chapter of the dissertation ternary fission process is considered in almost sequential mechanism: it is “almost” because intermediate time between ruptures of two necks (as three nuclei are placed in one line) is too small. This second chapter is based on the published paper by us [47].

Due to the small probability and unexpected collinearity of the momenta of the tripartition products, there are only a few experimental measurements of CCT, as given in Refs. [14-21]. Moreover, theoretical studies on ternary fission are very limited and some early works on this topic can be found, for example, in Refs. [48-51]. In these works, it was found that the ternary fission process in heavy nuclei occurs preferably in a collinear geometry, which was confirmed by the recent theoretical studies in Refs. [24,43,12]. In Ref. [24], the authors studied the difference between equatorial configurations and collinear configurations in ternary fission by calculating the potential energies for geometries of three fragments touching each other, i.e., a trinuclear system (TNS), where only the mass number of the central nucleus changes. On the other hand, the kinetic energies of the CCT products were evaluated in Ref. [43] to find that, in most cases, the velocity of the central fragment can be very small. This may be responsible for missing the third product in the experiments of Refs. [14-21]. In previous chapter (also Ref. [12]) the CCT process

has been considered as two sequential binary fissions. Namely, in the first stage, the excited compound nucleus decays into two fragments in an asymmetric channel, then the heavier fragment decays further into two fragments. Thus, three fragments are obtained with comparable masses. In that chapter only the yield of ternary fission fragments with comparable masses has been obtained and that is in agreement with the results observed in the experiments performed by the FOBOS group [17]. The theoretical results of the yield of ^{80}Ge and ^{84}Se isotopes as the first step for the CCT products and the products ^{70}Ni, ^{74,76}Zn, and ^{82}Ge in the second step in a sequential fission process are in good agreement with some of the corresponding experimental data on the mass distributions of the ^{252}Cf decay. This observation leads to the conclusion that these events can be associated with the sequential two step mechanism of CCT. However, the yields of ^{70}Ni, ^{82}Ge, and ^{84}Se in coincidence with ternary fission masses A=130-150 observed in Ref. [20] with a large probability were not completely explained in previous chapter.

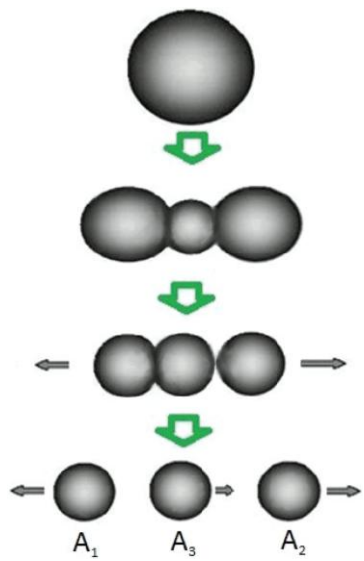

Fig. 2.1. The CCT fission mechanism of a heavy nucleus in a sequential decay [12]. A_1, A_2, and A_3 are mass numbers of the fragments formed in the trinuclear system.

Therefore, in the present chapter we consider the mechanism of a sequential ternary fission with a very short time between the ruptures of the two necks

connecting the middle cluster of the collinear TNS with its outer fragments. This mechanism is the almost simultaneous ternary fission, as illustrated in Fig. 2.1. The main goal of this chapter is to pursue the theoretical analysis of the ternary fission channels leading to the formation of the products of mass number A=132-140.

The collinear configuration of the TNS undergoing fission is defined as follows: First, the three fragments are situated on *one line* due to minimal value of the total energy of TNS. The border nuclei are numbered “1” and “2”, while the middle nucleus is labeled as “3”, as shown in Fig. 2.2. Consequently, there is no nuclear interaction between the outer fragments 1 and 2. However, the Coulomb interaction between them is taken into account because of its long-range property. In fact, it was found to have a nontrivial role in the decay of TNSs. The pre-scission barrier between fragments 1 and 3 decreases due to the Coulomb field of the fragment 2. For example, in the case of the sequential ternary fission of ^{236}U, when ^{132}Sn is formed as a fragment 2, the pre-scission barrier between fragments 2 and 3 is smaller than the one between the fragments 1 and 3 [12]. Certainly, the massive fragment 2 is separated at the first step, then occurs the rupture of the second neck between fragments 1 and 3. We will discuss the probability of the rupture at the second neck between 1 and 3, which decreases with increasing the distance R_{32} that induces the decrease of the Coulomb field of the massive fragment 2. The definitions of the variables of TNS used in this analysis are illustrated in Fig. 2.2.

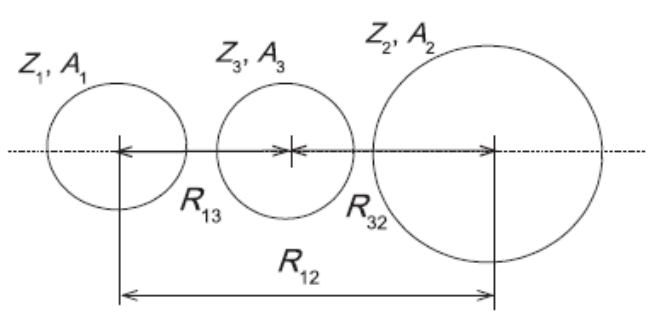

Fig. 2.2. The variables of the trinuclear system used in the analysis of the interaction energy between its fragments. Here, Z_i is the charge number of fragment i (i = 1,2,3) and R_{ij} is the distance between the mass centers of fragments i and j.

2.2. Theoretical approach: from a dinuclear system to a trinuclear system.

In order to explore the mechanisms of the CCT process, we apply the theoretical framework of the dinuclear system model [25-28]. In the present chapter, we estimate the total energy of the interacting system by calculating the sum of the binding energies of its constituents and the interaction potential energy between them. The minima of the potential-energy surfaces (PESs) are found by the variation of the charge and mass numbers of two fragments out of the three fragments and the distances between them. The PES is the two-dimensional driving potential which depends on the charge numbers of two fragments of the collinear TNS. The distances R_{13} and R_{32} between centers of mass of fragments are found from the minimum value of the nucleus-nucleus interaction.

The fission process is considered as a formation of the elongated mononucleus (for example, a superdeformed shape) which breaks down into two fragments as in the case of binary fission. The formation of the third cluster in the neck region and the splitting of this system into three fragments are related to the shape of the system such as hyperdeformation. Furthermore, the assumption of the formation of a heavier nucleus as the third fragment between the two main fission products is also introduced.

2.2.1. Total potential energy of a trinuclear system.

The study of the PES landscape is carried out to find minima and valleys, since at local minima, one can expect increased yields of the mass and charge distributions in the TNS undergoing the fission process. It should be noted that the transition from compound nucleus to the TNS configuration is not analyzed. Instead, we assume that the TNS is formed during fission of the compound nucleus into a binary system. This

process can occur in the sense of energy conservation. We refer to Ref. [51] for the hyperdeformed ^{236}U nucleus.

The PES is calculated as

$$U\left(Z_1, A_1, \beta^{(1)}, Z_2, A_2, \beta^{(2)}, Z_3, A_3, \beta^{(3)}, R_{13}, R_{32}\right) = V_{int}\left(Z_1, A_1, \beta^{(1)}, Z_2, A_2, \beta^{(2)}, Z_3, A_3, \beta^{(3)}, R_{13}, R_{32}\right) + Q_{ggg}\left(Z_1, A_1, Z_3, A_3\right), \quad (2.1)$$

where Z_i and A_i are the charge number and mass number of the ith fragment of the TNS (i=1,2,3), respectively, and R_{ij} is the distance between the mass centers of the ith and j^{th} fragments. Here, $\beta^{(i)} = \left\{\beta_2^{(i)}, \beta_3^{(i)}\right\}$ is a set of deformation parameters of fragment i, where $\beta_2^{(i)}$ and $\beta_3^{(i)}$ represent the quadrupole and octupole parts, respectively. The interaction potential V_{int} between the fragments of TNS can be written as

$$V_{int}\left(Z_1, A_1, \beta^{(1)}, Z_2, A_2, \beta^{(2)}, Z_3, A_3, \beta^{(3)}, R_{13}, R_{32}\right) = \sum_{i<j}^{3} V_{ij}\left(Z_i, A_i, \beta^{(i)}, Z_j, A_j, \beta^{(j)}, R_{ij}\right), \quad (2.2)$$

where V_{ij} is the two-body interaction potential between the nuclei "i" and "j". It contains two parts; namely, the nuclear part V_{nuc}^{ij} and the Coulomb part V_C^{ij}, so that

$$V_{ij}\left(Z_i, A_i, \beta^{(i)}, Z_j, A_j, \beta^{(j)}, R_{ij}\right) = V_{nuc}^{ij}\left(Z_i, A_i, \beta^{(i)}, Z_j, A_j, \beta^{(j)}, R_{ij}\right) + V_C^{ij}\left(Z_i, A_i, \beta^{(i)}, Z_j, A_j, \beta^{(j)}, R_{ij}\right). \quad (2.3)$$

It is clear that $V_{nuc}^{12} = 0$ since the fragments 1 and 2 are separated by the fragment 3 and, therefore, there is no overlap of their nucleon densities. The nuclear part of the nucleus-nucleus interaction V_{nuc}^{ij} is calculated by using the double folding procedure which is given in the Appendix, and the Coulomb part V_C^{ij} is estimated by the Wong expression.

In Eq. (2.1), Q_{ggg} is the reaction balance energy in ternary fission, which is written as

$$Q_{ggg}(Z_1, A_1, Z_3, A_3) = B_1(Z_1, A_1) + B_2(Z_2, A_2) + B_3(Z_3, A_3) - B_{CN}(Z_{CN}, A_{CN}). \quad (2.4)$$

The values of binding energies, B_i, for ground states are taken from Refs. [32,33]. In order to calculate the mass and charge distributions of the TNS in the pre-scission state, the minima and valleys of the PES are determined by computing the interaction potential V_{int} as a function of $(Z_1, A_1, Z_3, A_3, R_{13}, R_{32})$ since (Z_2, A_2) can be defined through (Z_1, A_1, Z_3, A_3) and $R_{12} = R_{13} + R_{32}$. This is done by taking V_{int} as a function of R_{13} and R_{32} for each configuration of $\{Z_1, A_1; Z_3, A_3; Z_2, A_2\}$ (see Fig. 2.2 for the geometry).

In order to find the dominant cluster states of the PES, the charge (and mass) numbers of the two fragments are varied in the range of $2<Z_1<Z_{CN}/2$ and $2<Z_3<Z_{CN}/2$ [$A_{1,\min}<A_1(Z_1)<A_{1,\max}$ and $A_{3,\min}<A_3(Z_3)<A_{3,\max}$]. The charge and mass numbers of the third fragment can be found from the corresponding conservation laws for them. The distances R_{13} and R_{32} between interacting nuclei are then varied to find $R_{13}^{(min)}$ and $R_{32}^{(min)}$ that correspond to the minimum values of the potential wells V_{13} and V_{32}, respectively. It should be noted again that the potentials are affected by the Coulomb interaction V_{12}^{C} of the border fragments.

This process allows us to find the mass number A_i that corresponds to the minimum value of the PES for a given value of Z_i. For example, the value of A_1 can be found by minimizing the PES for each value of A_3 at fixed values of Z_1 and Z_3. From the set of the results calculated for the PES as a function of $(Z_1, A_1, Z_3, A_3, R_{13}, R_{32})$ we can establish the driving potential demonstrating the configurations of the TNS with the well-pronounced cluster states having closed shells. The three-dimensional driving potential $U_{dr}(Z_1, A_1; Z_3, A_3)$ is determined by the values of the PES in Eq. (2.1) corresponding to the minimum values of the potential wells in the nucleus-nucleus interaction V_{int} between neighbor fragments as a function of the distances between their centers of mass:

$$U_{dr}\left(Z_1, A_1, \beta^{(1)}, \beta^{(2)}, Z_3, A_3, \beta^{(3)}\right) = U\left(Z_1, A_1, \beta^{(1)}, \beta^{(2)}, Z_3, A_3, \beta^{(3)}, R_{13}^{(min)}, R_{32}^{(min)}\right) \quad (2.5)$$

A change of A_i leads to the change of Q_{ggg} which depends on the binding energies B_i. As a result, U_{dr} is sensitive to the mass distribution between the TNS fragments.

2.2.2. Probability of the yield of ternary fission fragments.

The mass and charge distributions of the TNS fragments are related to the driving potential U_{dr}. Therefore, the knowledge of U_{dr} allows us to calculate the yield of the products of ternary fission as in previous chapter:

$$Y(Z_1, A_1; Z_3, A_3) = P(Z_1, A_1; Z_3, A_3) W_{13}(Z_1, A_1; Z_3, A_3) W_{32}(Z_2, A_2; Z_3, A_3) \quad (2.6)$$

where $Y(Z_1, A_1; Z_3, A_3)$ is the probability of the charge and mass distributions of the TNS fragments. The probability of the formation of a TNS, $P(Z_1, A_1; Z_3, A_3)$, can be found from the condition of statistical equilibrium as in Ref. [16], i.e. the TNS has an equilibrium state before scission:

$$P(Z_1, A_1; Z_3, A_3) = P_0 \exp\left[-\frac{U_{dr}(Z_1, A_1; Z_3, A_3)}{T_{TNS}(Z_1, A_1; Z_3, A_3)}\right], \quad (2.7)$$

where T_{TNS} is the effective temperature of the TNS and $U_{dr}(Z_1, A_1; Z_3, A_3)$ is determined by the formula (2.5). The normalization coefficient for the yield probability is represented by P_0.

In Eq. (2.6), W_{13} and W_{32} are the decay probabilities of the TNS that are caused by overcoming the pre-scission barriers B_{13} and B_{32} which correspond to the separation of the first and second nuclei, respectively. Their explicit expressions are given in the first chapter

$$W_{13}(Z_1, A_1; Z_3, A_3) = W_{13}^0 \exp\left[-\frac{B_{13}}{T_{13}}\right], \quad (2.8)$$

$$W_{32}(Z_2, A_2; Z_3, A_3) = W_{32}^0 \exp\left[-\frac{B_{32}}{T_{32}}\right], \tag{2.9}$$

where (B_{13},B_{32}) and (T_{13},T_{32}) are the pre-scission barriers and the effective temperatures on these barriers of the corresponding parts of the TNS. The barriers B_{13} and B_{32} prevent the separation of the outer fragments from the middle one. These pre-scission barriers are defined by the depth of the nucleus-nucleus potential well between neighbor fragments of the TNS. Here, W_{13}^0 and W_{32}^0 are normalization coefficients for the corresponding probability distributions.

The effective temperatures are determined by the excitation energy of the TNS which is generated by the descent of the system from the saddle point in binary fission. We assume that the third cluster is formed between the two parts of fissioning nuclei before their splitting. In this case, $E_{TNS}^*(Z_1, A_1, Z_3, A_3)$, the excitation energy of the system, is determined by the difference between the values at the saddle point and at the point of the minimum driving potential with the considered charge and mass numbers of clusters:

$$E_{TNS}^*(Z_1, A_1, Z_3, A_3) = E_{CN}^* - U_{dr}(Z_1, A_1; Z_3, A_3). \tag{2.10}$$

The effective temperatures of the TNS, necks 1-3 and 2-3 are defined by the excitation energies on the minimum of the driving potential and pre-scission barriers B_{13} and B_{32}, respectively:

$$T_{TNS} = \sqrt{\frac{12E_{TNS}^*}{A_{CN}}},$$

$$T_{13} = \sqrt{\frac{12E_{13}^*}{(A_1 + A_3)}}, \tag{2.11}$$

$$T_{32} = \sqrt{\frac{12E_{32}^*}{(A_2 + A_3)}},$$

where E_{13}^* and E_{32}^* are the excitation energies on the top of the pre-scission barrier of DNS 1-3 and 2-3, respectively; the level density parameter is taken as a=A/12. These

excitation energies are the result of sharing the TNS excitation energy between different degrees of freedom. The parts of E^*_{TNS} corresponding to the decay axes R_{13} and R_{32} are estimated by assuming that their inertial masses are $A_{13} = A_1(A_2 + A_3)/A_{CN}$ and $A_{32} = A_2(A_1 + A_3)/A_{CN}$, respectively. Then the values of E^*_{13} and E^*_{32} are found from the effective temperature of the TNS:

$$E^*_{13}(Z_1, A_1, Z_3, A_3) = \frac{T^2_{TNS} A_{13}}{12} - B_{13}, \tag{2.12}$$

$$E^*_{32}(Z_1, A_1, Z_3, A_3) = \frac{T^2_{TNS} A_{32}}{12} - B_{32}, \tag{2.13}$$

If the residual part of the TNS excitation energy, $E^*_{res} = E^*_{TNS} - E^*_{13} - E^*_{32}$, is larger than the energy B_n for the emission of neutrons from the TNS fragments, the ternary fission is accompanied by neutrons.

2.3. Investigation of tripartition at spontaneous fission of ^{252}Cf.

2.3.1. Potential energy surface showing cluster formation in trinuclear system.

In the experiment reported in Ref. [20], the ternary products were formed in the spontaneous fission of ^{252}Cf and the yields of ^{68}Ni, $^{80-82}$Ge, ^{94}Kr, ^{128,132}Sn, and ^{144}Ba were obtained. In the plot of the mass-mass distribution of two products (third one is missing) given in Fig. 10 of Ref. [20], these events were found form a rectangle. The authors of Ref. [20] assumed that the points in the right half of the rectangle likely reflect the shell effects around N=88.

The effect of the shell structure of the proton and neutron single-particle states in the formation of a trinuclear system and in its decay into the observed fission products is obviously seen in the mass-mass distribution data of Ref. [20]. This observation stimulates us to calculate the PES, i.e., $V(Z_1, Z_3, A_1, A_3, R_{13}, R_{32})$, and the driving potential $U_{dr}(Z_1, A_1, Z_3, A_3)$ for the intermediate system preceding their

formation. The products of a CCT decay should be formed before being separated from the other part of the system.

Our results for the PES are presented in Fig. 2.3. Each point in the driving potential $U_{dr}(Z_1, A_1, Z_3, A_3)$ for the TNS corresponds to a specific configuration (channel), which consists of three interacting nuclei placed in one line, as shown in Fig. 2.2. In calculating the PES, the distances between fragments are fixed at the values corresponding to the minimum values of the corresponding wells in the interaction potential between them (see Figs. 2.4 and 2.5). The quadrupole deformation parameters of the first-excited 2^+ state of nuclei [38] are used in calculation of the PES.

The rectangle "CCT" in Fig. 2.3 shows the area of the mass numbers $Z_1(A_1)$ and $Z_3(A_3)$ which corresponds to the CCT products. The rectangle "FFF" shows the area of formation of three fragments with similar mass numbers. The solid and dashed lines show the TNS configuration having ^{132}Sn and ^{134}Te, respectively, as the outer nucleus Z_2. So, we can see the valley, which is the minimal energy area (Z_2=50 and Z_2=52) and corresponds to the ^{252}Cf→f_1+f_3+^{132}Sn and ^{252}Cf→f_1+f_3+^{134}Te fission channels. The valley extends up to the area of about Z_3=28. As was mentioned earlier, Z_3 is the charge number of the middle cluster. The phase space of the configurations corresponding to the dark (blue) color region is large. Therefore, the probability of finding the TNS of configurations with a lower potential energy is larger. The configuration of Ni+Ca+Sn has large probability compared with the Ca+Ni+Sn configuration since the PES value of the latter configuration is about 12 MeV higher than that of the former configuration.

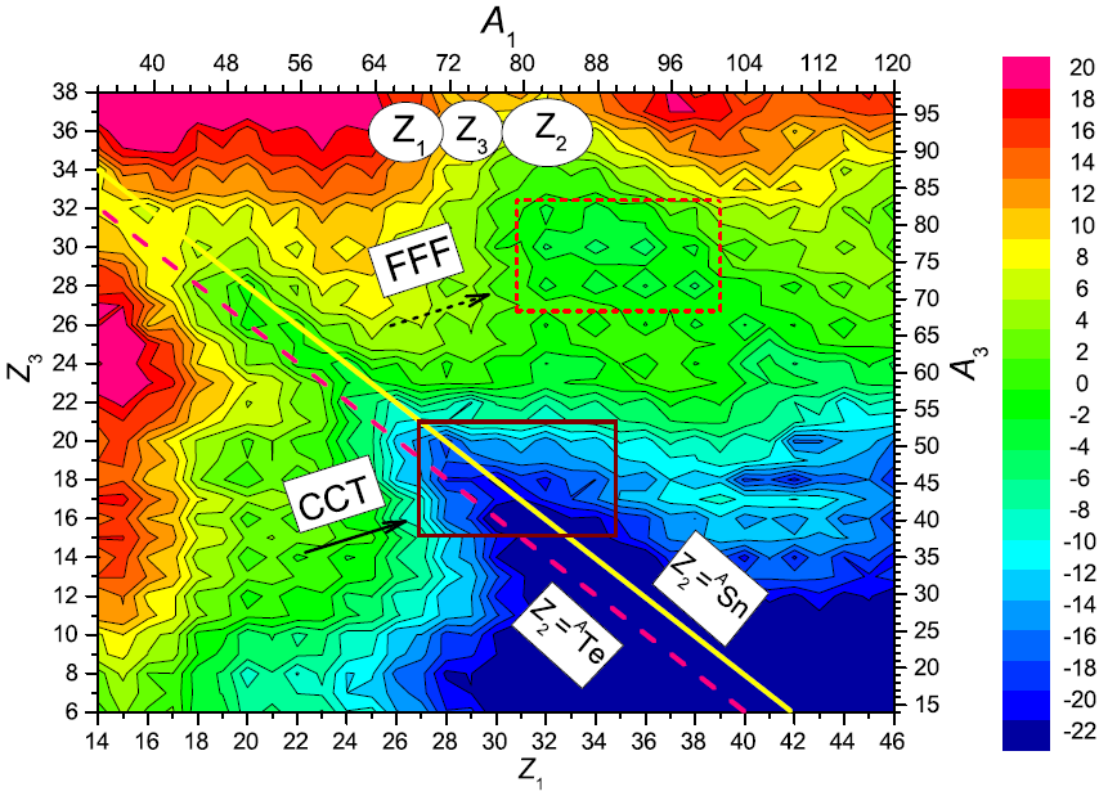

Fig. 2.3. The potential-energy surface of the ^{252}Cf (sf,fff) reaction. The wide solid rectangle "CCT" shows the area of the mass numbers $Z_1(A_1)$ and $Z_3(A_3)$ which corresponds to the CCT products. The red dashed rectangle "FFF" shows the area of formation of three fragments with similar mass numbers. The solid (yellow) and dashed (pink) lines show the TNS configurations having ^{132}Sn and ^{134}Te, respectively, as the outer nucleus Z_2.

The calculations were performed to find the yield of the CCT products from the collinear geometry based on the formula in Eq. (2.6). In these calculations, we found that the value of the pre-scission barrier plays important role. Therefore, in the next section we discuss the behavior of the barriers B_{13} and B_{32} for the CCT channel of the Ni+Ca+Sn configuration.

2.3.2. Decrease of pre-scission barrier due to Coulomb field of outer fragments.

The mechanism of almost sequential ruptures of the two necks connecting the fragments of a collinear TNS is suggested to explain the observed yields of heavy

clusters such as Ni, Ge, and Se isotopes that appear with products having a mass number of A=138-148 in the CCT of ^{252}Cf [18,20]. The PES shows the structure of valleys and local minima that correspond to the formation of heavy clusters observed in experiments as shown in Fig. 2.3. These fragments of a TNS should be emitted from the potential wells and, therefore, it is important to estimate the depths of the potential wells, since heavy clusters can exist during a definite long time. In Fig. 2.4 the potential wells calculated for the TNS of Ni+Ca+Sn, which forms a linear chain, are presented as functions of the distances between centers of the middle nucleus (Ca) and the outer nuclei (Ni and Sn). The values of these nucleus-nucleus potentials are shifted by the values of Q_{ggg} as the contour plot of the PES (see Fig. 2.3 and Eq. (2.1)) to take into account the change of the intrinsic energy of the TNS.

For the calculation of the interaction potential V_{CaSn}, the distance R_{NiCa} is fixed to the value corresponding to the minimum of V_{NiCa}, while the V_{NiCa} potential is calculated at the fixed value of R_{CaSn} that gives the minimum of V_{CaSn}. The results for the nucleus-nucleus interaction between the nuclei of the collinear TNS of Ni+Ca+Sn as a function of the independent variables $R_{13}(R_{\mathrm{NiCa}})$ and $R_{32}(R_{\mathrm{CaSn}})$ are given by a three-dimensional plot of the PES in Fig. 2.5. The contour lines of the PES presented in Fig. 2.3 are calculated at the minimum value of the nucleus-nucleus interaction, like at R_{13}=11 fm and R_{32}=12 fm shown in Fig. 2.5. The decay of the TNS occurs due to the motion of the system along R_{13} or R_{32}. The height of the pre-scission barrier is smaller in the direction along R_{32} (R_{CaSn} in Fig. 2.4) and, therefore, the massive fragment Sn is separated first from the TNS. This result is obtained using Eqs. (2.8) and (2.9). If the residual Ni+Ca part of the TNS does not decay, then the binary decay would be observed since the Ni+Ca system is considered as a superdeformed shape of ^{118}Cd.

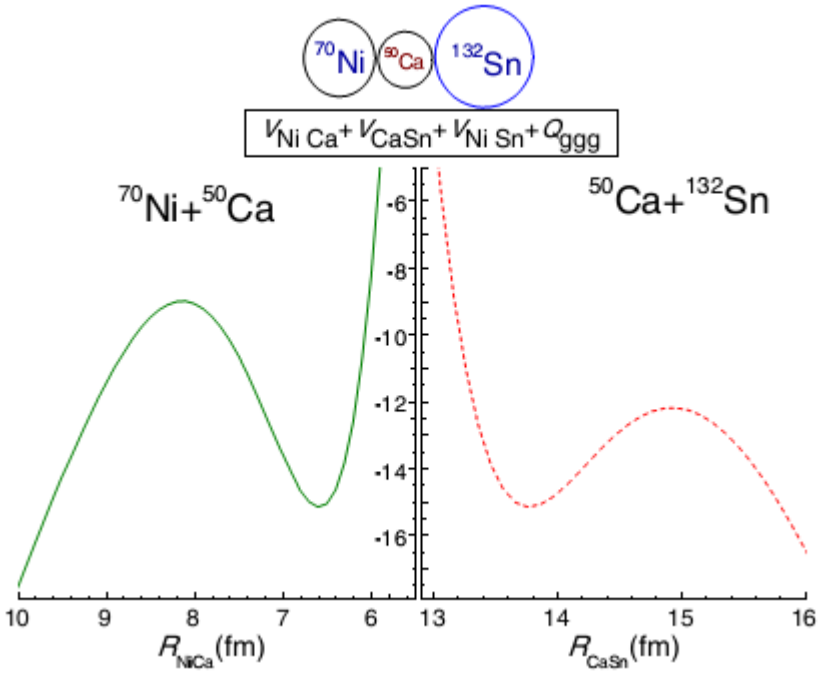

Fig. 2.4. The pre-scission barriers B_{NiCa} and B_{CaSn} keeping TNS fragments together.

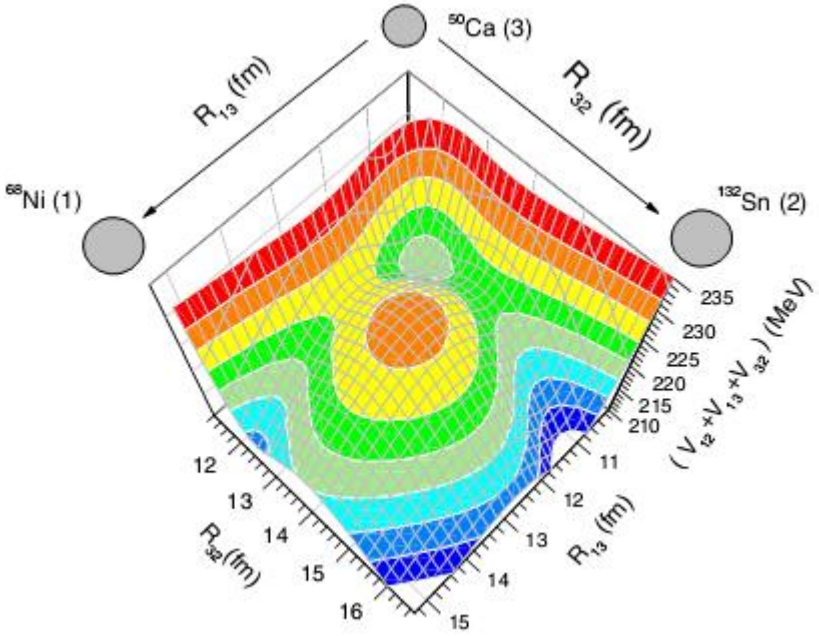

Fig. 2.5. The total nucleus-nucleus interaction potential V_{int} as a function of intercenter distances R_{13} and R_{32} between fragments of the TNS with collinear geometry.

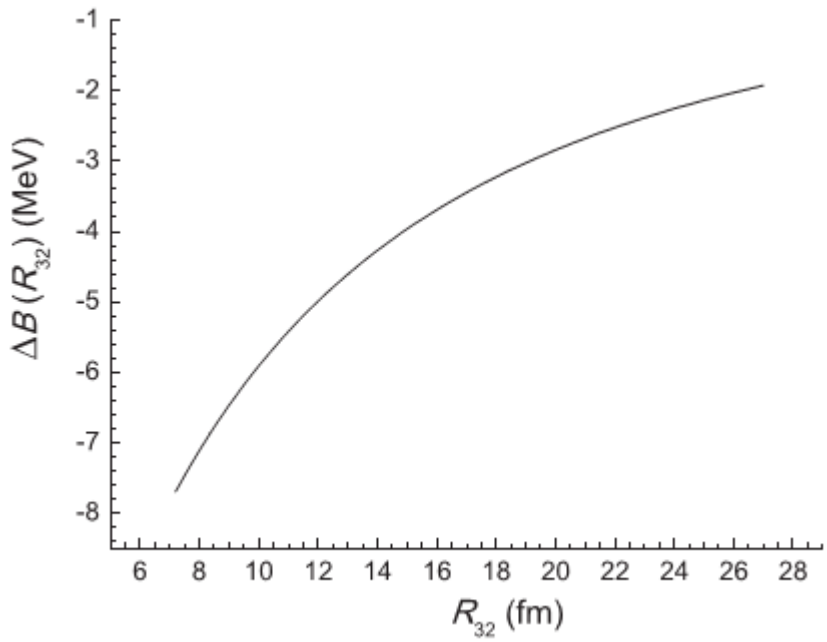

Fig. 2.6. The dependence of the change of the pre-scission barrier ΔB_{13} for the decay of the binary system Ni+Ca on the distance R_{32} due to the Coulomb interaction of the massive third fragment Sn in the collinear geometry.

The excitation energy of the residual Ni+Ca system should be large enough to its decay into Ni and Ca to observe them as CCT products. The probability of this event strongly depends on the position of the separated massive product, i.e., the Sn nucleus. The depth of the potential V_{NiSn}, which is the pre-scission barrier B_{NiSn}, changes as a function of the distance R_{32}. To show this phenomenon we estimate the change of the B_{13} barrier, which is the difference between the maximum (on the barrier) and the minimum values of V_{int} as a function of R_{13} in Eq. (2.2). As B_{13} is the Coulomb barrier, so the dependence of the change of the barrier B_{13} by the distance R_{32} can be reduced to a simple form of

$$\Delta B_{13}(R_{32}) = \frac{Z_1 Z_2 e^2}{R_{13}^{(B)} + R_{32}} - \frac{Z_1 Z_2 e^2}{R_{13}^{(min)} + R_{32}}, \tag{2.14}$$

where $e^2 = 1.44\ \mathrm{MeV} \cdot \mathrm{fm}$. The dependence of ΔB_{13} on R_{32} is presented in Fig. 2.6. The negative values mean the decrease of the depth of the potential well $[B_{13}(R_{32} \to \infty) + \Delta B_{13}(R_{32})]$ in the interaction of the Ni+Ca system. The main observation of the

present chapter is that the presence of the third fragment is important to cause the decay of the Ni+Ca system in an easier way. The presence of the third massive fragment Sn makes the pre-scission barrier shallower by 4 MeV, and thus the decay probability of the Ni+Ca system increases.

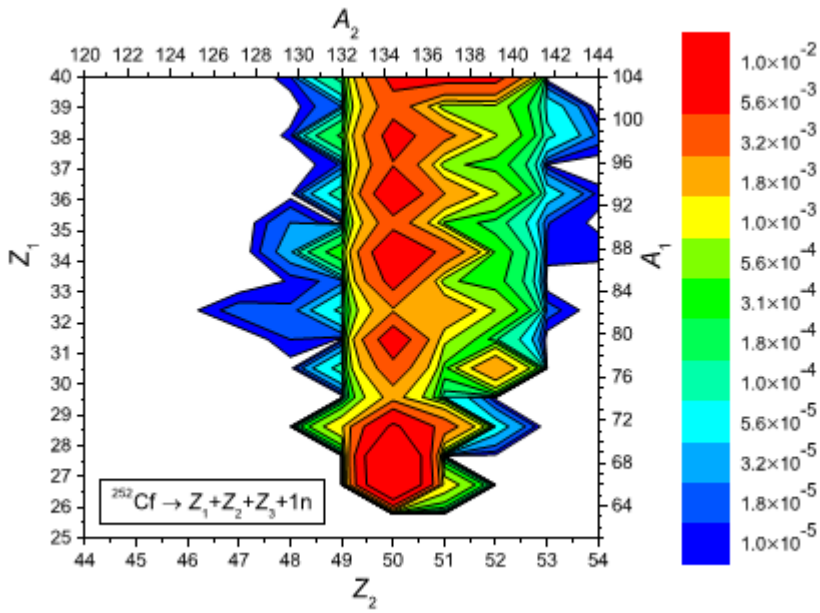

Fig. 2.7. Theoretical results for the yield of the outer fragments ${}^{A_1}Z_1$ and ${}^{A_2}Z_2$ of the TNS formed at the spontaneous fission of ^{252}Cf. The yield is high at Z_2~50.

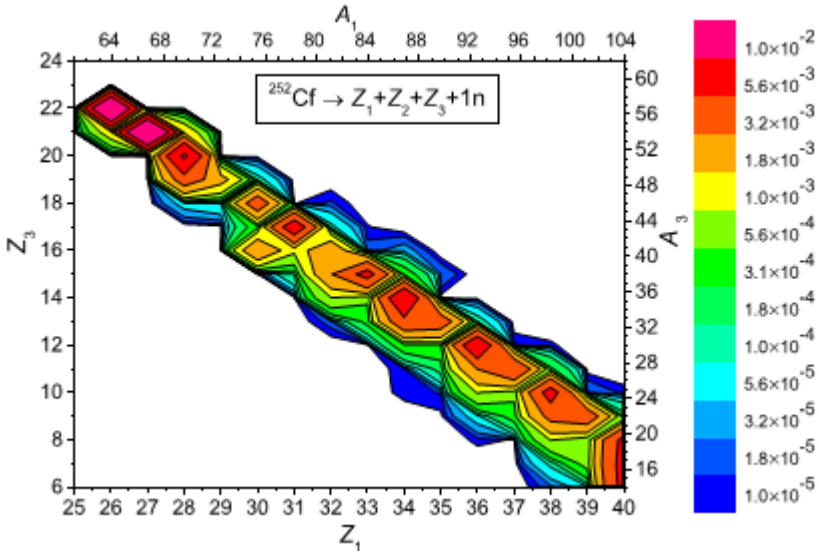

Fig. 2.8. Theoretical results for the yield of the outer ${}^{A_1}Z_1$ and middle ${}^{A_3}Z_3$ fragments of the TNS formed in the spontaneous fission of ^{252}Cf.

The reasonable results for the yields of the Ni isotopes followed by the emission of massive Sn isotopes from the formula in Eqs. (2.8) and (2.9) that includes the dependence on the pre-scission barriers B_{13} and B_{32}. The results are presented in Figs.2.7 and 2.8. In the former figure, we use $Z_1(A_1)$ and $Z_2(A_2)$ axes for the plot, while in the latter figure we use $Z_1(A_1)$ and $Z_3(A_3)$ axes.

Although the calculated yields of heavy clusters such as Ni, Ge, and Se isotopes are found to be in good agreement with the experimental data, there remains a difference between the mass numbers of the massive CCT products of ^{252}Cf observed in Refs. [18,20], namely A=138-148, which overlap with our results with A=132-140 presented in Figs. 2.7 and 2.8. The strong yield of the products with mass numbers A=132-140 indicates the important role of the magic number of neutrons at N=82. This difference may be ascribed to our use of the tabulated masses of Refs. [32,33] to obtain the binding energies of nuclei. This procedure, in fact, gives the binding energies of the ground states, but we may have deformed nuclei at the scission point, which is highly probable for massive nuclei. We should recall the procedure of calculating the PES by variation of the charge and mass numbers of the two fragments of TNS [$2<Z_1<Z_{CN}/2$ and $2<Z_3<Z_{CN}/2$, where $A_{1,min}<A_1(Z_1)<A_{1,max}$ and $A_{3,min}<A_3(Z_3)<A_{3,max}$]. The dependence of shell corrections on the deformation should be studied for most of the numerous (some thousands of) combinations. Since the primary goal of this chapter is to demonstrate the possibility of the formation of the Ni, Ge, and Se isotopes and their yields in the CCT mechanism, we leave the more accurate and sophisticated description of the production of massive isotopes of A=138-148 to future studies.

2.4. Estimate of kinetic energy of middle fragment of the trinuclear system.

The range of the kinetic energy of the middle fragment 3 can be estimated by applying the energy and momentum conservation laws. For simplicity, we assume

that the kinetic energy of the binary process is determined by the Coulomb barrier of the nucleus-nucleus interaction. The first step of the sequential collinear ternary fission is the separation of the right fragment 2 as shown in Fig. 2.1. The sum of the kinetic energies of this fragment and the residual part of the TNS is the same as the Coulomb repulsion between them, which leads to

$$\frac{Z_1 Z_2 e^2}{R_{13} + R_{23} + d} + \frac{Z_1 Z_2 e^2}{R_{23} + d} = \frac{m(A_1 + A_3)v_{13}^2}{2} + \frac{mA_2 v_2^2}{2}, \tag{2.15}$$

$$m(A_1 + A_3)v_{13} + mA_2 v_2 = 0, \tag{2.16}$$

where v_{13} and v_2 are the relative velocities of the DNS 1-3 and of the separated fragment 2, respectively, in the laboratory frame. The free parameter d is introduced to decrease the sum of the total Coulomb barriers that cannot be larger than the reaction-energy balance Q_{ggg} given in Eq. (2.4). The second step of the sequential collinear ternary fission is a decay of the DNS 1-3 into two fragments 1 and 3. The sum of their kinetic energies is then equal to the Coulomb repulsion between them so that

$$\begin{gathered} \frac{Z_1 Z_3 e^2}{R_{13}} = \frac{mA_1 v_1'^2}{2} + \frac{mA_3 v_3'^2}{2}, \\ mA_1 v_1' + mA_3 v_3' = 0, \end{gathered} \tag{2.17}$$

where v_1' and v_3' are the velocities of the fragments 1 and 3, respectively, in the moving frame with velocity v_{13} in the direction opposite to v_2. Therefore, we have

$$\begin{gathered} v_1 = v_1' + v_{13}, \\ v_3 = -v_3' + v_{13}. \end{gathered} \tag{2.18}$$

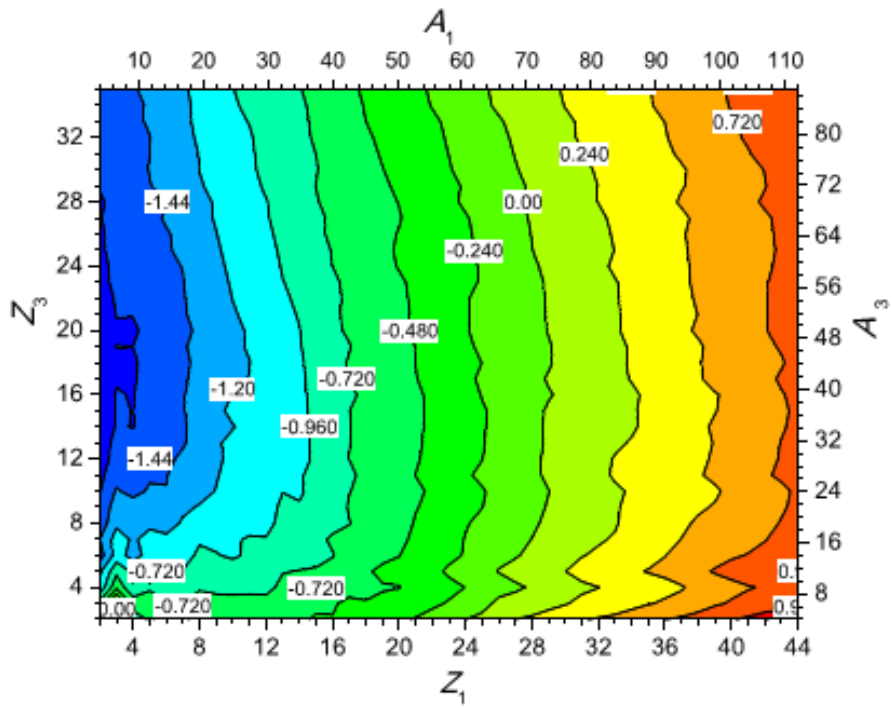

Fig. 2.9. The contour map of the calculated velocity v_3 (in cm/ns) of the middle ${}^{A_3}Z_3$ fragment of the TNS formed at the spontaneous fission of ^{252}Cf as a function of the charge and mass numbers of the outer fragments ${}^{A_1}Z_1$ and ${}^{A_2}Z_2$. The negative values of v_3 mean that its direction is opposite the direction of v_2.

We then obtain v_3 as a function of the mass numbers of the outer fragments ${}^{A_1}Z_1$ and ${}^{A_2}Z_2$ and the results are presented in Fig. 2.9. The negative values of v_3 mean that its direction is opposite to the direction of v_2. This figure also allows us to find the region of mass numbers A_1 and A_2 where the velocity of the middle cluster is large enough to be registered in experiments. One of the features in the experimental data on the collinear tripartition presented in Refs. [17,18,20] is the missing third fragment. As can be understood from this analysis, the main physical reason for this phenomenon is the smallness of the velocity of the "missing" third product.

In Fig. 2.9 one can see that the third product has a small velocity ($|v_3| < 0.25$ cm/ns) for the case of A_1=60-80 and A_3=24-64, which means that the range of mass numbers for the massive fragment is A_2=108-168. This region overlaps with the observed mass region, where a Ni-like product with a mass number of A_1=68-72 was

observed with a massive product of A_2=136-144 [17,18,20]. In the case of the symmetric masses, $A_1 \sim A_2 \sim A_3$, we have a small velocity of the middle fragment A_3; namely, we get $\upsilon_3 = 0.3 - 0.4$ cm/ns. The range of the mass numbers where the third middle fragment has an observable velocity is found to be A_1=100-120 and A_3=4-16 (i.e., A_2=116-148) which corresponds to the well-known ternary fission with emission of the light nuclei with a mass number of A_3=4-12 [53,54]. In the experiments reported in Refs. [53,54] all three ternary fission products were registered. The other range of mass numbers of the outer fragments of TNS which allows the observation of the middle fragment is A_1=104-112 and A_3=64-90 (A_2=50-84). The decay channel of A_2<100 has a very small probability to be realized since the pre-scission barrier B_{32} is sufficiently high. Our analysis on the sequential true ternary fission shows that the possibility of observing the middle fragment in this case is rather small.

2.5. Conclusion.

In present chapter, we suggested a sequential ternary fission process with a very short time between the ruptures of two necks connecting the middle cluster of the collinear trinuclear system. The necessity of this mechanism is revealed in the decrease of the pre-scission barrier of the residual part of the TNS due to the Coulomb field of the massive fragment being separated first. This mechanism leads to the probability of about 10^{-3} for the yield of massive clusters such as ^{70}Ni, $^{80\text{-}82}$Ge, ^{86}Se, and ^{94}Kr produced with a product of A=132-140 in the CCT of ^{252}Cf. The yields of such products were observed in coincidence with a massive product of A=138-148 with a relatively large probability in the experiments of the FOBOS group at the FLNR of the Joint Institute of Nuclear Research (Dubna).

To verify the realization of this mechanism, the total potential energy of the chain-like TNS was calculated as a sum of Q_{ggg} and the nucleus-nucleus interaction potential energy between its constituents. The minima and valleys of the PES related

to the shell effects in nuclei were determined by using the binding energies obtained from the well-known mass tables of Refs. [32,33] and the calculation of the interaction potential for the charge and mass numbers of the three fragments as a function of distances between their centers of mass. The distances R_{13} and R_{32} between interacting nuclei were varied to find the minimum values of the potential wells of V_{13} and V_{32}, respectively, which are affected by the Coulomb interaction V_{12}^{C} of the border fragments. The driving potential as a function of the charge and mass numbers of two fragments was obtained at the values of the distances $R_{13}^{(min)}$ and $R_{32}^{(min)}$ that correspond to the minimum values of the nucleus-nucleus interactions V_{13} and V_{32}, respectively.

In order to find the dominant cluster states of the TNS, the driving potential $U_{dr}(Z_1, A_1, Z_3, A_3)$ was calculated for the values of the charge (mass) numbers of the two fragments in the ranges of $2<Z_1<Z_{CN}/2$ and $2<Z_3<Z_{CN}/2$ [$A_{1,min}<A_1(Z_1)<A_{1,max}$ and $A_{3,min}<A_3(Z_3)<A_{3,max}$]. The analysis of the results allows us to find the mass number A_i corresponding to the minimum value of the PES for a given value of Z_i. The calculated total potential energy as a function of (Z_1, A_1, Z_3, A_3) enabled us to establish the three-dimensional driving potential that determines the configurations of TNS with probable cluster states in the pre-fission states.

Finally, the contour lines of the three-dimensional driving potential showed the structure of a valley corresponding to the formation of the outer cluster with Z_2=50 or N_2=82 at the ternary fission, which corresponds to the fission channel of $^{252}Cf \rightarrow f_1+f_3+^{132}Sn$. It was found that the valley extends up to the area of about Z_3=28 and the probability of a configuration having lower potential energy for the TNS is large. Therefore, the configuration of Ni+Ca+Sn has a large probability in comparison with the configuration of Ca+Ni+Sn since the PES value of the latter configuration is about 12 MeV higher than that of the former configuration. The dependence of the velocity of the middle cluster on the mass numbers A_1 and A_2 was also analyzed for

the case of the collinear tripartition of ^{252}Cf. The main physical reason associated with the collinear tripartition is the smallness of the missed third product. We found that the middle fragment has a very small velocity, when it is formed between fragments with the mass numbers A_1=60-80 and A_2=132-140 which agrees with the observed range of mass values presented in Refs. [17,18,20]. This means that it is indeed difficult to observe the middle product of a collinear tripartition of ^{252}Cf producing Ni with the second product having a mass number of A_2=132-140. In the case of the symmetric masses, $A_1 \sim A_2 \sim A_3$, we have a small velocity of the middle fragment A_3; namely, we get $\upsilon_3 = 0.3 - 0.4$ cm/ns. The smallness of the middle cluster velocity may explain why it is missing in the collinear tripartition in the ^{252}Cf(sf,fff) [18] and ^{235}U(n_{th},fff) [20] reactions.

The mass ranges of the two outer products, where the middle fragment can be observed, are (i) A_1=100-120 and A_2=130-140 which corresponds to the well-known ternary fission with emission of the light nucleus with A_3=4-12 [53,54] and (ii) A_1=90-110 and A_2=100-132.

The middle fragment may locate not in one line with edge fragments. So, possibility of its location will be considered in next chapter to estimate of collinearity of fission.

CHAPTER III. PRE-SCISSION CONFIGURATION OF THE TRINUCLEAR SYSTEM AT SPONTANEOUS TERNARY FISSION OF ^{252}Cf

3.1. Introduction

This chapter is dedicated to study various pre-scission configurations of tri-nuclear system. The main task is to check possibility of collinear ternary fission. This chapter is based on our published paper [55].

The mass and angle distribution, as well as kinetic energy of the ternary fission products are determined by the pre-scission configuration of trinuclear system. The appearance of the experimental results of the FOBOS (JINR, Dubna) group in Refs. [17,18,56] about the mass and energy distribution of the reaction products stimulated the theoretical studies of the main properties of the true ternary fission in Refs. [12,43,57-61]. The important conclusions of the experimental works [17,18,56] concern the collinearity of the velocities of the three reaction products and the cluster configuration of the pre-scission state of the ternary system. The ground-state shape of the actinide nuclei is prolate [33]. It is a result of the balance between the repulsive Coulomb and attractive surface tension forces. The oblate shape in the ground state seems to be favorable for the true equatorial fission but it is unfavorable energetically for the three massive fragments. Therefore, the prolate deformation of the fissioning nucleus favors the collinear ternary fission. The quantitative estimation of the potential energy and yields of the ternary fission products for the pre-scission oblate and prolate shapes of the TNS were made in Ref. [33]. The authors of Ref. [3] found that the potential energy of the collinear shape is significantly lower than the one for the equatorial (like triangular) shape and the yield of the ternary fission products is much larger for the prolate case than for the latter shape.

The yield of the true ternary fission fragments of comparable size A_i (A_i>36, i=1,2,3) has been observed in the experiments with the prolate deformed heavy nuclei

^{236}U and ^{252}Cf [18,20]. It is well known, and we will discuss in subsection 3.3 that the triangular shape of the vectors of the fission fragments at the pre-scission configuration is energetically not favorable for these massive nuclei. But this does not mean that the fragment yields of the true ternary fission can only be collinear.

The probability of cluster formation during the fission process is very high due to the shell effects in the structure in the nuclear fragments. Consequently, the yield of ternary events depends on the formation of intermediate mass fragments with specific mass A_3 and charge Z_3 numbers. These conclusions have been obtained from the analysis of the experimental data on the study of the true ternary fission described in Refs. [17,20,56] and from the theoretical investigations in Refs. [12,43,57-61]. The dependence on cluster structure with shell effects is seen in the study of the PES of the TNS as a function of the fragments mass *A* and charge *Z* as described in numerous Refs. [12,43,57-61].

For the discussion of the details of the decay process we need the PESs for the ternary fragmentation. The PES of the TNS is calculated as the sum of the binding energies B_1, B_2, B_3 of its fragments, the mass of the decaying nucleus, and the interaction potential energy between them:

$$U(B_1, B_2, B_3, Z_1, A_1, Z_3, A_3) = B_1 + B_2 + B_3 + V, \tag{3.1}$$

$$V = V_{12} + V_{13} + V_{23}, \tag{3.2}$$

where V_{ij} are the potential energy of the nucleus-nucleus interactions between fragments "*i*" and "*j*" (*i*>*j*) of the TNS. The method of calculations of V_{ij} is discussed in subsection 3.2.

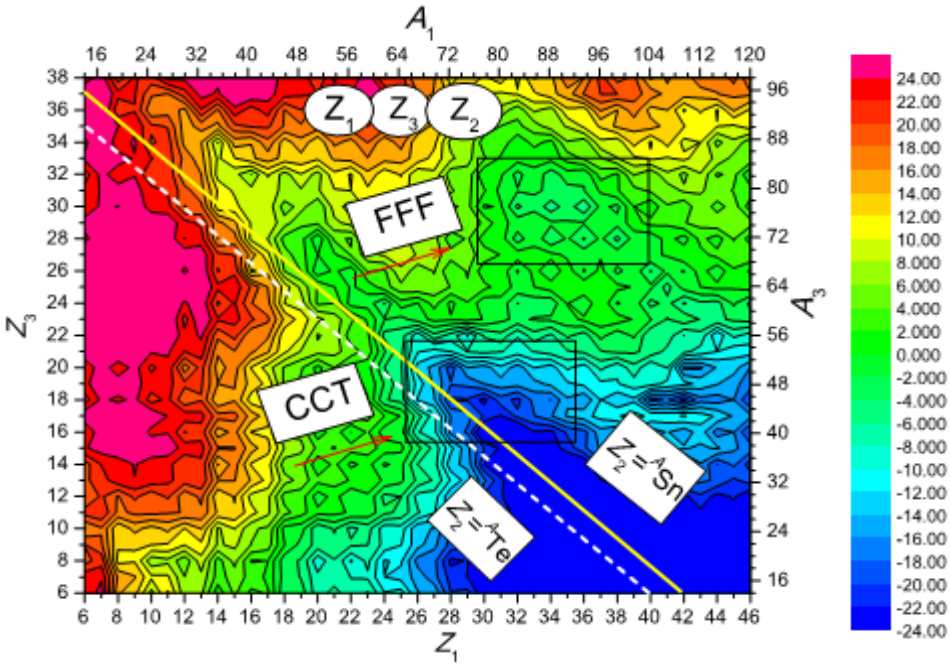

Fig. 3.1. The potential energy surface $U(B_1, B_2, B_3, Z_1, A_1, Z_3, A_3)$ of the trinuclear collinear system in a collinear arrangement as a function of the charge and mass numbers of the left outer (Z_1 and A_1) and middle (Z_3 and A_3) fragments. The binding energies B_1, B_2, B_3 of the fragments are obtained from the mass tables in Ref. [32,33], which include the nuclear shell effects.

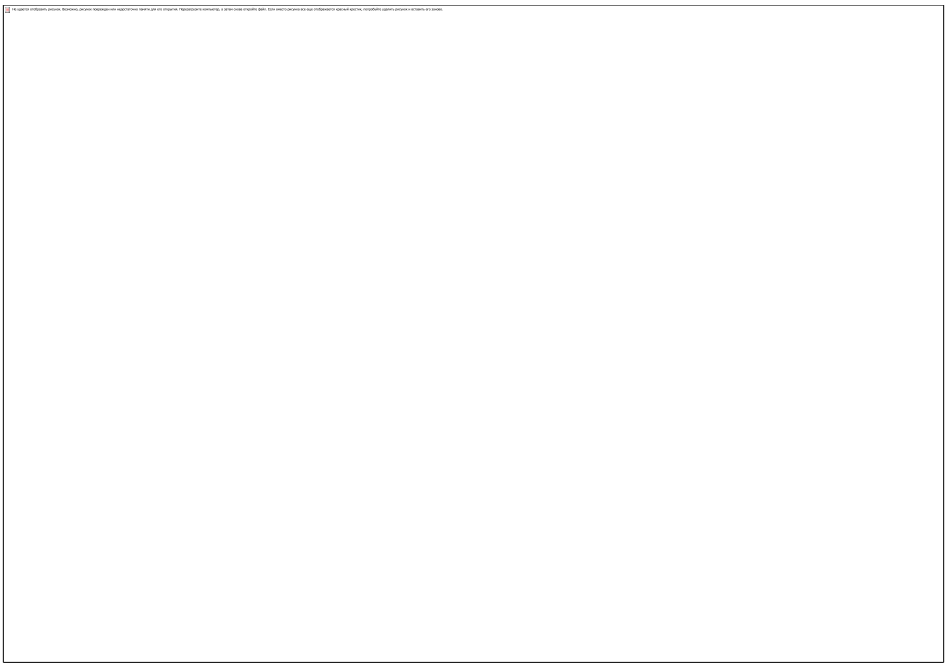

Fig. 3.2. The same as in Fig. 3.1 but the binding energies B_1, B_2, B_3 of the fragments have been obtained using the liquid-drop model.

The nuclear shell effects are included due to the use of the realistic binding energies B_1, B_2, B_3 obtained from the experimental mass tables [32], or from the values calculated by different theoretical methods (see [33,62,63]). To show the importance of the nuclear shell effects in the formation of the true ternary fission products we compare in Figs. 3.1 and 3.2, where we present the PESs calculated using binding energies of fragments obtained from the mass tables [33] and those from the liquid-drop model, respectively. The valleys corresponding to the formation of the isotopes of Sn (Z_2=50, solid line) and Te (Z_2=52, dashed line) in the TNS is seen in the PES presented in Fig. 3.1 as a function of the charge numbers Z_1 and Z_3 of the outer and middle fragments, respectively. The mass and charge number of the second outer fragment is determined from the conservation law of the proton and neutron numbers in the TNS: $A_2=A_{tot}-(A_1+A_3)$ and $Z_2=Z_{tot}-(Z_1+Z_3)$, where A_{tot} and Z_{tot} are mass and charge numbers of the fissioning nucleus. There are local minima pointing to the favored population of the charge (mass) distribution of the collinear TNS "1+3+2" with the formation of fragments having the charge numbers in the ranges Z_1=28-36; 40-46 and Z_3=6-20. The area of the collinear cluster tripartition labeled by the frame "CCT" in Fig. 3.1 is discussed in Refs. [18,20,56,59,61-52]. The area labeled "FFF" corresponds to the case of the formation of ternary fission products with almost equal mass numbers (A1≈A2≈A3). The probability for the population of this configuration is relatively small since the PES of the "FFF" area is placed higher than the one of the "CCT" region. The PES calculated by the liquid-drop model does not contain the "CCT" and "FFF" areas, which are related to the shell effects in the TNS fragments. The potential energy $V = V_{12} + V_{13} + V_{23}$ of the PES presented in Figs. 3.1 and 3.2 are calculated in the same way as described in Ref. [12,60]. The minimum values of V_{ij} correspond to the bottom of the potential wells in the interacting potential between fragments "*i*" and "*j*". Therefore, the difference between them is caused by the different ways of determining the values of binding energies B_1, B_2, B_3.

The extended version of the two-center shell model was used in Ref. [57] to calculate the PES as the adiabatic potential of the ternary system. The potential energy was found as a difference between the binding energy of the compound nucleus and the sum of the binding energies of three deformed fragments of the TNS. The comparison of the results of the PESs calculated by the liquid-drop model for the ternary fission of ^{248}Cm with the ones obtained by taking into account the nuclear shell corrections in the binding energies of the fragments, does not show distinctive changes in the PES in Ref. [64]. Therefore, the authors of this paper concluded that "for nuclei with Z<100 there is just not enough charge and mass to form two doubly magic tin-like nuclei plus a third heavy fragment". The observation of the yield of the true ternary fission products in the experiments of the FOBOS group [18,20] does not confirm this conclusion of the authors of Ref. [64].

A comparison of the results obtained for the PES with and without shell effects in the present chapter shows the strong effect of nuclear shells in the formation of the ternary fission fragments for ^{252}Cf. The nuclei with the closed shells in the number of protons and neutrons due to the single-particle structure appear as clusters in pre-scission states of the dinuclear and trinuclear systems. This fact is known from properties of the mass distribution of binary fission, since the nuclear shell effects play an important role in the formation of the binary fission products.

Certainly, the yield of ternary events depends on the mass and charge numbers A_i and Z_i of the fragments, particularly on the values of A_3 and Z_3 of the central fragment. How strong this dependence can be estimated by the theoretical methods presented in some of the papers, cited before. For example, in Refs. [12,24] the relative yield of the ternary fission products was estimated as a function of the mass and charge numbers of the product A_3 and Z_3 while in Ref. [60] the yield of the ternary fission products as a function of the mass and charge numbers of the outer products "1" and "2" has been explored. In the second chapter (see also Ref. [60]) we obtain a probability of about 5.6×10^{-3} per binary fission for the yield of massive

clusters such as ^{70}Ni, $^{80\text{-}82}$Ge, ^{86}Se, and ^{94}Kr in the ternary fission of ^{252}Cf. This result is close to the experimental value $4.6\cdot10^{-3}$ [20]. The yield of the true ternary fission products with comparable masses (^{82}Ge+^{72}Ni+^{82}Ge) in relation to binary fission events was estimated as $4\cdot10^{-4}$ in Ref. [12] where a sequential mechanism has been considered.

In the experiments of the FOBOS group for the true ternary fission process, two masses and two velocities are determined for two fragments observed at a relative angle of 180° [18,20]. The third fragment's mass was obtained from the mass conservation law. Thus, the mass distribution of the collinear lighter ternary fission fragments has been studied using the missing-mass method.

Results presented in Ref. [43,60] showed that the velocity of lighter ternary central fragments can become extremely small as a function of the excitation energy of the intermediate mass fragments, as well as of the two outer fragments. This implies that it is extremely difficult (even impossible) to observe the middle cluster in a triple coincidence experiment.

The aim of the present chapter is to test the collinearity in true ternary fission of ^{252}Cf, i.e. to study the range of the directions of the fragments after scission. Actually, the deviation from the collinearity of the momenta in true ternary fission has not been estimated yet. In our previous chapter, we suggested that the fragments move on the fission axes of the sequential decay of the ternary system, and that they are collinear [60]. The present chapter is devoted to the study of the potential energy between three nuclei as a function of the position of the middle lighter cluster, in order to clarify the possibility of a deviation from the collinearity in the TNS during its decay.

3.2. Trinuclear system model.

The theoretical approach is based on the TNS model, as in our previous chapter (Ref. [60]) we use the term "trinuclear system" based on a related model used for di-

nuclear systems [25,27,28]. The physical details of the TNS are the same as those for di-nuclear systems, but there are three interacting nuclei.

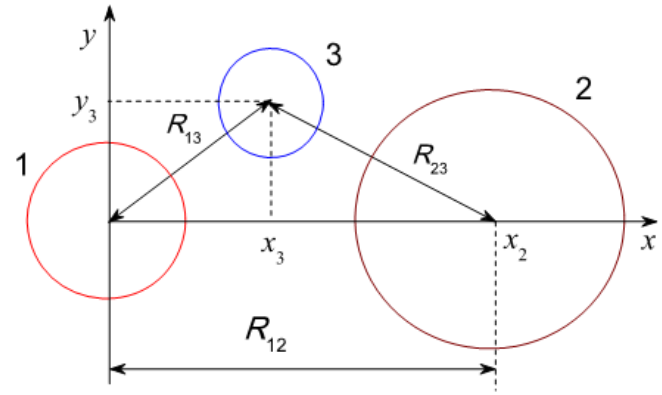

Fig. 3.3. The scheme showing the variables used in the calculation of the potential energy $V(R_{12}, x_3, y_3)$.

The potential energy is found as the sum of the nuclear and Coulomb interactions between three fragments:

$$V(R_{12}, x_3, y_3) = \sum_{i<j} V_{ij}(R_{12}, x_3, y_3), \tag{3.3}$$

$$V_{ij}(R_{12}, x_3, y_3) = V_{ij}^{(nuc)}(R_{12}, x_3, y_3) + V_{ij}^{(Coul)}(R_{12}, x_3, y_3), \tag{3.4}$$

where i,j=1,2,3 and $i<j$. The nucleus-nucleus potentials $V_{ij}(R_{12}, x_3, y_3)$ depend on the relative distances R_{ij} between fragments "i" and "j" (see Fig. 3.3). The x-axis of the coordinate system is directed along R_{12} connecting the centers of masses, of nuclei with "1" and "2". The coordinates of the third fragment are x_3 and y_3. These three variables are enough to obtain the potential energy of the three spherical nuclei. The relative distances $|\mathbf{R_{13}}|=|\mathbf{R_3}|$ and $|\mathbf{R_{23}}|=|\mathbf{R_2}-\mathbf{R_3}|$ can be found easily by the values of $|\mathbf{R_2}|=|\mathbf{R_{12}}|$, x_3 and y_3:

$$R_{13} = \sqrt{x_3^2 + y_3^2}, \tag{3.5}$$

$$R_{23} = \sqrt{(R_{12} - x_3)^2 + y_3^2}, \tag{3.6}$$

where $\mathbf{R_2}$ and $\mathbf{R_3}$ are the vectors showing the centers of mass of the nuclei "2" and "3" ($\mathbf{R_1}$=0).

The double-folding procedure is (similar which is given in the Appendix) used to calculate the nuclear interaction potential:

$$V_{ij}^{(nuc)}(R_{ij}) = \int \rho_i(r_i) f_{ij}(r_i, r_j) \rho_j(r_j) \mathrm{d}\mathbf{r}. \tag{3.7}$$

Here, ρ_i is the density of the *i*-th nucleus, f_{ij} is the effective nucleon-nucleon potential, which is taken from Migdal's book. So, they are defined as

$$f_{ij}(r_i, r_j) = C\left[f_{in} + (f_{ex} - f_{in})\frac{\rho_0 - \rho_i(r_i) - \rho_j(r_j)}{\rho_0}\right] \tag{3.8}$$

and

$$\rho_i(r_i) = \frac{\rho_0}{1 + \exp\left(\frac{r_i - R_{0i}}{a}\right)}, \tag{3.9}$$

where $r_i = |\mathbf{r} - \mathbf{R}_i|$ ($r_j = |\mathbf{r} - \mathbf{R}_j|$), $r_1 = r$, $R_{0i} = r_0 A_i^{1/3}$ is the radius of each nucleus. The constants in the potentials are C=300 MeV·fm^{-3}, $f_{in} = 0.09$, $f_{ex} = -2.59$, $\rho_0 = 0.17$ fm^{-3}, $r_0 = 1.17$ fm. As in a reaction, magic nuclei (clusters) are considered, so radii are for spherical shapes. Moreover, $\mathbf{R}_i$ is a position vector of the nucleus "*i*" relative to the centre of mass of the nucleus "1". Details of the calculation method of the nucleus-nucleus potential are presented in the Appendix and Ref. [10]. The Coulomb potential in the formula (3.4) is

$$V_C(R_{ij}) = \frac{Z_i Z_j e^2}{R_{ij}}. \tag{3.10}$$

3.3. Results of calculations of total interaction potential.

The calculations have been done for the configuration of the ternary nuclear system consisting of ^{70}Ni, ^{50}Ca and ^{132}Sn, which can be formed in the spontaneous fission of ^{252}Cf. The choice of this system is caused by the fact that, it was often

discussed in the publications related to the true ternary fission, see Refs. [65-67], and due to the relatively large probability of Ni in coincidence with the fission product with mass numbers A=134-138. It is easy to understand, that the configuration with the Ca in the middle between Ni and Sn, has the lower potential energy (see Refs. [61,68]). The potential energy of the TNS is calculated as a function of the Cartesian coordinates x and y, they depend on the distance R_{12} between the centers of mass of Ni and Sn nuclei. The analysis of the TNS potential energy as a function of R_{12}, x_3, and y_3 allows us to discuss its pre-scission state. Because the TNS fragments evolve to reach the state with the lower energy while they fluctuate around the minimum of the potential well. For example, at the given value of R_{12} the center-of-mass of the middle cluster tends to reach the minimum of the potential well of the ternary system since the middle cluster is Ca having smallest mass number and it is more mobile than the massive outer nuclei Ni and Sn.

We can observe three qualitatively different behaviors of the potential related to the probable positions of Ca relative to the Ni and Sn and to the line R_{12} as a function of its values.

It is seen from Figs. 3.4 and Fig. 3.5 that the ternary system has the triangular shape (y_3>0) for the distances R_{12}<22 fm since the repulsive Coulomb forces extrude Ca from the collinear position on the axis R_{12} connecting the centers of mass of Ni and Sn. It should be noted that the short-range nuclear force is repulsive at very small distances $R_{12}\leq 20$ fm between the centers of mass of the interacting fragments due to dependence of the effective nuclear interaction (see Eq. (3.8)). At small distances between fragments the overlap of their nucleon densities increases and the attractive nature of the nuclear forces becomes repulsive.

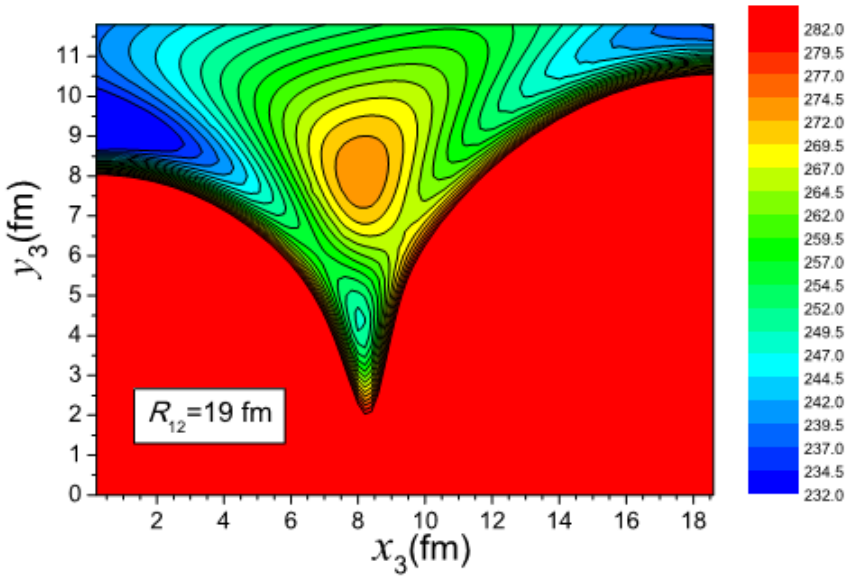

Fig. 3.4. The potential energy surface $V(R_{12}, x_3, y_3)$ as a function of the position x_3 and y_3 of the center-of-mass of the middle fragment "3" (Ca) at the value of R_{12}=19 fm of the relative distance between centers of mass of fragments "1" and "2". The minimum value of the potential well for Ca is V_{min} $(R_{12} = 19 \text{ fm},\ x_3 = 8.2 \text{ fm}, y_3 = 4.4 \text{ fm}) = 248.83$ MeV.

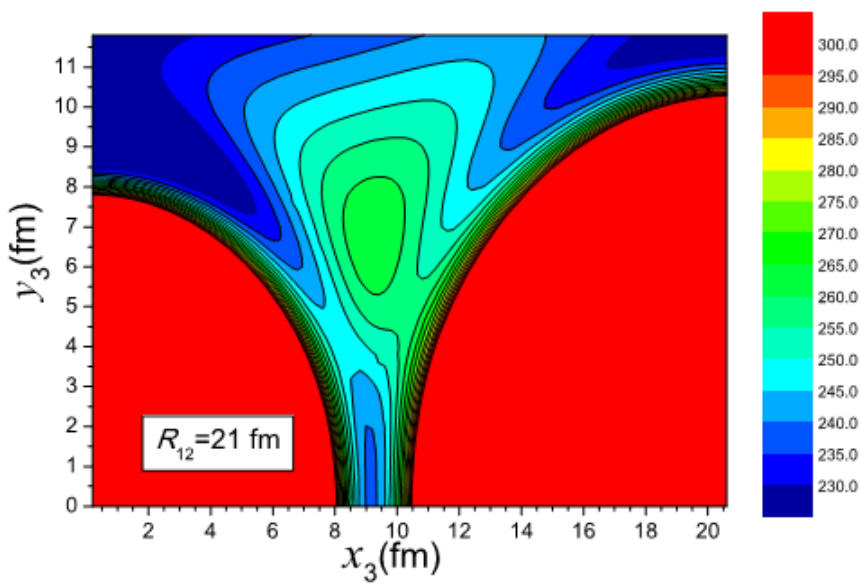

Fig. 3.5. The same as in Fig. 3.4 but for the distance R_{12}=21 fm. The minimum value of the potential well for Ca is V_{min} $(R_{12} = 21 \text{ fm},\ x_3 = 9.2 \text{ fm}, y_3 = 0 \text{ fm}) = 238.47$ MeV

The sign of the effective nucleon-nucleon forces depends on the subtraction $\rho_0 - \rho_i(r_i) - \rho_j(r_j)$ in (3.8): the case $\rho_0 < \rho_i(r_i) + \rho_j(r_j)$ corresponds to the distances when the internuclear distance is smaller than the sum of the radii of the interacting nuclei; the constant factor $\frac{f_{ex} - f_{in}}{\rho_0}$ is negative and, therefore, the nuclear force is positive $f_{ij}(r_i, r_j) > 0$, we have repulsive nuclear forces. When the internuclear distance is larger than the sum of the radii the overlap of the nucleon densities is not so strong and the case $\rho_0 > \rho_i(r_i) + \rho_j(r_j)$ takes place. In the last case, the nuclear forces are attractive.

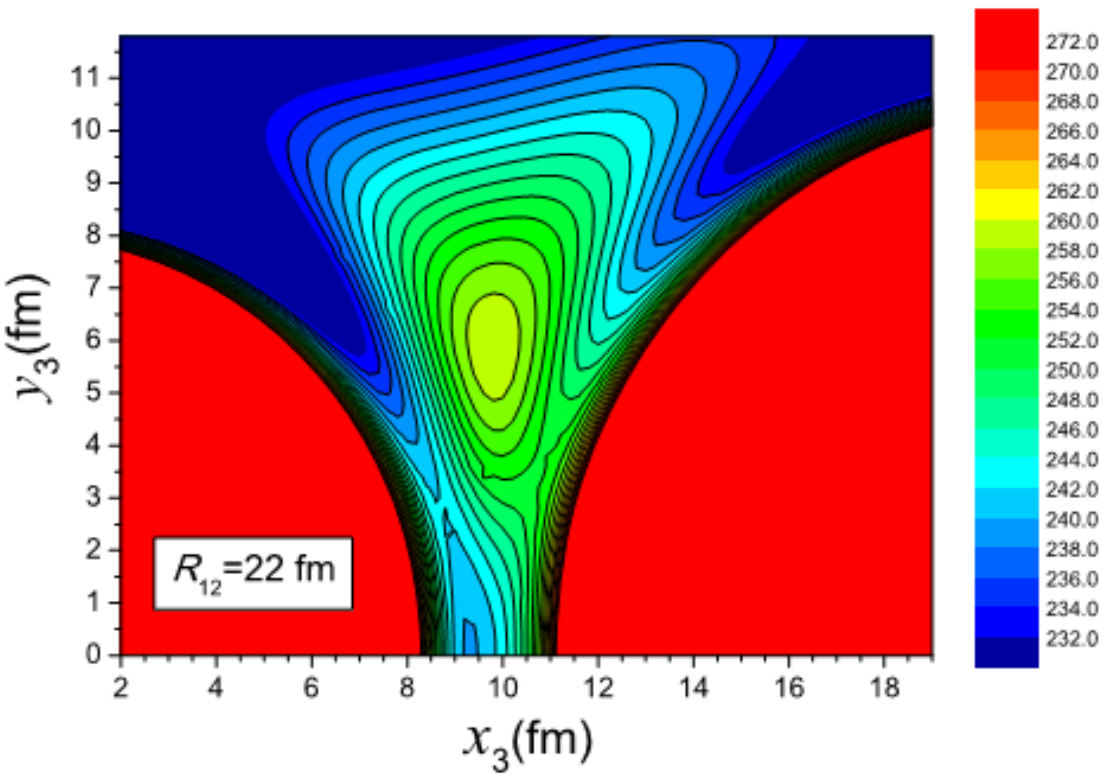

Fig. 3.6. The same as in Fig. 3.4 but for the distance R_{12}=22 fm. The minimum value of the potential well for Ca is $V_{min}\,(R_{12} = 22\text{ fm},\ x_3 = 9.4\text{ fm}, y_3 = 0\text{ fm}) = 239.75\text{ MeV}$.

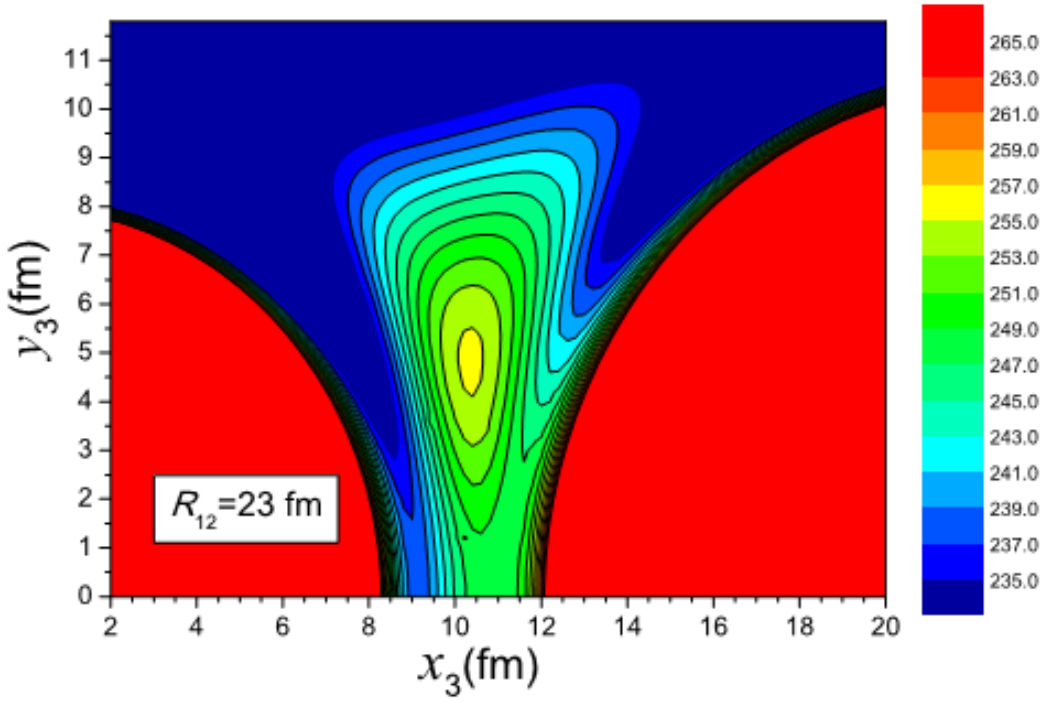

Fig. 3.7. The same as in Fig. 3.4 but for the distance R_{12}=23 fm. The minimum value of the potential well for Ca is V_{min} $(R_{12} = 22$ fm, $x_3 = 9.0$ fm, $y_3 = 2.2$ fm$) =$ 236.83 MeV.

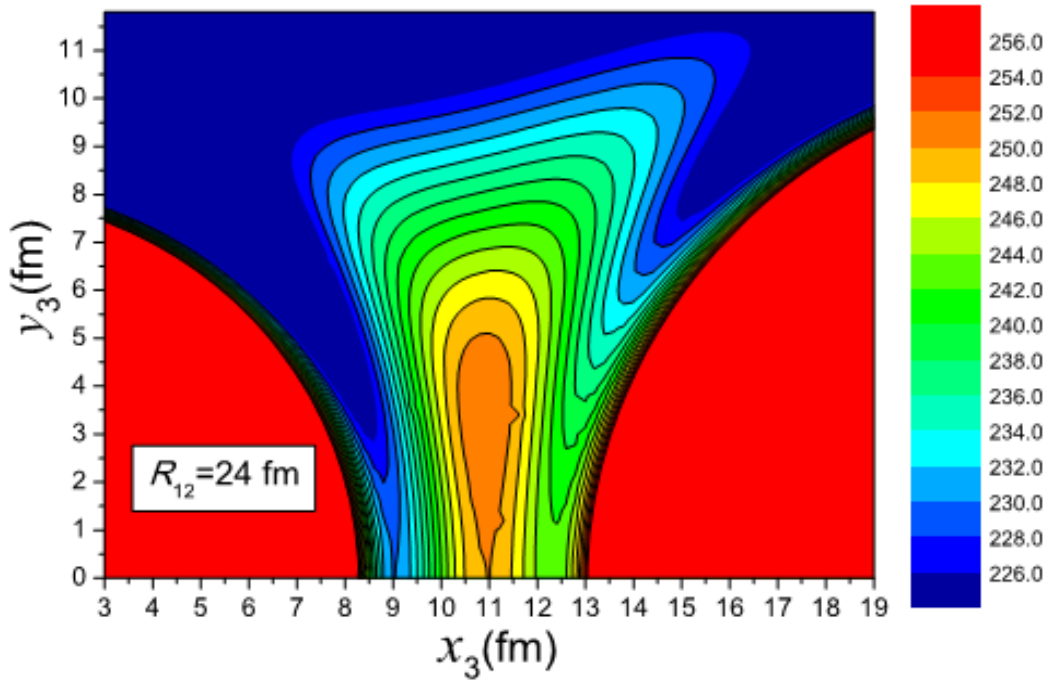

Fig. 3.8. The same as in Fig. 3.4 but for the distance R_{12}=24 fm. There is no minimum for Ca in the valley around Ni at x_3>0 fm, y_3>0 fm.

Therefore, the minimum value of the potential well for Ca is large, V_{min} (R_{12} = 19 fm, x_3 = 8.2 fm, y_3 = 4.4 fm) = 248.83 MeV. This is the first property of the Ca position relative to the line R_{12}. In this case, the position of Ca is similar to the pre-scission states of the light nuclei He, Li, Be, …, Si, which are placed between two massive nuclei and their emission trajectories are nearly perpendicular to the line R_{12} in the ternary fission (see Ref. [54]).

The second property for the position of the middle Ca nuclei relative to the collinearity axis R_{12} is the coincidence of the minimum of the potential well in $V(R_{12}, x_3, y_3)$ with R_{12}. The centre of the potential well moves to the line R_{12} by the increase of its value. This fact is seen from Fig. 3.5 and Fig. 3.6 showing the values of $V(R_{12}, x_3, y_3)$ obtained for the distances R_{12}=21 and 22 fm, respectively. The potential well is deeper and its minimum value is V_{min} (R_{12} = 21 fm, x_3 = 9.2 fm, y_3 = 0 fm) = 238.47 MeV and the minimum coincides with the R_{12} line (x-axis). In this case the geometry of the TNS is collinear and its potential energy is small due to the strong attraction by nuclear forces between neighboring fragments. The localized minimum appears for the potential well at larger values of R_{12}=22 fm and it is nearly at the same level V_{min} (R_{12} = 22 fm, x_3 = 9.4 fm, y_3 = 0 fm) = 239.75 MeV. The collinear shape of the TNS fragments remains favorable.

We can state, that the collinear configuration of the TNS is preferable for the values of R_{12}=21-22 fm but the fluctuation of the position of the middle Ca cluster from the collinearity axis can be observed due to the extension of the potential well in $V(R_{12}, x_3, y_3)$ up to 2 fm around the axis.

The increase of R_{12} values from the values 22 fm causes a decrease of the overlaps of the nucleon densities of the TNS nuclei, as a result the nuclear attraction decreases. At the same time the Coulomb repulsion decreases by the increase of R_{12} and the width of the potential well increases as well. As a result the potential well for Ca moves away from the x-axis at R_{12}=23 fm and its minimum value decreases: V_{min} (R_{12} = 22 fm, x_3 = 9.0 fm, y_3 = 2.2 fm) = 236.83 MeV.

The third property appears at larger values of R_{12}≥24 fm: the centre of the potential well moves along the surface of the Ni cluster and is transformed into a valley (see Figs. 3.7, 3.8) moving away from the collinearity axis R_{12}. The Ni+Ca system is bound stronger than Ca+Sn since the depth of the potential well of the Ca+Sn system is smaller than the one of the former system. At the same time the potential well of the interacting system Ca+Sn is higher than the one of the Ni+Ca system. Therefore, the probability of the binding of Ca cluster to Ni is larger than the probability of its binding to Sn. This fact indicates that at first Sn separates from the TNS system. This effect is the consequence of the complete disappearance of the simultaneous overlap of the nucleon density of the TNS nuclei. The details of the potential wells between neighboring nuclei will be analyzed in the next subsection 3.4.

The Coulomb force of the Sn nucleus pushes the Ca cluster, which is in the potential well of the Ca+Ni system, along the surface of the Ni cluster since the nuclear fields of the Ni and Ca nuclei overlap forming a DNS. When the Sn cluster separates first from the other part of the ternary system at R_{12}>24 fm, the usual binary spontaneous fission takes place since the probability of the decay of the DNS (Ni+Ca) is to small without the influence of the Coulomb field of the Sn cluster (see the second chapter).

The deviation from the collinearity of the velocities of the ternary fission products depends on the pre-scission geometrical configuration of the Ni+Ca system relative to the R_{12} line and the value of the relative motion momentum of its nuclei at break-up.

3.4. Potential energy of collinear trinuclear system.

The potential energy of the collinear TNS is calculated for the different values of the relative distance R_{12} between the outer fragments Ni and Sn. The results of the calculation for the five ranges of the R_{12} values are presented in Figs. 3.9 and 3.10.

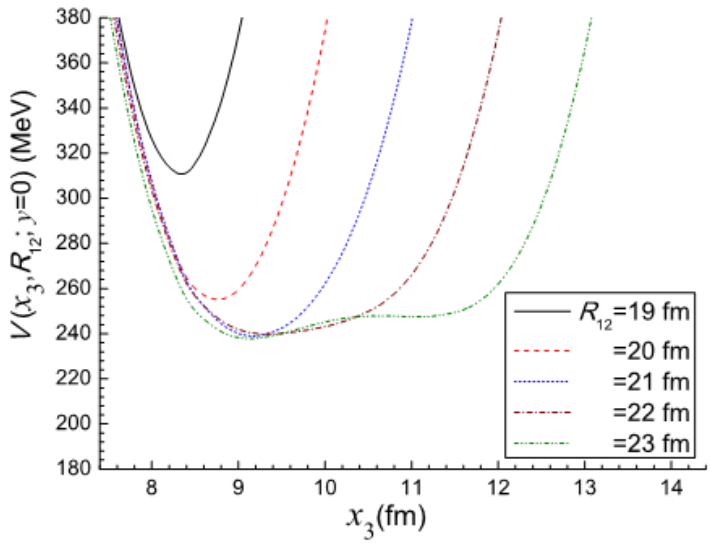

Fig. 3.9. The potential energy $V(R_{12}, x_3, y_3 = 0)$ of the TNS as a function of x_3 at different values of R_{12}=19-23 fm, the relative distances between centers of mass of the fragments "1" and "2".

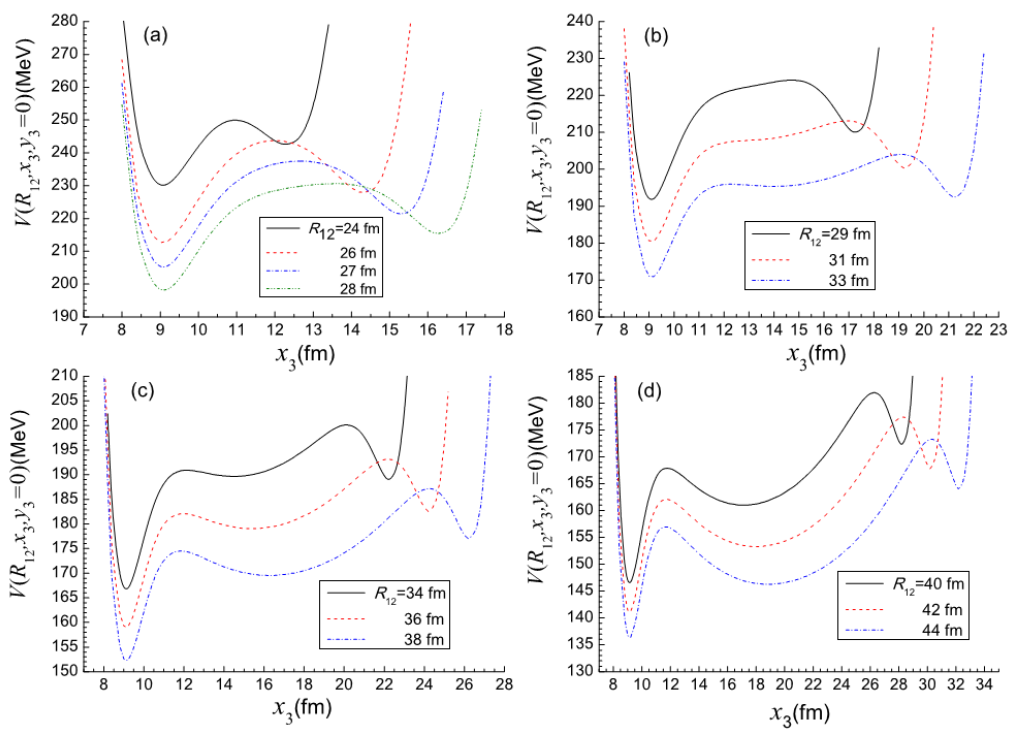

Fig. 3.10. The same as in Fig. 3.9 but for the distances R_{12}=24, 26, 27 and 28 fm (a); R_{12}=29, 31 and 33 fm (b); R_{12}=34, 36 and 38 fm (c); R_{12}=40, 42 and 44 fm (d).

Here 3 following qualitative properties of the potential energy as a function of R_{12} can be noted:

1) At small relative distances (R_{12}<22 fm) between the outer nuclei of the TNS, the overlap of the nucleon densities of its fragments is stronger, and therefore, the oscillator-like well in the potential energy of the system is formed due to the overlap of the potential wells of the V_{13}-and V_{23}-interactions (see Fig. 3.9). The size and minimum values $V_{\min}$ of the oscillator-like well depend on the distance R_{12}. At the distances R_{12}=19-21 fm the minimum values of the potential well do not coincide with the x-axis (y_3>0) and the TNS has the triangular shape (see Figs. 3.4–3.6). Consequently, the values of the potential energy on the x-axis (y_3=0) is large for the distances R_{12}=19–21 fm since the x-$V(R_{12}, x_3, y_3 = 0)$ plane cuts the potential well far from its minimum value.

2) The shape of the potential well on the x-axis is changed from the oscillator-like to the double well shape by the increase of R_{12}=22–24 fm (see figs. 3.9 and 3.10(a)). The minima of the potential well can be populated by the middle cluster ^{50}Ca in the pre-scission states during its motion in the TNS. This means that ^{50}Ca can be bound to the fragment "1"–^{70}Ni populating the potential well at x_3≈10.5 fm or it can be bound to the other massive cluster ^{132}Sn populating the potential well at x_3≈15.2 fm, for example, at R_{12}=27fm.

3) The potential well near the ^{132}Sn cluster is placed significantly higher than the one near ^{70}Ni. This means that the probability for the formation of the bound (^{50}Ca+^{132}Sn)-system is smaller than the one for the formation of the (^{70}Ni +^{50}Ca)-system at break-up of the initial TNS (^{70}Ni +^{50}Ca+^{132}Sn). One can say that the binding of the middle Ca cluster to the lighter ^{70}Ni nucleus is more favorable.

3.5. Conclusion.

The potential energy $V(R_{12}, x_3, y_3)$ for the pre-scission configurations of the TNS with the structure (^{70}Ni+^{50}Ca +^{132}Sn) for the spontaneous fission of ^{252}Cf has been calculated as a function of the center-of-mass coordinates of the middle fragment

“3” (Ca) for different values of the distance between the centers of the outer fragments “1” (Ni) and “2” (Sn). The analysis of the results show that when R_{12}<21 fm, the repulsive Coulomb forces extrude Ca from the collinear position between Ni and Sn and the ternary system has the triangular shape (y_3>0). It should be noted that the short-range nuclear force is repulsive at very small distances between the centers of mass of the interacting fragments due to the dependence of the effective nuclear interaction (Eq. (3.8)) on the nucleon density. At small distances between nuclei the overlap of their nucleon densities increases and the attractive nature of the nuclear forces becomes repulsive. Therefore, the minimum of the potential well for Ca corresponds to the triangular shape of the TNS with the fragmentation into (^{70}Ni+^{50}Ca +^{132}Sn). But the population of this equatorial configuration during the evolution of the TNS is small, because the potential well is placed higher, $V_{min}\,(R_{12} = 19\text{ fm},\ x_3 = 8.2\text{ fm},\ y_3 = 4.4\text{ fm}) = 248.83\text{ MeV}$.

At larger values of R_{12}=21–22 fm, the minimum of the potential well moves to the line R_{12} and the collinear shape of the TNS-(^{70}Ni+^{50}Ca +^{132}Sn) is favorable. The potential well is deeper and its minimum values are $V_{min}\,(R_{12} = 21\text{ fm},\ x_3 = 9.2\text{ fm}, y_3 = 0\text{ fm}) = 238.47\text{ MeV}$ and $V_{min}\,(R_{12} = 22\text{ fm},\ x_3 = 9.4\text{ fm},\ y_3 = 0\text{ fm}) = 239.75\text{ MeV}$.

We can state, that the collinear configuration of the TNS is preferable for the values of R_{12}=21-22 fm but the fluctuation of the position of the middle Ca cluster from the collinearity axis can be expected due to the extension of the potential well in $V(R_{12}, x_3, y_3)$ up to 2 fm around the axis.

The separation of the massive cluster ^{132}Sn occurs as the first step of the TNS break-up. Since the potential well near the ^{132}Sn cluster is significantly higher than the one near ^{70}Ni we expect, that at break-up of the TNS the middle Ca cluster is bound to the lighter ^{70}Ni nucleus, which is energetically more favorable energetically. The results show that the decay of the residual ^{70}Ni+^{50}Ca system can lead to the collinear tripartion of TNS when the relative distance between the centers of mass of ^{70}Ni and

^{132}Sn is about R_{12}>40 fm. If the decay of the residual (^{70}Ni+^{50}Ca) system does not occur the usual binary fission of ^{252}Cf will take place. It is well known that the yield of the binary fission products predominates the spontaneous fission of ^{252}Cf.

The calculation of the decay dynamics and the trajectory of the outgoing reaction products will be performed in next chapter to clarify the deviation of their trajectory from collinearity.

CHAPTER IV. DYNAMICS OF THE TRINUCLEAR SYSTEM AT SPONTANEOUS FISSION OF ^{252}Cf

4.1. Introduction

Recently, the two papers which were studied and analyzed the collinear cluster tripartition process have been published [69-71]. Author of the Ref. [69] estimated possible channels calculating interaction potential as the function of the radius of a compound nucleus and the mass of the middle fragment in the framework three-center shell model. In this manuscript only the collinear (prolate) configuration was considered. Authors of the Ref. [70] tried to summarize the current models and analyze the mechanisms of the collinear cluster tripartition process. Also, they estimated products kinetic energies for defined mechanisms. Moreover, they accepted the collinear cluster tripartition model – the almost sequential mechanism which is developed by us as one of successful models. Also, they confirmed results which are about deviation from collinearity and given in this chapter.

This last chapter of the dissertation is devoted to study dynamical properties of trinuclear system. The main aim is to find which initial cases of the system correspond to collinear ternary fission. This chapter is based on the published paper by us [72].

Studies of the spontaneous fission products of ^{252}Cf in the coincidences with the emitted neutrons has been performed in two missing-mass experiments [18,20]. These experiments demonstrated the interesting phenomenon – emission of the non equilibrium neutrons from the neck region of the fissioning system. The reason of this fact is explained by the neutron excess in the middle fragment. This peculiarity of CCT is reproduced by our calculations in both previous chapter and Ref. [61], and it is concluded that middle fragment is neutron-rich calcium nucleus.

At first, in collinear cluster tripartition (CCT) mode, the masses of nuclei are comparable, and nuclei are especially clusters, i.e. with a magic number of mass (or charge). At second, the collinearity of the momenta of the ternary fission fragments is proved by the fact that the two detectors registering Sn and Ni-like fragments are placed on the opposite sides from the fissioning source ^{252}Cf such that angle between them is 180^0. The observed probabilities of the yield of Ni and Sn nuclei were approximately 10^3 times less than the one of binary fission. The collinear cluster tri-partition observed by experimental group FOBOS (setup in the Flerov Laboratory for Nuclear Reactions of the Joint Institute for Nuclear Research, Dubna, Russia) has not been observed yet by other experimental group. There is no theoretical estimation the dynamics of the trajectories of the ternary fission products proving the collinearity of their momenta after decay. This mode of ternary fission differs from usual ternary fission which is binary fission with the emission of light fragments (He, Li, Be etc.) as the third (middle) nucleus in the perpendicular plane to the fission axis.

In previous chapter the possible channels of true ternary fission were studied. In the Ref. [20] it is shown that more possible channel of ternary fission in the ^{252}Cf(sf) reaction is ^{70}Ni+^{50}Ca+^{132}Sn which is theoretically proven in the third chapter. Our experience from the works [55,60] leads to the interesting question: how does trinuclear system evaluate during its decay? In fact, in those chapters it was not proven that the momenta of fission products are collinear or not. In present chapter, the dynamical changing the relative distance between nuclei and their velocities of the fission products of the ^{70}Ni+^{50}Ca+^{132}Sn system is studied.

Certainly, to get information about dynamics an equation of motion should be solved. Results of solution of the equation of motion depend on initial conditions. The dependence of the result on the initial condition is studied in detail to find the collinear flying of the ternary fission products. Thus, from results it will be easy to know what initial condition leads to collinear fission.

4.2. Equation of motion for decay of the trinuclear system.

The present theoretical model is based on the formation of the trinuclear system (TNS). The TNS is the system which has three interacting nuclei [55,60], and their interaction is studied on the basis of the DNS model [25-28]. The stage proceeding to formation of the TNS has not been studied. It is assumed that the system is formed, and any ternary fission of heavy nuclei passes through the TNS stage.

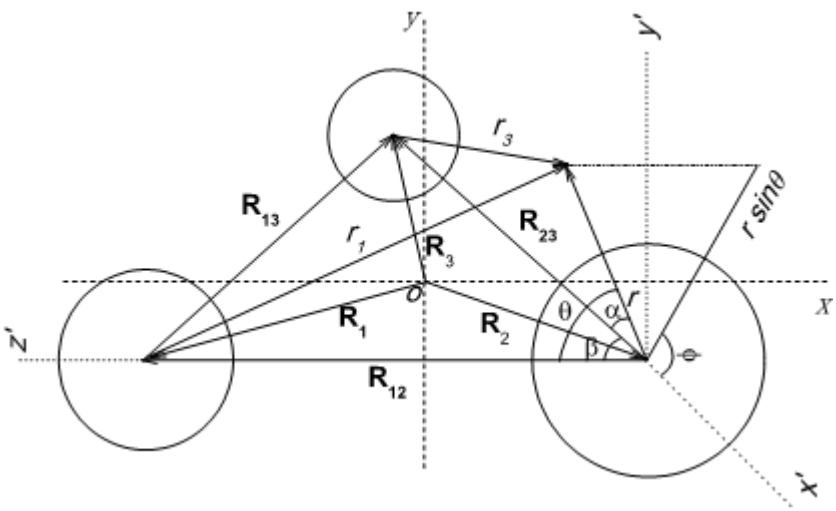

Fig. 4.1. Point ($\mathbf{R_k}$) and relative ($\mathbf{R_{ij}}$) vectors of trinuclear system. The point *O* (origin) corresponds to the center of mass of the whole system.

The main task is obtaining the classical Lagrange equations of motion, and solving them. First, the Lagrangian is $L=T-V$, where $T=\frac{1}{2}\sum_{i=1}^{3} m_i \dot{\mathbf{R}}_i^2$ – kinetic energy of the system, V – total interaction potential between fragments, m_i is the mass of the ith nucleus. Following system of equations can be written from the Fig. 4.1:

$$\begin{cases} \mathbf{R}_{12} = \mathbf{R}_1 - \mathbf{R}_2 \\ \mathbf{R}_{13} = \mathbf{R}_3 - \mathbf{R}_1 \\ \mathbf{R}_{23} = \mathbf{R}_3 - \mathbf{R}_2 \end{cases} \tag{4.1}$$

where $\mathbf{R}_k$ (k=1,2,3) are point vectors of nuclei and the magnitude of a vector $\mathbf{R}_{ij}$ is the relative distance between the ith and j^{th} nuclei.

Any kind of fission process occurs in one plane, i.e. it can be chosen the 2D space where fission fragments move. It means that the system does not have motion

on z-axis since there is no force on the axis. So any $\mathbf{R}_i$ vector can be described only with x and y components (R_{ix} and R_{iy}) in the Cartesian system. Correspondingly, velocities are defined as $\upsilon_{ix} = \dot{R}_{ix}$ and $\upsilon_{iy} = \dot{R}_{iy}$, therefore, the kinetic energy can be written as

$$T = \frac{1}{2}\sum_{i=1}^{3} m_i(\upsilon_{ix}^2 + \upsilon_{iy}^2). \tag{4.2}$$

4.2.1. The Lagrange equation of motion.

In the framework of the classical Lagrange formalism 3 equations of motion for the x variable and 3 for the y variable can be obtained:

$$\frac{d}{dt}\frac{\partial T}{\partial \upsilon_{ix}} - \frac{\partial T}{\partial R_{ix}} = -\frac{\partial V}{\partial R_{ix}}$$

$$\frac{d}{dt}\frac{\partial T}{\partial \upsilon_{iy}} - \frac{\partial T}{\partial R_{iy}} = -\frac{\partial V}{\partial R_{iy}}$$

The kinetic energy does not depend on a distance R_i, i.e. $\frac{\partial T}{\partial R_{ix}} = \frac{\partial T}{\partial R_{iy}} = 0$. Therefore,

$$m_i\dot{\upsilon}_{ix} = -\frac{\partial V}{\partial R_{ix}} \tag{4.3}$$

$$m_i\dot{\upsilon}_{iy} = -\frac{\partial V}{\partial R_{iy}} \tag{4.4}$$

The magnitude of a $\mathbf{R}_{ij}$ vector is $R_{ij} = \sqrt{R_{ijx}^2 + R_{ijy}^2}$. Potential energy V depends only on relative distance R_{ij} (or R_{ik}). So

$$\frac{\partial V}{\partial R_{ix}} = \frac{\partial V}{\partial R_{ijx}}\frac{\partial R_{ijx}}{\partial R_{ix}} + \frac{\partial V}{\partial R_{ikx}}\frac{\partial R_{ikx}}{\partial R_{ix}} = \frac{\partial V}{\partial R_{ij}}\frac{\partial R_{ij}}{\partial R_{ijx}}\frac{\partial R_{ijx}}{\partial R_{ix}} + \frac{\partial V}{\partial R_{ik}}\frac{\partial R_{ik}}{\partial R_{ikx}}\frac{\partial R_{ikx}}{\partial R_{ix}}. \tag{4.5}$$

It can be noted that $R_{ij} = R_{ji}$ and $R_{ik} = R_{ki}$. When the equation (4.3) is written for each nucleus, then using (4.5) following equations will be obtained:

$$\begin{cases} m_1\dot{\upsilon}_{1x} = -\dfrac{R_{12x}}{R_{12}}\dfrac{\partial V}{\partial R_{12}} + \dfrac{R_{13x}}{R_{13}}\dfrac{\partial V}{\partial R_{13}} \\ m_2\dot{\upsilon}_{2x} = \quad \dfrac{R_{12x}}{R_{12}}\dfrac{\partial V}{\partial R_{12}} + \dfrac{R_{23x}}{R_{23}}\dfrac{\partial V}{\partial R_{23}} \\ m_3\dot{\upsilon}_{3x} = -\dfrac{R_{23x}}{R_{23}}\dfrac{\partial V}{\partial R_{23}} - \dfrac{R_{13x}}{R_{13}}\dfrac{\partial V}{\partial R_{13}} \end{cases} \tag{4.6}$$

The relation between R_i (or R_{ix}) and R_{ij} (or R_{ijx}) is found from the system of equations (4.1). Symmetric three equations can be obtained for the *y* component:

$$\begin{cases} m_1\dot{\upsilon}_{1y} = -\dfrac{R_{12y}}{R_{12}}\dfrac{\partial V}{\partial R_{12}} + \dfrac{R_{13y}}{R_{13}}\dfrac{\partial V}{\partial R_{13}} \\ m_2\dot{\upsilon}_{2y} = \quad \dfrac{R_{12y}}{R_{12}}\dfrac{\partial V}{\partial R_{12}} + \dfrac{R_{23y}}{R_{23}}\dfrac{\partial V}{\partial R_{23}} \\ m_3\dot{\upsilon}_{3y} = -\dfrac{R_{23y}}{R_{23}}\dfrac{\partial V}{\partial R_{23}} - \dfrac{R_{13y}}{R_{13}}\dfrac{\partial V}{\partial R_{13}} \end{cases} \tag{4.7}$$

Considering the conservation law of linear momentum $\sum_{i=1}^{3} m_i\upsilon_{ix} = 0$ (since $\mathbf{P}_{c.m.} = 0$ for the spontaneous fission of ^{252}Cf) one of the equations in formulas (4.6) and (4.7) can be excluded. It means that υ_{3x} and R_{3x} are found as

$$\begin{cases} \upsilon_{3x} = -\dfrac{m_1\upsilon_{1x} + m_2\upsilon_{2x}}{m_3} \\ R_{3x} = -\dfrac{m_1R_{1x} + m_2R_{2x}}{m_3} \end{cases} \tag{4.8}$$

As the origin is placed at the center of mass so there is no "*const*" term in the definition of R_{3x}. Equations for *y* component are similar to the last equations.

4.2.2. Derivative of total interaction potential.

It is clear from the Eqs. (4.6), (4.7) and (4.8) that the dynamics of motion strongly depends on the derivative of the total interaction potential. The total interaction potential consists of two parts: coulomb and nuclear

$$V = V_C + V_{nuc}\,. \tag{4.9}$$

As there are three interacting nuclei so there are three terms on each part. To calculate the nuclear part the double folding procedure is used

$$V_C(R_{12}, R_{23}, R_{13}) = e^2 \sum_{i<j}^{3} \frac{Z_i Z_j}{R_{ij}}, \tag{4.10}$$

$$V_{nuc}(R_{12}, R_{23}, R_{13}) = \int \sum_{i<j}^{3} \rho_i(r_i) f(r_i, r_j)\, \rho_j(r_j) \mathrm{d}\mathbf{r}. \tag{4.11}$$

Following formulas are necessary to calculate the nuclear part:

$$f_{ij}(r_i, r_j) = C\left[f_{in} + (f_{ex} - f_{in})\frac{\rho_0 - \rho_i(r_i) - \rho_j(r_j)}{\rho_0}\right],$$

$$\rho_i(r_i) = \frac{\rho_0}{1 + \exp\left(\frac{r_i - R_{0i}}{a_d}\right)},$$

$$r_1(R_{12}) = \sqrt{r^2 + R_{12}^2 - 2rR_{12}\cos\theta},$$

$$r_2 = r$$

$$r_3(R_{12}, R_{23}, R_{13}) = \sqrt{r^2 + R_{23}^2 - 2rR_{23}\cos\alpha},$$

$$\cos\alpha = \cos\theta\cos\beta + \sin\theta\sin\beta\sin\varphi,$$

$$\cos\beta = \frac{R_{12}^2 + R_{23}^2 - R_{13}^2}{2R_{12}R_{23}}.$$

Here, r_i is the radial distance of the ith nucleus (see Fig. 4.1), r, θ and φ are variables of the spherical coordinate system, $R_{0i}=r_0A^{1/3}$ – the radius of the ith spherical nucleus, all parameters of interaction potential r_0, ρ_0, a_d, C, f_{in}, f_{ex} are taken as in Appendix, f_{ij} is the effective nuclear-nuclear force which is taken from the Ref. [73]. Calculation of total interaction potential of the trinuclear system was given in previous chapter, but the difference is that the origin of coordinate system is located at another place.

From equation (4.9) the derivative of the total interaction potential is found as

$$\frac{\partial V}{\partial R_{ij}} = -e^2 \frac{Z_i Z_j}{R_{ij}^2} + \frac{\partial V_{nuc}}{\partial R_{ij}},$$

$$\frac{\partial V_{nuc}}{\partial R_{ij}} = \int (F_{12} + F_{23} + F_{13})\, \mathrm{d}\mathbf{r},$$

$$F_{12} = \rho_2 \left[f_{12} - \frac{\rho_1}{\rho_0} C(f_{ex} - f_{in}) \right] \frac{\partial \rho_1}{\partial R_{ij}},$$

$$F_{23} = \rho_2 \left[f_{23} - \frac{\rho_3}{\rho_0} C(f_{ex} - f_{in}) \right] \frac{\partial \rho_3}{\partial R_{ij}},$$

$$F_{13} = \rho_3 \left[f_{13} - \frac{\rho_1}{\rho_0} C(f_{ex} - f_{in}) \right] \frac{\partial \rho_1}{\partial R_{ij}} + \rho_1 \left[f_{13} - \frac{\rho_3}{\rho_0} C(f_{ex} - f_{in}) \right] \frac{\partial \rho_3}{\partial R_{ij}},$$

$$\frac{\partial \rho_1}{\partial R_{ij}} = \frac{\rho_1(\rho_1 - \rho_0)}{a\rho_0} \frac{\partial r_1}{\partial R_{ij}},$$

$$\frac{\partial \rho_3}{\partial R_{ij}} = \frac{\rho_3(\rho_3 - \rho_0)}{a\rho_0} \frac{\partial r_3}{\partial R_{ij}}.$$

The derivatives $\frac{\partial r_1}{\partial R_{ij}}$ and $\frac{\partial r_3}{\partial R_{ij}}$ are calculated as follows

$$\frac{\partial r_1}{\partial R_{12}} = \frac{R_{12} - r\cos\theta}{r_1},$$

$$\frac{\partial r_1}{\partial R_{23}} = \frac{\partial r_1}{\partial R_{13}} = 0,$$

$$\frac{\partial r_3}{\partial R_{12}} = (R_{23}\cos\beta - R_{12})h(r),$$

$$\frac{\partial r_3}{\partial R_{23}} = \frac{R_{23} - r\cos\alpha}{r_3} - (R_{23} - R_{12}\cos\beta)h(r),$$

$$\frac{\partial r_3}{\partial R_{23}} = R_{13}h(r),$$

where $h(r) = \frac{r}{R_{12}r_3}(\cos\theta - \cot\beta\sin\theta\sin\varphi)$.

Note that the integration in (4.11) is provided in the (x', y', z') system (see Fig. 4.1), and if $\varphi = \pi/2$ then $\theta = \alpha + \beta$.

4.3. Solution of the equation of motion.

As mentioned above the channel for spontaneous ternary fission of ^{252}Cf nucleus is chosen as ^{70}Ni+^{50}Ca+^{132}Sn. ^{70}Ni is the first nucleus (placed left side), ^{132}Sn is the second nucleus (placed right side) and ^{50}Ca is the third one (placed in the middle) in the Fig. 4.1. The collinearity of the momenta of the tri-partition is determined by the dynamics of the middle fragment ^{50}Ca since the heavier fragment ^{132}Sn is separated firstly and then the middle fragment separates from ^{70}Ni. This sequence of ternary fission was discussed in the Ref. [60] and it is confirmed by the solution of dynamical equations in this chapter.

It is interesting to discuss how the total interaction potential looks as a function of R_{3x} and R_{3y}. It is shown in figures 4.2-4.7 for different values of R_{12} (relative distance between Ni and Sn nuclei). The origin (which is not shown) corresponds to the center of mass. There is local minimum at point R_{3x}=−2.9 fm and R_{3y}=0 fm (see Figs. 4.2 and 4.4). By increasing of R_{12} the minimum goes to left (to the side of Ni nucleus) but starting from R_{12}=22 fm it is transferred into a saddle point.

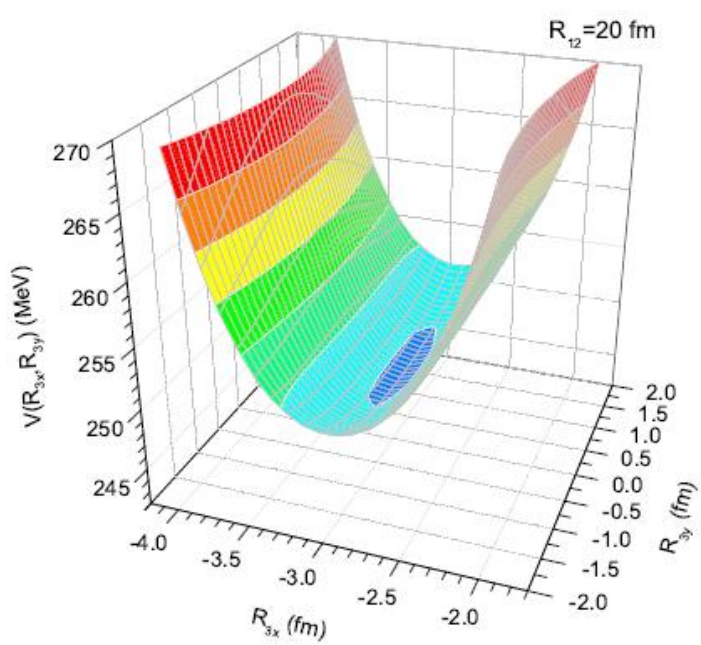

Fig. 4.2. The total interaction potential as the function of R_{3x} and R_{3y} when R_{12}=20 fm.

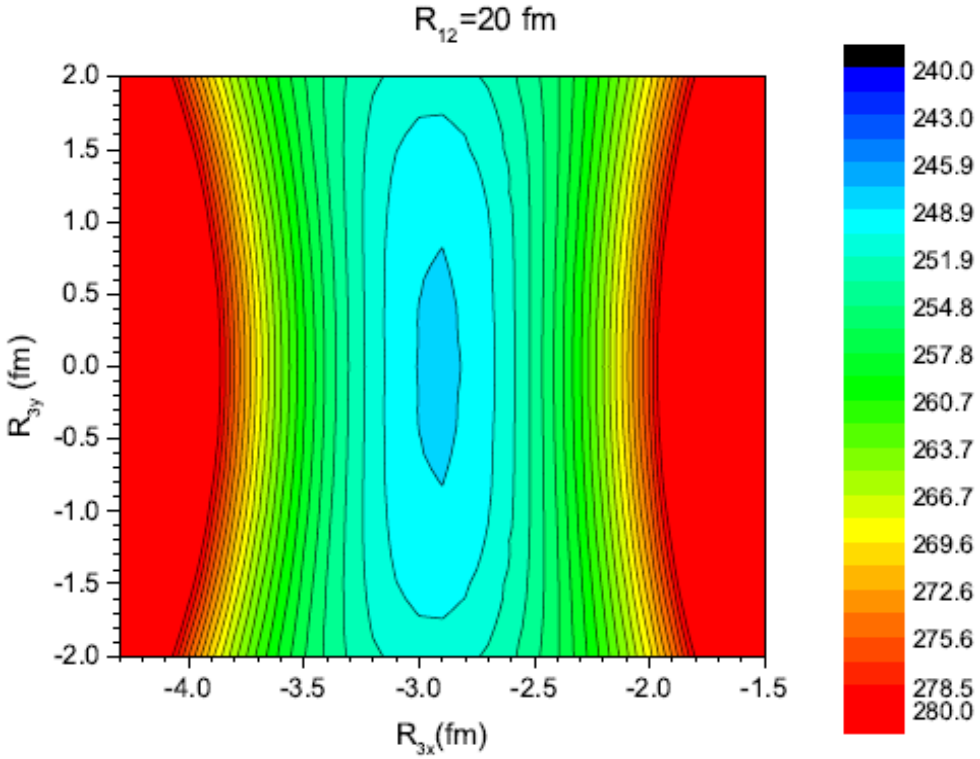

Fig. 4.3. Contour plot of the Fig. 4.2.

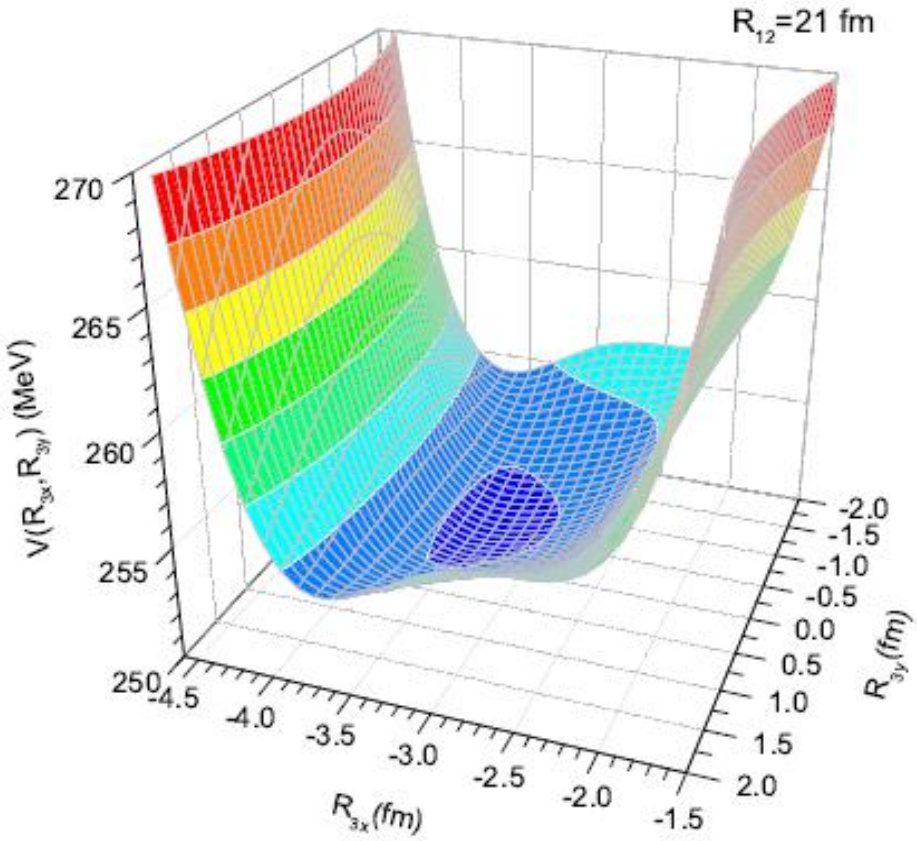

Fig. 4.4. The same as Fig. 4.2 but for R_{12}=21 fm.

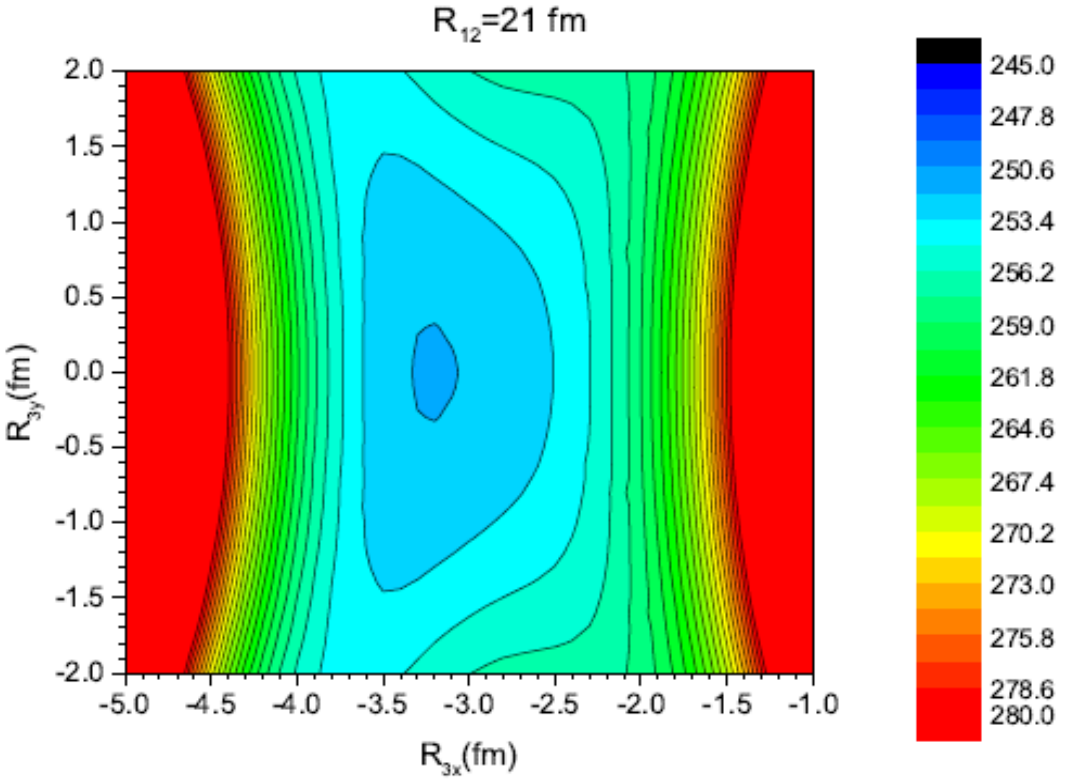

Fig. 4.5. The same as Fig. 4.3 but for R_{12}=21 fm.

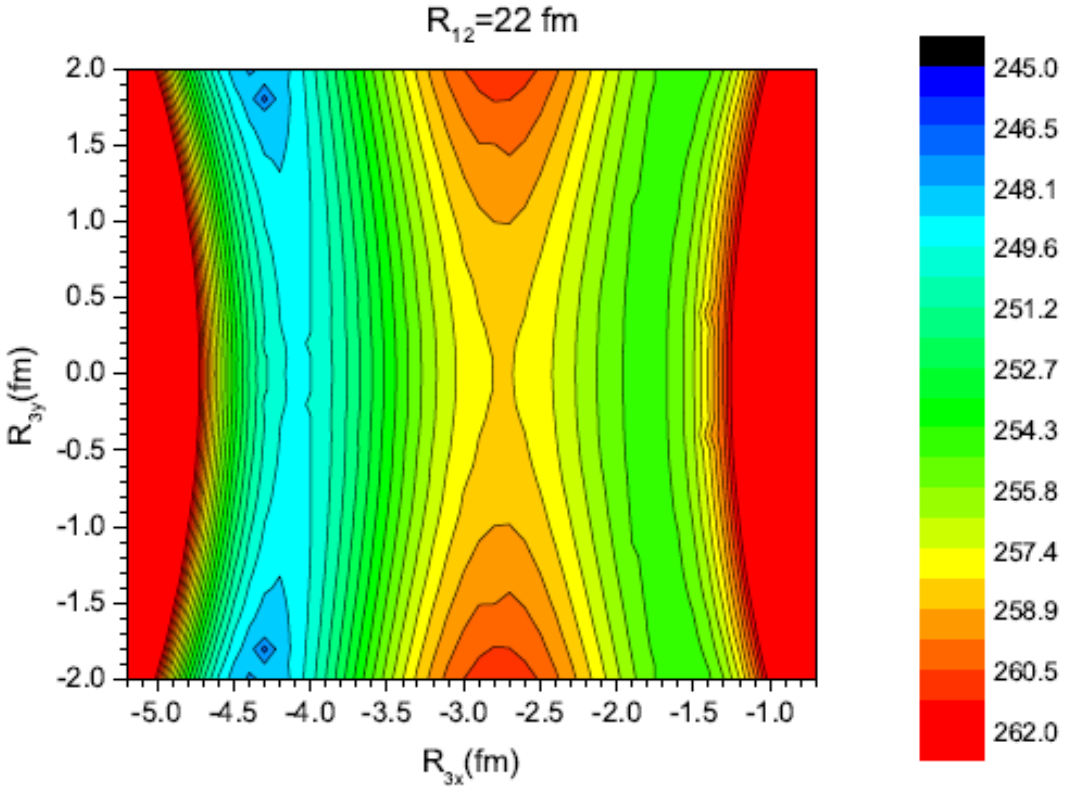

Fig. 4.6. The same as Fig. 4.3 but for R_{12}=22 fm.

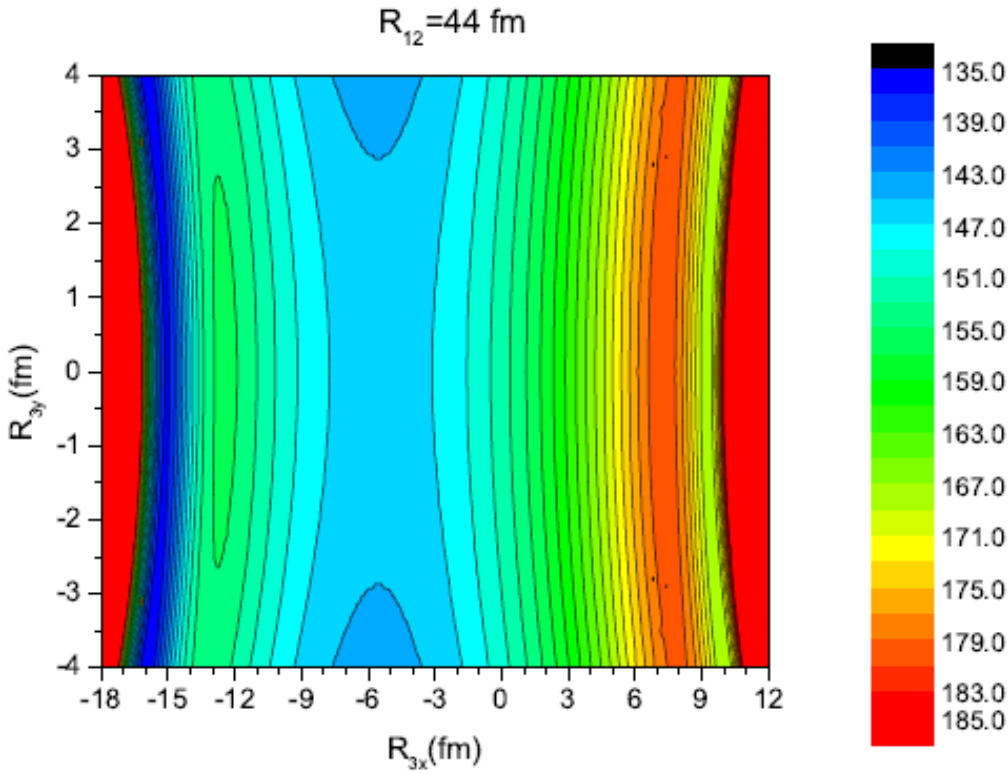

Fig. 4.6. The same as Fig. 4.3 but for R_{12}=44 fm.

Let's consider 3 cases of initial conditions which correspond to Cauchy problem. In the first case it is considered that initially all nuclei are placed in one line which means $R_{1y}(t = 0) = R_{2y}(t = 0) = R_{3y}(t = 0) = 0$, since the energy of the collinear configuration in the pre-scission state is the smallest, and x coordinates of that nuclei (or relative distance between nuclei) correspond to the local minimum in the Fig. 4.2, i.e. $R_{1x}(t = 0) = -12.3$ fm, $R_{2x}(t = 0) = 7.7$ fm, $R_{3x}(t = 0) = -2.9$ fm. Both components (x and y) of initial velocities of the three nuclei are zero. In other words formation of fragments of the TNS so slow that fragments have zero (or too small) velocities. Nevertheless, the assumption of all initial velocities are zero means that there is no the net force which acts to nuclei in the equilibrium state. Results of solution of the equations of motion (4.6) and (4.7) (together with (4.8)) with the mentioned above initial conditions are shown in the Fig. 4.8. It is shown that from the beginning Sn nucleus is going to break up from the Ni+Ca system, and then at $t \approx 13.5\times10^{-22}$ s the Ni+Ca system has decayed. Moreover, as an important result has been obtained that

the third nucleus (Ca) almost does not change its coordinate, because its velocity is about zero. It means the detecting the middle nucleus (Ca) is almost impossible experimentally. This conclusion proves the assumption done in the second chapter. Only this condition leads to collinear fission of the trinuclear system.

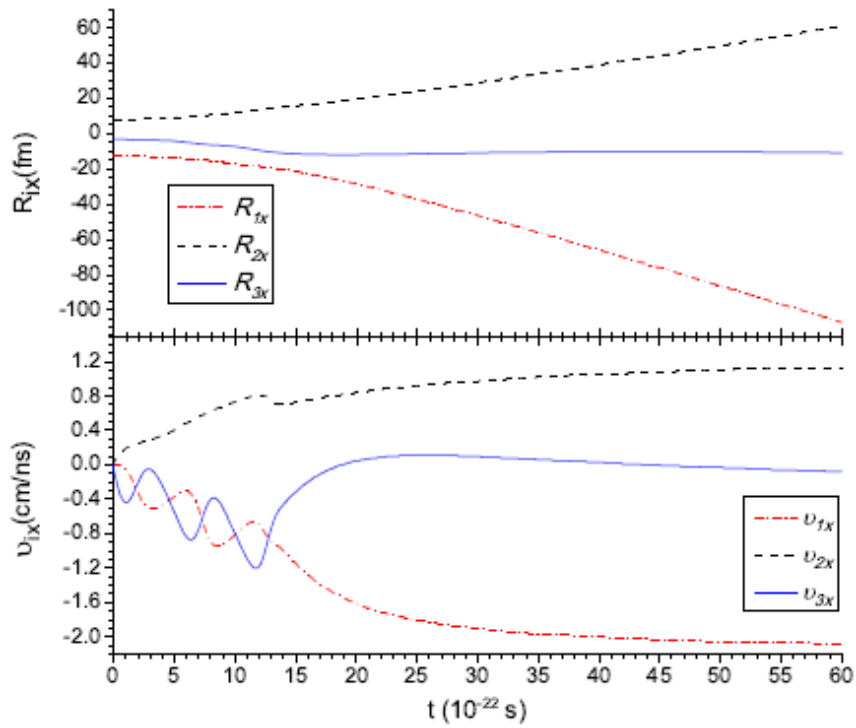

Fig. 4.8. *x* component of coordinates (upper) and velocities (lower) of three nuclei as functions of time.

In the second case the velocities of all nuclei are zero, but the middle nucleus (Ca) is placed a little bit upper, i.e. $R_{3y}(t = 0) = 0.5$ fm, $R_{1x}(t = 0) = -12.3$ fm, $R_{2x}(t = 0) = 7.7$ fm, $R_{3x}(t = 0) = -2.9$ fm and $R_{1y}(t = 0) = R_{2y}(t = 0) = 0$. Results of calculation are shown in the Fig. 4.9. It is clear from the figure that the deviation of the location of calcium nucleus on 0.5 fm on *y*-axis from the origin is enough to get non-collinear fission. Moreover, the sequence of the non-collinear fission is similar to the one of the collinear fission: at first Sn is separated from Ni+Ca, then, Ni+Ca system is broken up. It is interesting that the decay time of the trinuclear system is $t \approx 13.2\times10^{-22}$ *s* which is almost the same with the time of collinear ternary fission.

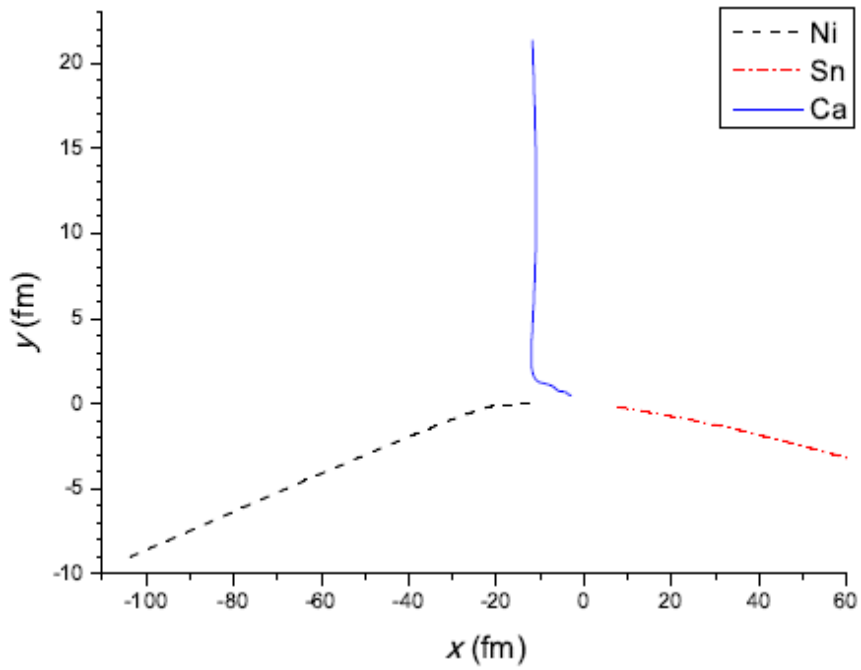

Fig. 4.9. Trajectories of three decaying nuclei when $R_{3y}(t = 0) = 0.5$ fm and the same initial velocities as in Fig. 4.8.

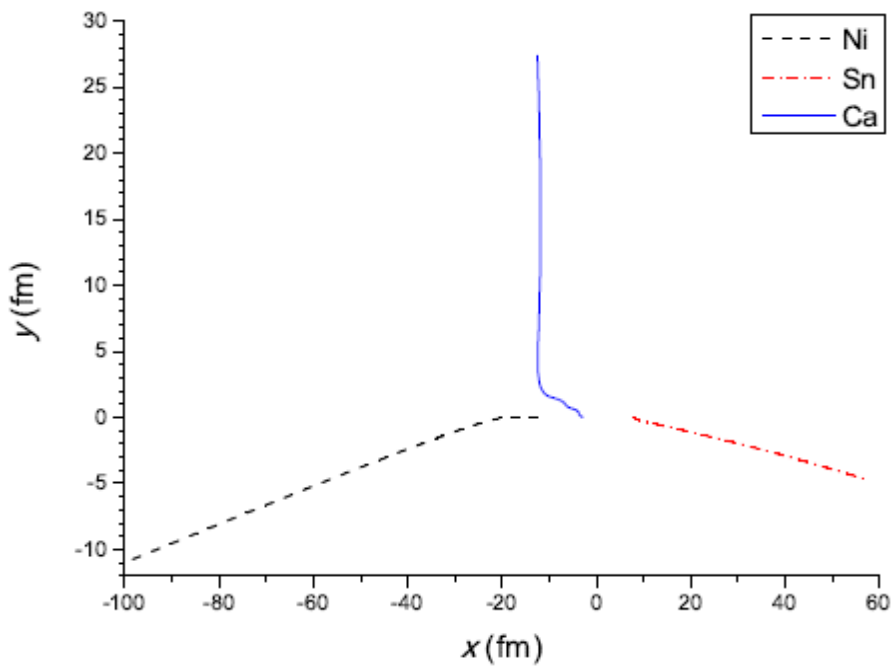

Fig. 4.10. Trajectories of three decaying nuclei when $v_{3y}(t = 0) = 0.1$ cm/ns and the same initial coordinates as in Fig. 4.8.

In the third case initial location of all nuclei are the same as in the first case, i.e. $R_{1y}(t=0)=R_{2y}(t=0)=R_{3y}(t=0)=0$, $R_{1x}(t=0)=-12.3$ fm, $R_{2x}(t=0)=7.7$ fm, $R_{3x}(t=0)=-2.9$fm.

But the initial velocity of the middle fragment is $\upsilon_{3y}(t=0)=0.1$ cm/ns, and other initial velocities are zero: $\upsilon_{1x}(t=0)=\upsilon_{2x}(t=0)=\upsilon_{3x}(t=0)=\upsilon_{1y}(t=0)=\upsilon_{2y}(t=0)=0$. The Fig. 4.10 shows that if y component of the initial velocity of the Ca nucleus is not zero, ternary fission will be non-collinear. Also, it should be noted that in this case the decay time of the TNS is $t \approx 13.4\times10^{-22}$ s which is almost the same with the time of the previous cases. From the comparison of Figs. 4.9 and 4.10 is seen that the final paths of the all fragments are similar despite difference in the initial conditions of the second and third cases.

From the figures 4.8-4.10, it can be concluded that there is collinear fission only when all three nuclei are located in one line ($R_{iy}=0$) and there is not y component of the initial velocity of the middle fragment ($\upsilon_{3y}=0$).

4.4. Summary.

We conclude that if in the pre-scission stage all nuclei are placed collinearly which corresponds to the minimum in the potential energy surface and there is no the net force on the third nucleus (Ca) on y-axis (or y component of its initial velocity is zero), then the trinuclear system can be broken up collinearly. This theoretical result proves the experimental results of the collinear cluster tripartition in the Ref. [20]. The experiment shows that collinear ternary fission can be observed. Therefore, in the framework of the TNS model the initial condition which leads to collinear fission have a place in the nature.

From the comparison of the potential energy surfaces in the Figs. 4.2-4.7 it can be concluded that as R_{12} (relative distance between Ni and Sn nuclei) increases the minimum at the point when $R_{3x}=-2.9$ fm and $R_{3y}=0$ fm in the Fig. 4.2 disappears, and instead of this minimum the saddle point emerges (see Fig. 4.7). It means the TNS with value of R_{12} higher than 22 fm is an unstable system.

Moreover, from the Figs. 4.9 and 4.10 as conclusion it can be emphasized that non-collinear ternary fission occurs in the following initial conditions: the deviation in *y*-axis of location from the origin of the middle (Ca) nucleus or the difference from zero of the *y* component of the velocity of that nucleus.

Nevertheless, it is interesting that in all cases the decay time of the TNS has nearly the same value. It means the time almost does not depend on initial conditions.

This is because of the sequence of the fission: firstly, Sn nucleus is separated from the Ni+Ca system, and then Ni is separated from Ca nucleus.

As the collinearity of the ternary fission depends on initial conditions so the probability (or the weight) of each initial condition's population is an open question which will be studied in future investigations.

MAIN RESULTS AND CONCLUSIONS

The analysis of the main results of the theoretical research carried out on the theme of the PhD dissertation “Mechanisms of collinear cluster tripartition” has leaded to the following conclusions:

1. If the excited compound nucleus $^{236}U^{*}$ formed in the in the $^{235}U(n_{th},f)$ reaction can undergo the collinear cluster tripartition by the sequential mechanism, then products will be $^{82}Ge^{*}$, $^{72}Ni^{*}$ and $^{82}Ge^{*}$. The probability of this channel is maximum comparing with other channels for CCT, and it is equal to $3\cdot10^{-4}$ relative to binary fission. The value of the yield is close to the value which is obtained in experiment. But the yield of products with mass number M=132-138 was not obtained in this mechanism.

2. The second mechanism of CCT, which is called “almost sequential mechanism”, has been suggested to reproduce the yield of the massive fragment (^{132}Sn nucleus) in spontaneous fission of ^{252}Cf together with ^{70}Ni and ^{50}Ca nuclei. The advance of this mechanism is taking into account the decrease of the pre-scission barrier in the interaction between ^{70}Ni and ^{50}Ca nuclei due to the Coulomb field of the massive fragment (^{132}Sn nucleus). It means the location of ^{132}Sn should be close to $^{70}Ni+^{50}Ca$ system for its separation.

3. The solution of the equations related with the energy and momentum conservation laws shows that the velocity of the middle fragment (Ca) is about zero in the $^{252}Cf\rightarrow^{70}Ni+^{50}Ca+^{132}Sn$ reaction. That is why Ca nucleus is hard to observe in experiment.

4. From results of calculation of the total interaction potential for the spontaneous fission of ^{252}Cf we can conclude that R_{12} (line connecting centers of the outer fragments Ni and Sn) is smaller than 21 fm outer fragments extrude the middle fragment (Ca) from collinear position, TNS has the triangular shape. At larger values

of R_{12}=21-22 fm, the minimum of the potential well moves to the line R_{12} and the collinear shape of the TNS is favorable.

5. In the pre-scission stage if all nuclei of TNS are placed collinearly which corresponds to the minimum in the potential energy surface and there is no the net force on the third nucleus (Ca) on y-axis (or *y* component of its initial velocity is zero), then the trinuclear system can be broken up collinearly. Other initial cases lead to non-collinear ternary fission.

6. In all cases the decay time of the TNS (^{70}Ni+^{50}Ca+^{132}Sn) is nearly the same value, around 1.4×10^{-21} s. It means the time almost does not depend on initial conditions. It is because of the sequence of the fission: firstly, Sn nucleus is separated from the Ni+Ca system, and then Ni is decayed from Ca nucleus.

Acknowledgements

The author deeply grateful to A. K. Nasirov for supporting to solve and discuss problems during research. The author thanks to A. V. Khugaev, P. N. Usmanov, A. Rakhimov and S. V. Artemov for interest and discussion. The author also thanks to D.V. Kamanin for supporting to stay in Dubna.

BIBLIOGRAPHY

1. G. Farwell, E. Segre and C. Wiegand, “Long range alpha-particles emitted in connection with fission. Preliminary report”, Physical Review, American Physical Society (USA), 1947, v. 71, p. 327.

2. F. K. Goward, E. W. Titterton, and J. J. Wilkins, “Photo-fission of uranium with possible emission of a beryllium nucleus”, Nature, v. 164, n. 4172, p. 661 (1949).

3. K. W. Allen and J. T. Dewan, “The emission of short-range charged particles in the slow neutron fission of uranium”, Physical Review, American Physical Society (USA), 1951, v. 82, p. 527.

4. L. Rosen and A. M. Hudson, “Symmetrical tripartition of U^{235} by thermal neutrons”, Physical Review, American Physical Society (USA), 1950, v. 78, p. 533.

5. W. J. Swiatecki, “Deformation energy of a charged drop. III. Further developments”, in Proceedings of the 2nd UN Conference on the Peaceful Uses of Atomic Energy, Geneva (Sweden), 1958, v. 15, paper/651, p. 248.

6. M. L. Muga, H. R. Bowman, and S. G. Thompson, “Tripartition in the spontaneous-fission decay of Cf^{252}”, Physical Review, American Physical Society (USA), 1961, v. 121, p. 270.

7. V. M. Strutinsky, N. Ya. Lyashchenko and N. A. Popov, “Symmetrical shapes of equilibrium for a liquid drop model”, Nuclear Physics, Elsevier (Netherland), 1963, v. 46, pp. 639-659.

8. H. Diehl and W. Greiner, “Theory of ternary fission in the liquid drop model”, Nuclear Physics A, Elsevier (Netherland), 1974, v. 229, pp. 29-46.

9. A. R. Degheidy and J. A. Maruhn, “A three-center shell model for ternary fission”, Zeitschrift Physik A, Springer (Germany), 1979, v. 290, pp. 205-212.

10. P. Schall, P. Heeg, M. Mutterer and J.P. Theobald, “On symmetric tripartition in the spontaneous fission of ^{252}Cf”, Physics Letters B, Elsevier (Netherland), 1987, v. 191, n. 4, pp. 339-342.

11. J. P. Theobald, P. Heeg and M. Mutterer, “Low-energy ternary fission”, Nuclear Physics A, Elsevier (Netherland), 1989, v. 502, pp. 343-362.

12. R. B. Tashkhodjaev, A. K. Nasirov, and W. Scheid, “Collinear cluster tripartition as sequential binary fission in the ^{235}U(n_{th},f) reaction”, European Physical Journal A, Springer-SIF (Germany), 2011, v. 47, p. 136.

13. F. Gönnenwein, “Ternary and quaternary fission”, Nuclear Physics A, Elsevier (Netherland), 2004, v. 734, p. 213.

14. Yu. V. Pyatkov, Yu. E. Penionzhkevich, W. H. Trzaska, O. I. Osetrov, A. A. Alexandrov, I. A. Alexandrova, J. Äystö, K.-Th. Brinkmann, S. V. Khlebnikov, V. F. Kushniruk, A. V. Kuznetsov, V. G. Lyapin, V. A. Maslov, M. Mutterer, Z. Radivojevich, V. A. Rubchenya, Yu.G.Sobolev, G. P. Tiourine, D. N. Vakhtin, “Peculiarities in fragment mass distribution in the ^{238}U+^{40}Ar (243 MeV) reaction”, European Physical Journal A, Springer-SIF (Germany), 2001, v. 10, pp. 171-175.

15. Yu. V. Pyatkov, D. V. Kamanin, A. A. Alexandrov, I. A. Alexandrova, S. V. Khlebnikov, S. V. Mitrofanov, V. V. Pashkevich, Yu. E. Penionzhkevich, Yu. V. Ryabov, E. A. Sokol, V. G. Tishchenko, A. N. Tyukavkin, A. V. Unzhakova and S. R. Yamaletdinov, “New Indications of Collinear Tripartition in ^{252}Cf(sf) Studied at the Modified FOBOS Setup”, Physics of Atomic Nuclei, Springer (Germany), 2003, v. 66, p. 1631.

16. Yu. V. Pyatkov, V. V. Pashkevich, W. H. Trzaska, G. G. Adamian, N. V. Antonenko, D. V. Kamanin, V. A. Maslov, V. G. Tishchenko, and A. V. Unzhakova, “Nontrivial Manifestation of Clustering in Fission of Heavy Nuclei at Low and Middle Excitations”, Physics of Atomic Nuclei, Springer (Germany), 2004, v. 67, p. 1726.

17. Yu. V. Pyatkov, D. V. Kamanin, Yu. N. Kopach, A. A. Alexandrov, I. A. Alexandrova, S. B. Borzakov, Yu. N. Voronov, V. E. Zhuchko, E. A. Kuznetsova, Ts. Panteleev, and A. N. Tyukavkin, "Collinear cluster tripartition channel in the reaction $^{235}U(n_{th},f)$", Physics of Atomic Nuclei, Springer (Germany), 2010, v. 73, p. 1309.

18. Yu. V. Pyatkov, D.V. Kamanin, W. von Oertzen, A.A. Alexandrov, I.A. Alexandrova, O.V. Falomkina, N.A. Kondratjev, Yu.N. Kopatch, E.A. Kuznetsova, Yu.E. Lavrova, A.N. Tyukavkin, W. Trzaska and V.E. Zhuhcko, "Collinear cluster tripartition of $^{252}Cf(sf)$ and in the $^{235}U(n_{th},f)$ reaction", European Physical Journal A, Springer-SIF (Germany), 2010, v. 45, p. 29.

19. Yu. V. Pyatkov, D. V. Kamanin, A. A. Alexandrov, I. A. Alexandrova, N. A. Kondratjev, E. A. Kuznetsova, N. Jacobs, V. Malaza, D. Phan Minh, and V. E. Zhuchko, "Presumable scenario of one of the collinear cluster tri-partition modes", International Journal of Modern Physics E, World Scientific (Singapore), 2011, v. 20, p. 1008.

20. Yu. V. Pyatkov, D.V. Kamanin, W. von Oertzen, A.A. Alexandrov, I.A. Alexandrova, O.V. Falomkina, N. Jacobs, N.A. Kondratjev, E.A. Kuznetsova, Yu.E. Lavrova, V. Malaza, Yu.V. Ryabov, O.V. Strekalovsky, A.N. Tyukavkin and V.E. Zhuchko, "The collinear cluster tri-partition (CCT) of $^{252}Cf(sf)$: New aspects from neutron gated data", European Physical Journal A, Springer-SIF (Germany), 2012, v. 48, p. 94.

21. Yu. V. Pyatkov, D. V. Kamanin, A. A. Alexandrov, I. A. Alexandrova, E. A. Kuznetsova, Yu. E. Lavrova, A. O. Strekalovsky, O. V. Strekalovsky, V. E. Zhuchko, "First results on observation of new shape isomers", Physics Procedia, Elsevier (Netherland), 2015, v. 74, pp. 67-73.

22. K. Manimaran and M. Balasubramaniam, "Three-cluster model for the α-accompanied fission of californium nuclei", Physical Review C, American Physical Society (USA), 2009, v. 79, id 024610.

23. K. Manimaran, M. Balasubramaniam, “Ternary fission fragmentation of ^{252}Cf for all possible third fragments”, European Physical Journal A, Springer-SIF (Germany), 2010, v. 45, p. 293.

24. K. Manimaran and M. Balasubramaniam, “All possible ternary fragmentations of ^{252}Cf in collinear configuration”, Physical Review C, American Physical Society (USA), 2011, v. 83, id 034609.

25. N. V. Antonenko, E. A. Cherepanov, A. K. Nasirov, V. P. Permjakov and V. V. Volkov, “Competition between complete fusion and quasi-fission in reactions between massive nuclei. The fusion barrier”, Physics Letters B, Elsevier (Netherland), 1993, v. 319, pp. 425-430.

26. N. V. Antonenko, E. A. Cherepanov, A. K. Nasirov, V. P. Permjakov, and V. V. Volkov, “Compound nucleus formation in reactions between massive nuclei: Fusion barrier”, Physical Review C, American Physical Society (USA), 1995, v. 51, id 2635.

27. V. V. Volkov, “From deep inelastic transfer reactions to complete fusion of nuclei”, Acta Physica Polonica B, Jagiellonian University (Poland), 1999, v. 30, n. 5, pp. 1517-1526.

28. Avazbek Nasirov, Akira Fukushima, Yuka Toyoshima, Yoshihiro Aritomo, Akhtam Muminov, Shuhrat Kalandarov, Ravshanbek Utamuratov, “The role of orientation of nucleus symmetry axis in fusion dynamics”, Nuclear Physics A, Elsevier (Netherland), 2005, v. 759, pp. 342-369.

29. A.V. Andreev, G.G. Adamian, N.V. Antonenko, S.P. Ivanova, S.N. Kuklin, and W. Scheid, “Ternary fission within statistical approach”, European Physical Journal A, Springer-SIF (Germany), 2006, v. 30, p. 579.

30. G. G. Adamian, R.V. Jolos, A.K. Nasirov, “Partition of excitation energy between reaction products in heavy ion collisions”, Zeitschrift Physik A, Springer (Germany), 1994, v. 347, pp. 203-210.

31. A. K. Nasirov, G. Giardina, G. Mandaglio, M. Manganaro, F. Hanappe, S. Heinz, S. Hofmann, A. I. Muminov, and W. Scheid, "Quasifission and fusion-fission in reactions with massive nuclei: Comparison of reactions leading to the Z=120 element", Physical Review C, American Physical Society (USA), 2009, v. 79, id 024606.

32. G. Audi, A. H. Wapstra, C. Thibault, "The AME2003 atomic mass evaluation. (II). Tables, graphs and references", Nuclear Physics A, Elsevier (Netherland), 2003, v. 729, pp. 337-676.

33. P. Möller, J. R. Nix, W. D. Myers, and W. J. Swiatecki, "Nuclear ground-state masses and deformations", Atomic Data and Nuclear Data Tables, Elsevier (Netherland), 1995, v. 59, p. 185.

34. G. Royer and B. Remaud, "On the fission barrier of heavy and superheavy nuclei", Journal of Physics G: Nuclear Physics, IOP Publishing (United Kingdom), 1984, v. 10, n. 11, p. 1541.

35. D. J. Hinde, D. Hilscher, H. Rossner, B. Gebauer, M. Lehmann, and M. Wilpert, Physical Review C, American Physical Society (USA), 1992, v. 45, id 1229.

36. L. G. Moretto and J. S. Sventek, "A theoretical approach to the problem of partial equilibration in heavy ion reactions", Physics Letters, Elsevier (Netherland), 1975, v. 58B, pp. 26-30.

37. V. V. Pashkevich, A. Ya. Rusanov, "The ^{226}Th fission valleys", Nuclear Physics A, Elsevier (Netherland), 2008, v. 810, pp. 77-90.

38. S. Raman, C. H. Malarkey, W. T. Milner, C. W. Nestor, Jr, P. H. Stelson, "Transition Probability, B(E2)↑, from the Ground to the First-Excited 2^+ State of Even-Even Nuclides", Atomic Data and Nuclear Data Tables, Elsevier (Netherland), 1987, v. 36, p. 1.

39. Yu. V. Pyatkov, V. G. Tishchenko, V. V. Pashkevich, V. A. Maslov, D. V. Kamanin, I. V. Kljuev, W. H. Trzaska, "Manifestation of fine structures in the fission fragment mass-energy distribution of the ^{233}U(n_{th},f) reaction", Nuclear

Instruments and Methods in Physics Research Section A, Elsevier (Netherland), 2002, v. 488, pp. 381-399.

40. A. J. Sierk, “Macroscopic model of rotating nuclei”, Physical Review C, American Physical Society (USA), 1986, v. 33, id. 2039.

41. A. V. Andreev, G. G. Adamian, N. V. Antonenko, S. P. Ivanova, S. N. Kuklin, W. Scheid “Cluster aspects of binary and ternary fission” Physics of Atomic Nuclei, Springer (Germany), 2007, v. 70, n. 9, pp. 1-5 (2007).

42. A.A. Goverdovsky, V.F. Mitrofanov, V.A. Khryachkov, “Cold deformed fission of uranium in the high mass asymmetry area”, Physics of Atomic Nuclei, Springer (Germany), 1995, v. 58, n. 9, p. 1460.

43. K. R. Vijayaraghavan, W. von Oertzen, and M. Balasubramaniam, “Kinetic energies of cluster fragments in ternary fission of ^{252}Cf”, European Physical Journal A, Springer-SIF (Germany), 2012, v. 48, p. 27 (2012).

44. K. R. Vijayaraghavan, M. Balasubramaniam, W. von Oertzen, “Collinear versus triangular geometry: A ternary fission study”, Physical Review C, American Physical Society (USA), 2014, v. 90, id 024601.

45. K. P. Santhosh, Sreejith Krishnan and B. Priyanka, “^{34}Si accompanied ternary fission of ^{242}Cm in equatorial and collinear configuration”, Int. J. Mod. Phys. E, v. 23, n. 11, 1450071 (2014).

46. K. R. Vijayaraghavan, M. Balasubramaniam, W. von Oertzen, “True ternary fission”, Physical Review C, American Physical Society (USA), 2015, v. 91, id 044616.

47. R. B. Tashkhodjaev, A. I. Muminov, A. K. Nasirov, W. von Oertzen, Yongseok Oh, “Theoretical study of the almost sequential mechanism of true ternary fission”, Physical Review C, American Physical Society (USA), 2015, v. 91, id 054612.

48. H. Diehl and W. Greiner, “Theory of ternary fission in the liquid drop model”, Nuclear Physics A, Elsevier (Netherland), 1974, v. 229, pp. 29-46.

49. G. Royer, “On the fission of ^{56}Ni and ^{48}Cr rotating nuclei”, Journal of Physics G, IOP Publishing (United Kingdom), 1995, v. 21, p. 249.

50. J. A. Maruhn and W. Greiner, “Collective effects on mass asymmetry in fission”, Physical Review C, American Physical Society (USA), 1976, v. 13, id 2404.

51. D. N. Poenaru, R. A. Gherghescu, and W. Greiner, “Complex fission phenomena”, Nuclear Physics A, Elsevier (Netherland), 2005, v. 747, p. 182.

52. M. Csatlòs, A. Krasznahorskay, P.G. Thirolf, D. Habs, Y. Eisermann, T Faestermann, G. Graw, J. Gulyas, M. N. Harakeh, R. Hertenberger, M. Hunyadi, H. J. Maier, Z. Màtè, O. Schaile, H. F. Wirth, “Resonant tunneling through the triple-humped fission barrier of ^{236}U”, Physics Letters B, Elsevier (Netherland), 2005, v. 615, p. 175.

53. V. K. Rao, V. K. Bhargava, S. G. Marathe, S. M. Sahakundu, R. H. Iyer, “Shoulders in the very asymmetric mass distribution for reactor-neutron-induced fission of ^{238}U” Physical Review C, American Physical Society (USA), 1979, v. 19, id. 1372.

54. F. Gönnenwein, M. Mutterer, and Y. Kopatch, “Ternary and quaternary fission”, Europhysics News, European Physical Society (France), 2005, v. 36, p. 11.

55. A. K. Nasirov, R. B. Tashkhodjaev, W. von Oertzen, “Pre-scission configuration of the trinuclear system at spontaneous ternary fission of ^{252}Cf”, European Physical Journal A, Springer-SIF (Germany), 2016, v. 52, pp. 135-141.

56. Yu.V. Pyatkov, D.V. Kamanin, A. A. Alexandrov, I. A. Alexandrova, N. Mkaza, V. E. Zhuchko, N. A. Kondratjev, E. A. Kuznetsova, G. V. Mishinsky, V. Malaza, A. O. Strekalovsky, O. V. Strekalovsky, “Status and prospects of investigations into the collinear cluster decay of heavy nuclei”, Physics of Atomic Nuclei, Springer (Germany), 2014, v. 77, pp. 1518-1524.

57. V. I. Zagrebaev, A. V. Karpov, Walter Greiner, “True ternary fission of superheavy nuclei”, Physical Review C, American Physical Society (USA), 2010, v. 81, id 044608.

58. K. R. Vijayaraghavan, M. Balasubramaniam, W. von Oertzen, “True ternary fission”, Physical Review C, American Physical Society (USA), 2015, v. 91, id 044616.

59. W. von Oertzen, A.K. Nasirov, R.B. Tashkhodjaev, “Multi-modal fission in collinear ternary cluster decay of ^{252}Cf(sf,fff)”, Physics Letters B, Elsevier (Netherland), 2015, v. 746, pp. 223-229.

60. R. B. Tashkhodjaev, A. I. Muminov, A. K. Nasirov, W. von Oertzen, Yongseok Oh, “Theoretical study of the almost sequential mechanism of true ternary fission”, Physical Review C, American Physical Society (USA), 2015, v. 91, id 054612.

61. A.K. Nasirov, W. von Oertzen, A.I. Muminov, R.B. Tashkhodjaev, “Peculiarities of cluster formation in true ternary fission of ^{252}Cf and ^{236}U*”, Physica Scripta, IOP Publishing (United Kingdom), 2014, v. 89, id 054022.

62. I. Muntian, Z. Patyk, A. Sobiczewski, “Calculated masses of heaviest nuclei”, Physics of Atomic Nuclei, Springer (Germany), 2003, v. 66, pp. 1015-1019.

63. Ning Wang, Min Liu, Xizhen Wu, “Modification of nuclear mass by considering isospin effects”, Physical Review C, American Physical Society (USA), 2010, v. 81, id 044322.

64. A. V. Daniel, G. M. Ter-Akopian, J. H. Hamilton, A. V. Ramayya, J. Kormicki, G. S. Popeko, A. S. Fomichev, A. M. Rodin, Yu. Ts. Oganessian, J. D. Cole, J. K. Hwang, Y. X. Luo, D. Fong, P. Gore, M. Jandel, J. Kliman, L. Krupa, J. O. Rasmussen, S. C. Wu, I. Y. Lee, M. A. Stoyer, R. Donangelo, W. Greiner, “Ternary fission of ^{252}Cf: 3368 keV γ radiation from ^{10}Be fragments”, Physical Review C, American Physical Society (USA), 2004, v. 69, id 041305(R).

65. R. K. Gupta, W. Scheid, and W. Greiner, “Theory of Charge Dispersion in Nuclear Fission”, Physical Review Letters, American Physical Society (USA), 1975, v. 35, p. 353-356.

66. V. M. Strutinsky, “Shell effects in nuclear masses and deformation energies”, Nuclear Physics A, Elsevier (Netherland), 1967, v. 95, pp. 420-442.

67. V. M. Strutinsky, ““Shells” in deformed nuclei”, Nuclear Physics A, Elsevier (Netherland), 1968, v. 122, pp. 1-33.

68. W. von Oertzen, A. K. Nasirov, “True ternary fission, the collinear decay into fragments of similar size in the ^{252}Cf(sf) and ^{235}U(n_{th},f) reactions”, Physics Letters B, Elsevier (Netherland), 2014, v. 734, p. 234.

69. A. V. Karpov, “Ternary fission of a heavy nuclear system within a three-center shell model”, Physical Review C, American Physical Society (USA), 2016, v. 94, id 064615.

70. P. Holmvall, U. Köster, A. Heinz, T. Nilsson, “Collinear cluster tri-partition: Kinematics constraints and stability of collinearity”, Physical Review C, American Physical Society (USA), 2017, v. 95, id 014602.

71. V. Yu. Denisov, N. A. Pilipenko, I. Yu. Sedykh, “Interaction of three fission fragments and yields of various ternary fragments”, Physical Review C, American Physical Society (USA), 2017, v. 95, id 014605.

72. R. B. Tashkhodjaev, A. K. Nasirov, E. Kh. Alpomeshev, “Dynamics of the trinuclear system at spontaneous fission of ^{252}Cf”, Physical Review C, American Physical Society (USA), 2016, v. 94, id 054614.

73. Migdal A. B., “Theory of the Finite Fermi Systems and Properties of Atomic Nuclei”, Nauka (Russia), 1983.

74. N. M. Korobov, “Theoretical-numerical method in approximate analysis”, Fizmatlit (Russia), 1963, 224 p.

75. C. Y. Wong, “Interaction barrier in charged-particle nuclear reactions”, Physical Review Letters, American Physical Society (USA), 1973, v. 31, pp. 766-769 (1973).

The method of calculation is applicable at the stage of fission when two fragments are connected with a neck of a small size in comparison with the whole size of the DNS. In this case the interaction between the fragments of the DNS may be described by the diabatic nucleus-nucleus potential for well-deformed nuclei with a repulsive core and gives the relaxation of the charge asymmetry degree of freedom.

We use the nucleus-nucleus potential consisting of three parts:

$$V_{int}(R,Z,A,l,\beta) = V_{nuc}(R,A,\beta) + V_C(R,Z,\beta) + V_{rot}(R,Z,l) \qquad \text{(A.1)}$$

where V_{nuc} and V_C are the nuclear and Coulomb parts of the nucleus-nucleus potential, respectively; V_{rot} is the rotational energy of the DNS. In ternary fission of ^{236}U (caused by thermal neutrons) and ^{252}Cf (spontaneous fission) discussed in this work the rotational energy can be neglected due to the smallness of the partial wave number l. Therefore, the rotation of the DNS is not considered in this work.

The nuclear part V_{nuc} is calculated by the double folding potential:

$$V_{nuc}(R) = \int \rho_1(r')f_{eff}[\rho(r,r')]\,\rho_2(r)\mathrm{d}\mathbf{r}, \qquad \text{(A.2)}$$

$$\mathbf{r}' = \mathbf{r} - \mathbf{R},$$

where ρ_1 and ρ_2 are the nucleon density distributions of the interacting nuclei; f_{eff} is the effective nucleon-nucleon potential taken from Ref. [73]. The advantage of these Migdal forces is their dependence on the nuclear density of the nuclei:

$$f_{eff}[\rho(r,r')] = C\left[f_{in} + (f_{ex} - f_{in})\frac{\rho_0 - \rho(r,r')}{\rho_0}\right], \qquad \text{(A.3)}$$

where $C = 300$ MeV·fm^3, $f_{in} = 0.09$ and $f_{ex} = -2.59$ are constants from Ref. [73]. When $\rho(r,r') > \rho_0$ the nuclear part becomes repulsive that corresponds to the appearance of the Pauli blocking principle. For the nucleon density distribution of nuclei we use Fermi functions placed at the center of mass of the nuclei which have the distance R between them,

$$\rho_1(r') = \frac{\rho_0}{1 + \exp\left(\frac{r' - R_1}{a_d}\right)}, \tag{A.4}$$

$$\rho_2(r) = \frac{\rho_0}{1 + \exp\left(\frac{r - R_2}{a_d}\right)}, \tag{A.5}$$

and

$$\rho(r, r') = \rho_1(r') + \rho_2(r). \tag{A.6}$$

Here, $r' = |\mathbf{r} - \mathbf{R}| = \sqrt{r^2 + R^2 - 2rR\cos\theta}$, $R_i = r_0 A_i^{1/3}\left(1 + \beta_2^{(i)} Y_{20}(\theta_i)\right)$ is the radius of the *i*-th nucleus, $r_0 = 1.16$ fm is radius parameter, $\rho_0 = 0.17$ fm^{-3} is nuclear density at center, $a_d = 0.54$ fm is diffuseness parameter, and $\beta_2^{(i)}$ are the quadrupole deformation parameters. Also r, θ and $\varphi = 2\pi$ (2π is because of axial symmetry) are variables of spherical coordinates. $Y_{20}(\theta_i)$ is the spherical function of the deformed *i*-th nucleus, and θ_i angles are defined as $\theta_1 = \cos^{-1}\left(\frac{r\cos\theta - R}{r'}\right)$ and $\theta_2 = \theta$. The orientation angles of the axial symmetry axes of the interacting nuclei are taken as $\Theta_1 = 0^0$ and $\Theta_2 = 180^0$ in both the stages of the sequential binary fission.

The integral in equation (A.2) can be calculated by using the Korobov's numerical method [74].

The Coulomb potential between the nuclei of the DNS is found by the formula of Wong [75]:

$$V_C(R, Z_1, Z_2) = \frac{Z_1 Z_2 e^2}{R} + \\ + \frac{Z_1 Z_2 e^2}{R^3}\sqrt{\frac{9}{20\pi}}\sum_{i=1}^{2} R_{0i}^2 \beta_2^{(i)} + \frac{Z_1 Z_2 e^2}{R^3}\frac{3}{7\pi}\sum_{i=1}^{2} R_{0i}^2 \left(\beta_2^{(i)}\right)^2, \tag{A.7}$$

here, $R_{0i} = r_0 A_i^{1/3}$ is the radius of the *i*-th spherical nucleus.